



universität
wien

DIPLOMARBEIT

Titel der Diplomarbeit

Interfacing the L1 Global Trigger of the CMS experiment at LHC with
physics

angestrebter akademischer Grad

Magister der Naturwissenschaften (Mag. rer.nat.)

Verfasser:	Philipp Wagner
Matrikel-Nummer:	0505989
Studienrichtung (lt. Studienblatt):	Physik (411)
Betreuerin:	Claudia-Elisabeth Wulz

Wien, November 2010

The Large Hadron Collider at CERN, Geneva, Switzerland was designed to answer the last open questions of Standard Model of particle physics and is expected to open the doors for the discovery of new physics beyond the SM since it allows to investigate energy scales, that have not been accessed so far. It produces a relatively huge amount of data at each collision and delivers collisions with a frequency of 40 MHz. To deal with this data the experiments at Large Hadron Collider are equipped with a trigger system which separates the events that are interesting from a physicist's point of view from the huge amount of background events, that do not carry new information. At the CMS experiment the trigger system consists of two parts, the hardware-based Level-1 Trigger and a software-based High-Level Trigger. The latter can only deal with an input rate of 100 kHz, therefore the Level-1 Trigger has to reduce the event rate by a factor of 10^7 . The core of the Level-1 Trigger System is the Global Trigger that provides a largely programmable logic system which can deal with complex algorithms consisting of physics objects and decides whether an event is forwarded to the High-Level Trigger or irrecoverably discarded. The goal of this thesis was to develop an interface within the existing CMS software infrastructure to generate these physics algorithms and make the logic unit of the Global Trigger easily adaptable to any physics requirements. The information about the logic in use must also be recorded in the CMS configuration database in order to make it accessible by the High-Level Trigger and for further data analysis.

Contents

1	Introduction	6
2	High Energy Physics in 2010	8
2.1	Standard Model Physics	8
2.1.1	Elementary particles	8
2.1.2	Interactions within the Standard Model	9
2.1.3	Spontaneous symmetry breaking and the Higgs Mechanism	13
2.1.4	Experimental search of the Higgs boson	14
2.1.5	B-physics and top quarks	17
2.2	Supersymmetry	18
2.2.1	Naturalness and the hierarchy problem	18
2.2.2	Supersymmetric particles	19
2.2.3	R-Parity	20
2.2.4	Supersymmetry, Dark Energy and Dark Matter	20
2.2.5	The MSSM and mSUGRA	20
2.3	Beyond the Standard Model and Supersymmetry	21
2.3.1	The Little Higgs Model of electroweak symmetry breaking	21
2.3.2	Extra Dimensions and Black Holes	22
2.3.3	Technicolor	23
3	Experiments at the Large Hadron Collider	25
3.1	The LHC - Characteristics and parameters	25
3.2	Summary of the different experiments and their goals	26
4	The Compact Muon Solenoid Detector	29
4.1	The CMS coordinate frame	30
4.2	The Superconducting Solenoid	32
4.3	The Tracking System	32
4.4	The CMS Calorimeters	33
4.4.1	The Electromagnetic Calorimeter	33
4.4.2	The Hadron Calorimeter	35
4.4.3	The Muon system	37
4.4.4	Forward detectors	38
4.4.4.1	Castor	38
4.4.4.2	Zero Degree Calorimeter	39
4.4.5	Trigger and Data Acquisition	39

5	The CMS L1-Trigger System	42
5.1	Trigger objects	42
5.2	Design of the L1-Trigger	44
5.2.1	The Calorimeter Trigger	44
5.2.2	The Muon Trigger	45
5.2.3	The Global Trigger	48
5.2.3.1	The logic processor	51
5.2.3.2	Trigger Partitioning and the Final-OR	53
5.3	The Level-1 Trigger Menu	53
5.3.1	Condition types	54
5.3.2	Algorithms	57
5.3.3	Scales	57
6	Online Software at the CMS Experiment	58
6.1	Basic systems for operation and data taking	58
6.1.1	Run Control and Monitor System	58
6.1.2	Detector Control System	58
6.1.3	Cross-Platform DAQ Framework	59
6.1.4	Trigger Supervisor framework	59
6.2	Online configuration database	60
7	The L1 Trigger Menu Editor	63
7.1	Requirements	63
7.1.1	Functional requirements	63
7.1.2	Non-functional requirements	64
7.2	Concept and first steps	64
7.2.1	The TME as TS Cell	65
7.2.2	Integration of the CMSSW Classes	67
7.2.3	Shared features with the GT Cell	67
7.3	VHDL Writer and the VHDL code for the GTL	68
7.4	Lookup tables in the VHDL code and mirror operations	70
7.4.1	VME Addresses	71
7.5	Scales	72
7.5.1	Available scales	72
7.5.2	Scales management	73
7.5.3	Scale-dependent implementation of algorithms	73
7.5.4	Interpretation of hardware differences of spatial correlations	73
7.6	Implementation details of the L1 Trigger Menu Editor TS Cell	77
7.6.1	The user interface	77
7.6.2	Non - visible classes	82
7.6.3	Automatic condition name generation	83
7.6.4	Consistency checks	83
7.6.5	The Trigger Menu HTML file	85
7.6.6	Database access	85
7.6.7	The VME mode	86
7.6.8	Operation of the L1 TME on a server and password protection	86
7.6.9	Firmware deployment	88

<i>CONTENTS</i>	5
8 Performance and Basic Rates Analysis	89
8.1 Analysis of trigger rates and trigger correlations	89
8.1.1 The total trigger rate versus luminosity	90
8.1.2 The rate of particular triggers versus luminosity	93
8.1.3 Correlations between different triggers	95
8.1.4 The work flow from the raw data to the root trees	95
8.2 A first result of the CMS experiment	97
9 Summary and Perspectives	99
Bibliography	102
A The VHDL Writer Mirror Operations	108
B Class Scheme of the L1 Trigger Menu Editor	111
C Trigger Rate Analysis Material	112
D Kurzzusammenfassung	114

Chapter 1

Introduction

The Large Hadron Collider (LHC) [1] in Geneva, Switzerland will allow physicists to investigate completely new scales of energy and distance beyond the TeV range [2] that have never been accessed before. It is expected to open the doors for new physics and answer the last open questions of the Standard Model of particle physics. The Higgs Boson, which explains mass within the Standard Model, is of particular interest. Up to now neither the Large Electron Positron Collider (LEP) at CERN nor the Tevatron at Fermilab have managed to provide sufficient prove for its existence. Furthermore, there are great expectations that the LHC will bring clues to answer some of the most urgent questions of todays physics such as the matter-antimatter asymmetry in the universe, the unification of the fundamental forces or reconciliation of general relativity with quantum physics. One promising approach to some of these problems is Supersymmetry. It assigns a supersymmetric partner to each Standard Model particle, but is not considered to be an exact symmetry. At energies larger than 10^{16} GeV it opens a way to unify the strong, the electromagnetic and the weak force. On the other hand it provides a clear candidate for the dark matter that emerges in the theories of astrophysics, which still is one of the big enigmas of modern physics. Some theorists expect the LHC to discover extra dimensions as they are needed by string theory for example. Whatever turns out at the LHC, the discoveries will have a lasting impact on physics and boost our understanding of the structure of matter.

There are four big experiments at the LHC, one of which is the Compact Muon Solenoid (CMS) experiment. It was designed as a general-purpose detector to deal with the enormous amount of events that will be produced by LHC with a frequency of 40 MHz. It is optimized for the search for the Higgs Boson, the only particle in the Standard Model that has not been discovered yet and also to look for supersymmetric particles. Since it is only possible to record few hundred of Hz to the storage, the event rate has to be reduced from 40 MHz to about 100 Hz. Therefore the detector is equipped with a trigger system that has to separate the events that are considered to carry information about new physics from those which just can be considered to be background. This selection process takes place in two steps. The first part of the trigger system called Level-1 Trigger (L1-Trigger) is hardware based while the second part, the High-Level Trigger (HLT) consists of a huge computing farm.

- The task of the L1-Trigger is to reduce the event rate by a factor of 10^7 from 40 MHz to less than 100 kHz, a frequency the HLT can deal with. The core of the L1-Trigger System is the Global Trigger with a largely programmable logic processor that can deal with complex trigger algorithms consisting of logic combinations of certain trigger objects (called “conditions” in the following). The number of trigger algorithms is limited by hardware to 128 at a given time. For each collision there is a decision whether the event will be accepted or discarded forever. The L1 algorithms can apply energy and momentum thresholds, but also more complex topological and quality conditions are possible.
- The High-Level Trigger, consisting of a big computing farm, reduces the rate to about 100 Hz taking into account the full readout of the detector, including alignment and calibration parameters, for its decision.

The principal goal of this thesis is to develop a user interface for physicists to define the L1-Trigger algorithms in order to make the L1 Global Trigger of CMS easily adaptable to physics requirements. It should be integrated in the existing software infrastructure of the experiment, using common classes with the CMS offline software and communicate with the online configuration database to store the information about the trigger algorithms in use. A set of trigger algorithms combined with some additional, so-called technical triggers (logical values sent by detectors to the Global Trigger) is called L1 trigger menu. The Global Trigger hardware uses Fully-Programmable Gate Arrays (FPGA) technology; it uses FPGA chips that are programmable in Very High Speed Integrated Circuit Hardware Description Language (VHDL), a language which is very close to the hardware level. Therefore the physics definitions have to be translated to VHDL code which can be compiled to binary files by commercial software and are loaded to Global Trigger hardware.

The last chapter of this thesis is dedicated to some analysis of trigger rates during the commissioning of CMS and the LHC. Since during this process the luminosity of the accelerator is continuously increased by both adding more protons to the circulating bunches and adding more bunches to the LHC orbit, it is important to understand how the L1 trigger rate at CMS is influenced by these changes in order to be able to keep it within a reasonable range. Furthermore, the rates of particular triggers and their correlations are analyzed.

Chapter 2

High Energy Physics in 2010

2.1 Standard Model Physics

The Standard Model (SM) conceptually unifies Einstein's theory of special relativity with quantum mechanics resulting in a relativistic quantum field theory where point-like particles correspond to fields. These fields are described by their Lagrangian or more precisely Lagrangian density. The dependence of the actions on these two quantities is as follows: $S = \int L dt$ and $S = \int \mathcal{L} d^4x$ where L means Lagrangian and \mathcal{L} Lagrangian density with $L = \int \mathcal{L} d^3x$. The core principle of the Standard Model is the gauge invariance of its Lagrangian (density) under $SU(3) \otimes SU(2) \otimes U(1)$ transformations. Here $SU(3)$ is the symmetry group of the strong interaction, while $SU(2) \otimes U(1)$ is the underlying symmetry group of the theory of electroweak unification. In total the Standard Model has 18 free parameters which have to be determined by experiment. These free parameters are:

- The electromagnetic coupling constant, also called fine structure constant $\alpha = \frac{e^2}{4\pi\epsilon_0\hbar} \approx \frac{1}{137}$
- The strong coupling constant α_s
- The weak coupling constant α_w
- The mass of the Z^0 boson ($m_Z = 91.1876 \pm 0.0021$ GeV)
- The three CKM mixing angles and a additional complex phase
- In total nine fermion masses
- The mass of the Higgs boson

2.1.1 Elementary particles

The Standard Model knows three generations of elementary particles that can be divided in two classes each (Table 2.1). The fermions with spin 1/2 are ingredients of the matter that is surrounding us. The bosons with spin 1 on the other hand are considered as the mediators of the fundamental interactions. The leptons of the Standard Model can be classified by a doublet for each

Leptons			Bosons
e	μ	τ	γ
ν_e	ν_μ	ν_τ	Z^0
Quarks			$W^{+/-}$
u	c	t	8 gluons
d	s	b	H

Table 2.1: The particle content of the Standard Model.

generation consisting of an electron, muon or tauon and its associated neutrino. The quark content of the Standard Model shows a similar pattern. The lightest generation consists of the up and down quarks, followed by a duplet of charmed and strange, and top and bottom. On the boson side we have the massless photon, transmitting the electromagnetic interaction, the relatively heavy W^+ , W^- and Z^0 bosons responsible for the weak interaction and the 8 massless gluons that mediate the strong interaction. Last but not least, there is the so called Higgs boson that is needed to explain the mass within the SM.

At the Large Electron Positron Collider (LEP) it was shown that the number of light neutrinos is limited to three and therefore no more generations of elementary particles of the structure described above can exist. This result was obtained by precision measurements of the Z^0 resonance since the decay of a Z^0 in a pair consisting of a neutrino and a anti-neutrino contributes to the branching ratio of the Z^0 decays and therefore the number of generations of neutrinos influences the shape of the Z^0 resonance.

$$\Gamma_z = \Gamma(Z \rightarrow \text{Hadrons}) + 3\Gamma(l^+l^-) + N_\nu\Gamma(\nu - \bar{\nu}) \quad (2.1.1)$$

The shape of the Z^0 resonance gave clear experimental evidence for only three and no more generations existing since more (or fewer) generations would mean more decay channels into neutrinos and therefore lead to a different shape as Fig. 2.1.1 shows. For N_ν equal to three the simulated curve exactly fits the experimental data [3].

2.1.2 Interactions within the Standard Model

As already mentioned before the Standard Model knows three fundamental interactions that are mediated by gauge bosons. One great breakthrough in the SM was the unification of the electromagnetic and the weak interaction. However, the strong interaction is not included into the framework of electroweak unification and therefore has a separate description. The gravitation is neglected in the SM since it appears extremely weak compared to the other three forces: (Strong :1; EM: 1/137; Weak: 10^{-6} ; Gravitation: 10^{-39}).

The Electromagnetic Interaction If we consider the Lagrangian of a free fermion (which leads to the Dirac equation, introducing it into the Euler - Lagrange equations)

$$\mathcal{L} = i\bar{\psi}(x)\gamma^\mu\partial_\mu\psi(x) - m\bar{\psi}(x)\psi(x) \quad (2.1.2)$$

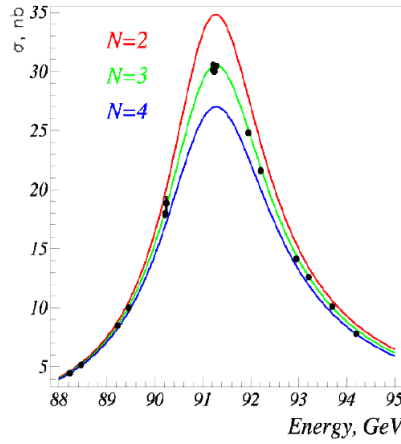


Figure 2.1.1: The experimental data fits the predicted Breit-Wigner curve for only three generations of light neutrinos existing.

we note that its invariant under a global gauge transformation

$$\psi' = e^{i\Theta} \psi \quad (2.1.3)$$

However, this global symmetry is not very handsome since it would mean having to apply the same phase transformation to all fermions in the entire universe at the same time which definitely would lead to some theoretical and experimental complications. Therefore local U(1) transformations are of special interest, where Θ is replaced by $\Theta(x)$. The transformation

$$\psi' = e^{i\Theta(x)} \psi \quad (2.1.4)$$

is called a local gauge transformation. Applying it to our Lagrangian we get an extra term which destroys our invariance:

$$\mathcal{L}' = i\bar{\psi}(x)\gamma^\mu\partial_\mu\psi(x) - m\bar{\psi}(x)\psi(x) - \bar{\psi}\gamma^\mu\partial_\mu\Theta(x)\psi \quad (2.1.5)$$

This disturbing term can be canceled by introducing an additional field that should transform like

$$A'_\mu = A_\mu - \frac{1}{e}\partial_\mu\Theta(x) \quad (2.1.6)$$

We can include this field into our Lagrangian by replacing the common derivative by the so called covariant derivative D_μ .

$$D_\mu = \partial_\mu + ieA_\mu \quad (2.1.7)$$

Arriving at the desired local gauge invariance we are left with a new vector field A_μ that we had to introduce. Of course this field has its own free Lagrangian that should not violate gauge invariance. The expression $F_{\mu\nu} = \partial_\mu A_\nu - \partial_\nu A_\mu$ transforms as it should. $A_\mu A^\mu$, corresponding to a mass term according to the Proca Lagrangian for a vector Spin 1 field with mass m , however, does not. The Proca Lagrangian can be written as follows:

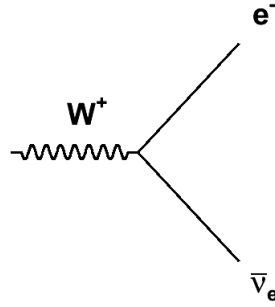


Figure 2.1.2: Example of a charged weak current with the coupling $\frac{-ig_w}{\sqrt{2}}\gamma^\mu\left(\frac{1-\gamma^5}{2}\right)$.

$$\mathcal{L} = -\frac{1}{4}F_{\mu\nu}F^{\mu\nu} + \frac{1}{2}m^2 A_\mu A^\mu - j_\mu A^\mu \quad (2.1.8)$$

Considering Eq. (2.1.8) we see that our spin-1 field has to be massless ($m=0$) since the $A_\mu A^\mu$ dependency, a mass term would bring, destroys the local gauge invariance we demand. Therefore A_μ turns out to be equivalent to the electromagnetic vector potential. Any m different from zero would imply a massive photon with mass m . Indeed the entire electrodynamics emerges by simply demanding local gauge invariance for the Lagrangian of free fermions.

The Strong Interaction Since the focus on this chapter is set on electroweak symmetry breaking the strong interaction will only shortly be described for completeness. A good introduction to the subject can be found in Ref. [4] for example. The strong interaction is (approximately) obeying a non-abelian SU(3) symmetry and is described by Quantum Chromodynamics (QCD) at present. The underlying charge is called color. The strong interaction is mediated by eight gluons which also carry a color charge. The coupling constant of the strong interaction increases with distance, at short ranges it is relatively weak. This effect has the important consequence that no free quarks can be observed in nature. Furthermore, baryons and mesons only exist as color singlets. Gluons, however, have mixed colors which allows a green quark to be changed into a red one, for example, emitting a red-anti-green gluon. Like in QED, for the Lagrangian of QCD local gauge invariance is demanded and the corresponding covariant derivative is

$$D^\mu = \partial^\mu + ig_s \frac{\lambda^a}{2} G_a^\mu(x) \quad (2.1.9)$$

with a running from 1 to 8. This covariant derivative implies the eight gluon fields.

The Weak Interaction and Electroweak Unification A description of the weak interaction is complicated since it is maximally parity-violating (chiral) due to its V-A structure: considering the vertex factor of a charged weak current (e.g. electron - neutrino scattering, Fig. 2.1.2) it turns out to contain both vector and axial vector components. Therefore $\gamma^\mu(1-\gamma^5)$ where γ^μ is a vector and γ^5 is an axial vector is called V-A-form. A definition of the gamma matrices can be

found in Ref. [4]. This addition of a vector and an axial vector leads to a parity violation. Consequently for the transformation behavior of fermions it plays a role whether they are left-handed or right-handed. Left-handed fermions are appearing in duplets building fundamental representations of $SU(2)$, the weak isospin symmetry group. Right-handed particles on the other hand are singlets. Right-handed neutrinos do not exist within the standard model. Performing gauge transformations we get a different transformation behavior for left-handed and for the right handed fields:

$$\begin{pmatrix} \psi_\nu \\ \psi \end{pmatrix}'_L = e^{i\alpha(x)_k * T^k} \begin{pmatrix} \psi_\nu \\ \psi \end{pmatrix}_L \quad (2.1.10)$$

$$\psi'_r = e^{i\alpha(x)*Y} \psi_r \quad (2.1.11)$$

with

$$\begin{pmatrix} \psi_\nu \\ \psi \end{pmatrix}'_L = \frac{1 - \gamma^5}{2} \begin{pmatrix} \psi_\nu \\ \psi \end{pmatrix} \quad \text{and} \quad \psi_r = \frac{1 + \gamma^5}{2} \psi \quad (2.1.12)$$

T_k (with T standing for the weak isospin) are the three generators of the $SU(2)$ symmetry group while the weak hypercharge Y is a generator of the $U(1)$ symmetry group. There is an important relation between weak hypercharge, the third component of the isospin and electric charge:

$$Q = T_3 + \frac{Y}{2} \quad (2.1.13)$$

In electroweak unification the weak hypercharge plays a central role. Therefore the underlying symmetry group of electroweak unification is a non-abelian $SU(2)_L \times U(1)_Y$ group. The $U(1)$ symmetry is closely related to the weak hypercharge, which allows a relation between the electric charge and isospin. Again, in analogy to the QED case, the covariant derivatives for the doublet and the right handed singlets have to be introduced. For the left-handed doublet it can be written as [5]:

$$D_\mu = \partial_\mu - igW_\mu - i\frac{g'}{2}YB_\mu \quad (2.1.14)$$

W_μ is a $SU(2)_L$ matrix field:

$$W_\mu = \frac{T_i}{2} W_\mu^i(x) \quad (2.1.15)$$

For the two right-handed singlets there are two derivatives of the form

$$D_\mu = \partial_\mu - i\frac{g'}{2}YB_\mu \quad (2.1.16)$$

The gauge fields introduced in the previous step result in describing the $W^{+/-}$, Z bosons and the photon. They cannot explain the W and Z mass so far [5, 6]. The weak interaction shows some very characteristic properties:

- It is the only interaction that can take place between different flavors.
- It has a finite range since its gauge bosons have a mass different from zero.
- It violates the CP symmetry that is conserved by all other interactions within the SM.

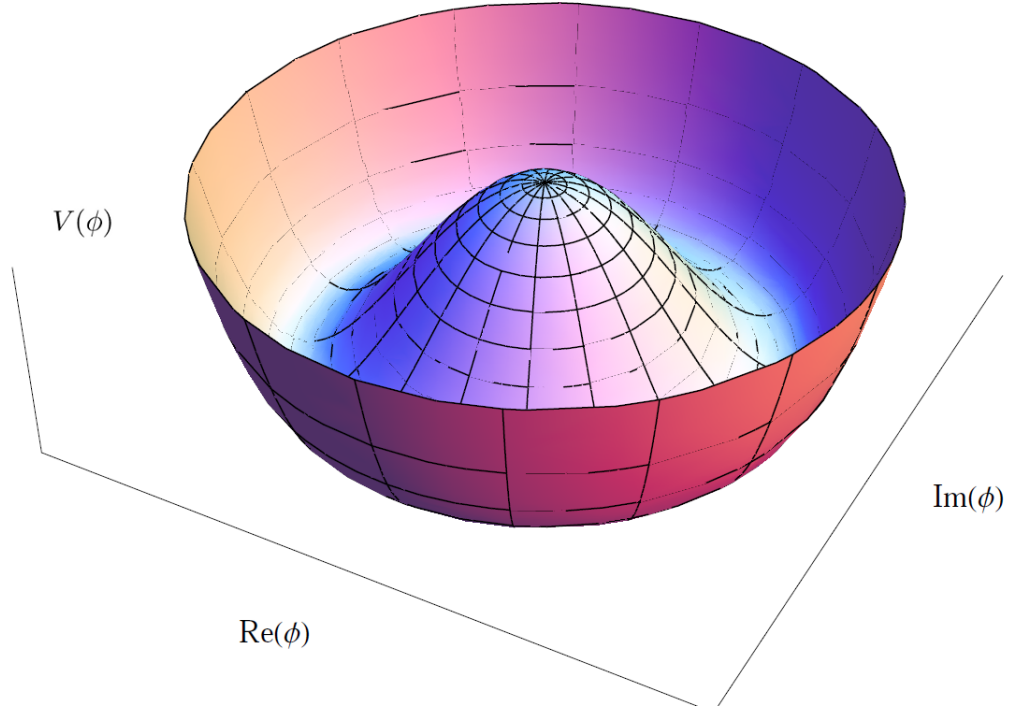


Figure 2.1.3: The potential $V(\phi)$. Because of its characteristic shape it is often called mexican hat potential.

2.1.3 Spontaneous symmetry breaking and the Higgs Mechanism

Electromagnetic and strong interactions can be described well by the concepts presented above since the gauge bosons of these interactions are massless. For weak interaction, however, the situation differs: due to the finite range of this interaction the gauge bosons have a rest mass different from zero which has been confirmed by the experiment. A method was needed to unify this fact with the concept of local gauge invariance. This method is called spontaneous symmetry breaking. It involves the fact that in quantum field theory the quantized fields can be considered to be perturbations, the development of which starts at a ground-state of minimum energy. The Lagrangian of electroweak unification with massless W and Z Bosons has a trivial minimum $\phi_0 = 0$ (ϕ is a complex scalar field in that Lagrangian). Adding the potential

$$V(\phi) = \mu^2 \phi^\dagger \phi + (\phi^\dagger \phi)^2 \quad (2.1.17)$$

to the Lagrangian, the ground or vacuum state changes. If the coefficient $h > 0$ is real and $\mu^2 < 0$ we get a degenerate, continuous ground state with a minimum energy which is itself symmetric:

$$\phi_0 = \sqrt{-\frac{\mu^2}{2h}} e^{i\theta} \quad (2.1.18)$$

However, if we arbitrarily choose a minimum (e.g. $\theta = 0$) for the parametrization of our field the symmetry is broken spontaneously, since the entire system, particle and field is not symmetric any longer. The minima are located on a circle in the complex plane as it is illustrated in Fig. 2.1.3. We can express our complex field by two real fields φ_1 and φ_2 :

$$\phi(x) = \frac{1}{\sqrt{2}} [v + \varphi_1(x) + i\varphi_2(x)] \quad (2.1.19)$$

v is called vacuum expectation value of the Higgs field. It is important to understand that this variable change does not at all change the physics described by the system. However, the shape of the potential changes. For $\mu^2 < 0$, φ_2 corresponds to a massive particle moving along the flat direction of the potential. This fact is a fundamental result about spontaneous symmetry breaking, the so-called Goldstone theorem. If a Lagrangian is invariant under a continuous symmetry group G , but the vacuum is only invariant under a subgroup H of G , then there must exist as many massless spin-0 particles (Goldstone bosons) as broken generators (i.e., generators of G which do not belong to H). To explain the mass of the W and Z boson, one has to make use of the local gauge invariance of the electroweak Lagrangian. Applying a $SU(2)_L \times U(1)_Y$ transformation, the $SU(2)_L$ dependence makes the dependence on $i\theta(x)$ disappear, which corresponds to the massless Goldstone bosons that are generated by the spontaneous symmetry breaking mechanism. Skipping the details which would surpass the scope of this experimental thesis one arrives at a dependence of the vacuum expectation value of the Higgs field [6].

$$m_W = \frac{1}{2}gv, \quad m_Z = \frac{m_W}{\cos(\theta_W)} \quad (2.1.20)$$

g is a constant, defining the strength of the $U(2)_L$ coupling. θ_W stands for the electroweak mixing angle which can be obtained from the experimental values for the W and Z masses:

$$\sin^2 \theta_W = 1 - \frac{m_W^2}{m_Z^2} = 0.223 \quad (2.1.21)$$

The Higgs field corresponds to a new particle, the Higgs boson.

2.1.4 Experimental search of the Higgs boson

The Higgs boson is the only particle, predicted by the Standard Model, that has not been discovered yet. Since the Higgs boson appears in quantum loop corrections of distinct SM processes, an upper limit for its mass range can be determined, which depends on other well measured quantities as e.g. the masses of the weak bosons. The lower limit has been determined by the experiments at LEP and Tevatron. Therefore the most probable mass range for the Higgs boson is $114.4 \text{ GeV} \leq m_H \leq 158 \text{ GeV}$. Furthermore, Tevatron at Fermilab could exclude the Higgs in the range of 158 - 175 GeV [7]. The next paragraphs of this thesis closely follow Ref. [8]. There are various mechanisms to produce the

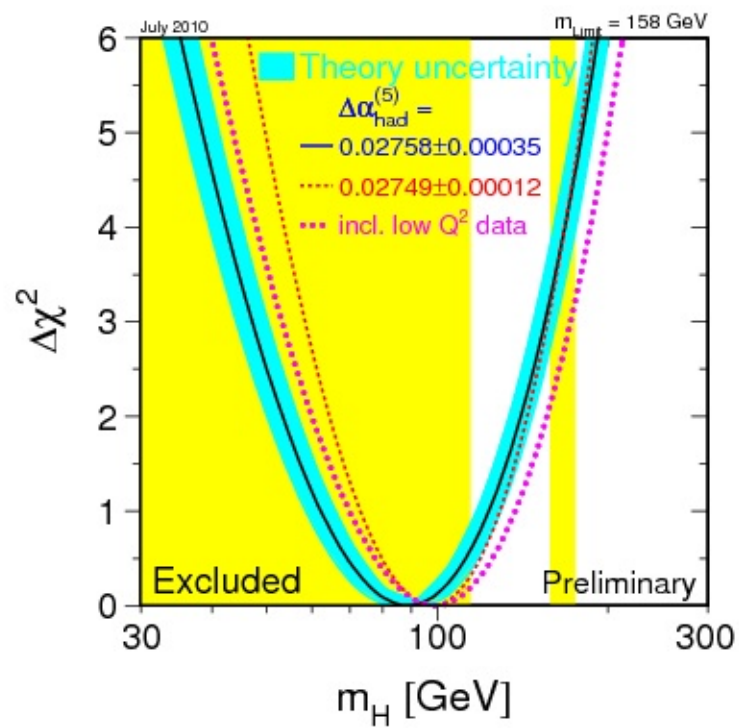


Figure 2.1.4: $\Delta\chi^2$ plotted vs probability. From experimental evidence and this fit it follows that $114.4 \text{ GeV} \leq m_H \leq 158 \text{ GeV}$. Tevatron excluded the Higgs for a mass range from 158 - 175 GeV.

Higgs at LHC. The most important production mechanism is gluon-gluon fusion ($gg \rightarrow H$) with a cross section of 20–40 pb for the most likely range of the Higgs mass from 114–185 GeV. The vector-boson-fusion (VBF) ($qq \rightarrow qqH$), the cross section of which is a factor eight smaller, is another way to produce the Higgs boson. It is accompanied by two jets which mainly are directed in forward direction with a large gap in pseudorapidity in-between in most cases. There are additional ways to produce the Higgs with a lot smaller cross sections. To detect the Higgs boson experimentally its decay channels play a crucial role. It is predicted to decay in many different ways with the branching ratios of the different channels depending on its mass (Fig. 2.1.5). For a very low Higgs mass the decay mode via $b\bar{b}$ is dominant which is not suitable for a discovery unfortunately due to its high QCD backgrounds. Due to extensive Monte Carlo studies performed by the CMS and ATLAS collaborations the best channels for a discovery of the Higgs boson seem to be the following ones:

- The most important channel for a discovery of the Higgs is $H \rightarrow ZZ^* \rightarrow 4l$ which is good for a wide mass range except for $m_H \leq 130$ GeV and $m_H \approx 2m_W$. A dominant background is the ZZ^* continuum containing smaller contributions by $b\bar{b}$ and $t\bar{t}$. Using impact parameters and lepton isolation requirements the latter two can be significantly reduced. The 4μ , $2e2\mu$ and $4e$ final states of ZZ^* decays are often referred to as “golden channels” and should allow a 5σ discovery of the Higgs in a wide range of the allowed mass space with less than 30 fb^{-1} of integrated LHC luminosity.
- A further possibility is the channel $H \rightarrow WW^*$ for the mass range $2m_W \leq m_H \leq 2m_Z$ due to the high branching ratio of this process. It can be used at lower mass ranges (down to 130 GeV) and very high mass ranges at the same time. The two final states, being taken into consideration are: $l\nu l\nu$ and $lvqq$. Because of neutrinos occurring in the final state a complete mass reconstruction is not possible, which leads to complications estimating the background. For the Higgs signal without jets the dominant background is $q\bar{q}, g\bar{g}$ to WW^* . However, this background can be suppressed, considering the spin correlation between the final lepton states. On the other hand, for Higgs to two jets the $t\bar{t}$ production is the main background which can be reduced by “forward jet tagging” and “central jet veto”. According to NLO-level studies less than 2 fb^{-1} integrated luminosity are expected to be sufficient for a 5σ Higgs discovery with $m(H) = 160\text{--}170$ GeV.
- $H \rightarrow \gamma\gamma$ Although this channel has a very small branching ratio of only 0,2 % in a mass region from 120 - 140 GeV it is important since it produces a very clear signal. There are some irreducible backgrounds from diphoton production $gg, qq \rightarrow \gamma\gamma$. Reducible backgrounds are due to γ jet and jet-jet events. For an integrated luminosity of 30 fb^{-1} one can obtain a significance $> 5\sigma$ at the CMS experiment for the mass range of 115–140 GeV.
- The channel $H \rightarrow t\bar{t}$, produced by gluon fusion, is not very promising because of large backgrounds which are hard to reduce.

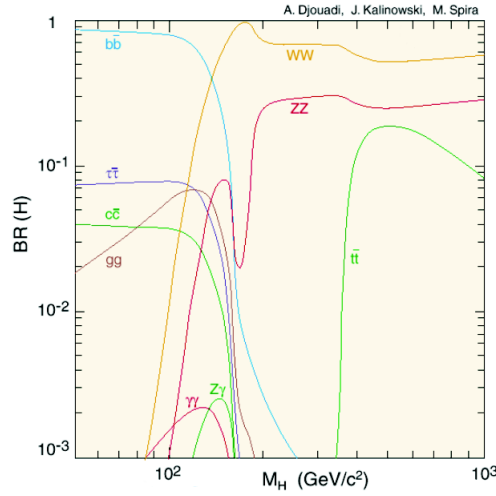


Figure 2.1.5: The branching ratios of the Higgs particle versus its mass.

2.1.5 B-physics and top quarks

Due to the high production rate of B-mesons, precision measurements of their properties will be possible. A investigation of the decay of heavy flavored hardrons is also a way of measuring directly some elements of the Cabibbo-Kobayashi-Maskawa (CKM) matrix, which describes the mixing of quarks in weak interactions:

$$\begin{pmatrix} d' \\ s' \\ b' \end{pmatrix} = \begin{pmatrix} V_{ud} & V_{us} & V_{ub} \\ V_{cd} & V_{cs} & V_{cb} \\ V_{td} & V_{ts} & V_{tb} \end{pmatrix} \begin{pmatrix} d \\ s \\ b \end{pmatrix} \quad (2.1.22)$$

The decay $B_s^0 \rightarrow J/\Psi\phi \rightarrow \mu^- \mu^+ K^+ K^-$ has three final state helicity configurations, the linear combination of which are eigenstates of the CP operator. Measuring three angles and the B_s^0 proper time the weak phase $\delta \equiv \text{Arg}(V_{ub}^* V_{cb} / V_{us}^* V_{cs})$, where V_{ij} are elements of the CKM matrix, and other parameters can be extracted. Therefore a deviation from the Standard Model could be detected if it is existing. A presence of phases in the CKM Matrix which is describing charge changing weak interactions is one possible explanation for CP - violation. Last but not least the LHC produces a huge amount of top quarks and therefore this particle, discovered in 1993 at Tevatron, can be studied in detail (precision measurements of its mass, proper time etc.) Understanding the top quark well can improve the estimations of the background during the search of new physics [9, 10]. Very recently the D0 Collaboration from Fermilab observed a CP violation in $B_s - \bar{B}_s$ meson mixing that significantly exceeds the one predicted by the SM. The deviation from the SM prediction is about 2.9σ . In Ref. [11] it is claimed that this discrepancy could be explained by “uplifted supersymmetry”, which is an adapted version of the Minimal Supersymmetric Standard Model (MSSM) described in the next section.

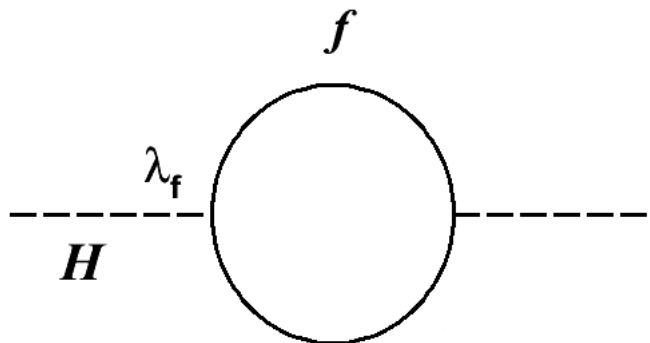


Figure 2.2.1: One loop correction to m_H^2 by the coupling of a fermion to the Higgs field.

2.2 Supersymmetry

2.2.1 Naturalness and the hierarchy problem

The so-called hierarchy problem is closely related to the concept of “naturalness” which was founded by ’t Hooft in 1979 as an order of magnitude restriction for parameters of a theory that has to be valid for all energy scales. According to ’t Hooft’s definition a system is “natural” under the following circumstances: considering the system “at any energy scale μ , a physical parameter or set of parameters $\alpha_i(\mu)$, is allowed to be very small only if the replacement $\alpha_i(\mu) = 0$ would increase the symmetry of the system” [12]. An example to illustrate this principle is the electron mass at an energy scale of 50 MeV. The electron mass at this scale is at the order of magnitude 10^{-5} and therefore can be considered to be small. With respect to the concept of naturalness there is no problem about this since an electron mass of 0 would lead to an additional chiral symmetry in order to have a separate conservation of left handed and right handed leptons. Therefore the small electron mass is natural according to the definition from above. “Unnaturalness” on the other hand occurs whenever fundamental scalars (scalar particles that are not composite) are present in a theory. The Higgs mass squared m_H^2 can be considered to be such a fundamental scalar of the electroweak Lagrangian that is small at energy scales $\mu \gg m_H$. According to naturalness a new symmetry should emerge for the limit $m_H \rightarrow 0$. This is not the case within known concepts for some theoretical reasons explained in Ref. [12]. Assuming that the Standard Model is a good theory beyond the electroweak scale, let us say until the Planck scale for example where gravitation starts to play a role, the Higgs mass gets increasingly unnatural, since it is small compared to the considered energy scale due to reasons that have been described in the section about the SM. On the other hand the square of the Higgs mass m_H^2 receives quantum corrections by every particle that couples to the Higgs field. The coupling of a fermion (Fig. 2.2.1) for example leads to a contribution of

$$\Delta m_H^2 = -\frac{|\lambda_f|^2}{8\pi^2} \Lambda_{UV}^2 \quad (2.2.1)$$

Λ_{UV} , called ultraviolet momentum cutoff regulates the loop integral. It cuts it off at energy scales at which we expect the SM no longer to be a proper theory. This is certainly valid for the Planck scale but probably already much below. Taking into account that m_H is expected to be about 150 GeV, m_H^2 should be roughly in the order of magnitude of $(100 \text{ GeV})^2$. However, considering a cut-off in the region of the Planck scale and comparing m_H^2 with its quantum correction there is a discrepancy of about 30 orders of magnitude, which is basically the essence of the hierarchy problem. To get rid of this ugly discrepancy rigorous fine tuning or new concepts are needed. Within the SM only the Higgs boson is affected by this problem since the corrections to fermions and gauge bosons do not have a quadratic sensitivity to λ . There are several ways to escape from this dilemma, two of which are:

1. To assume that the Higgs boson is not a fundamental scalar and therefore composite. This would allow a cutoff in the region of TeV and therefore no hierarchy problem emerges.
2. A second, with respect to naturalness much more promising one is the following: One could assume that there is an unknown approximate symmetry that is responsible for the small Higgs mass and leads to contributions to the loop integral that more or less cancel the terms that boost m_H^2 .

This postulated, fundamental symmetry is called Supersymmetry (SUSY) and will be described in this section. Supersymmetry introduces a bosonic superpartner for each fermion (and vice versa) that leads to a contribution to the quantum correction of each fermion which exactly cancels the quadratic terms. Therefore only a term that is logarithmic in lambda remains as leading contribution:

$$m_H^2 \cong (m_H^0)^2 - \frac{1}{16\pi^2} (m_b^2 - m_f^2) \ln\left(\frac{\lambda}{m_f}\right) + \dots \quad (2.2.2)$$

The couplings of fermions and their superpartners are assumed to be the same in this equation: $\lambda = \lambda_f = \lambda_b$. Because of the logarithmic dependency the quantum corrections stay reasonable even for very big lambdas, however, the masses of the supersymmetric partners cannot exceed the TeV scale too far because that again would boost the quantum corrections to m_H^2 . If SUSY were an exact symmetry (e.g. mass of fermion = mass of the supersymmetric partner) even the contribution to the quantum correction, that is logarithmic in λ would vanish [13, 14, 15].

2.2.2 Supersymmetric particles

Supersymmetry is one possible extension of the Standard Model that was introduced to solve the hierarchy problem as described in the previous section. Moreover, SUSY particle content has also particles that could be a candidate for dark matter (Table 2.2). The basic idea is to attribute a fermionic superpartner to each boson and the other way round which are differing by spin 1/2. Consequently fermionic states are related to bosonic states by a symmetry transformation and the other way round. However, SUSY cannot be an exact symmetry since the superpartners would already have been discovered in that case since a particle and its superpartner would have exactly the same mass.

The coupling lambda of particles and superpartners is required to be identical. The Lagrangian can be split up in a part conserving supersymmetry \mathcal{L}_{SUSY} and another part, \mathcal{L}_{SOFT} , which is breaking supersymmetry.

$$\mathcal{L} = \mathcal{L}_{SUSY} + \mathcal{L}_{SOFT} \quad (2.2.3)$$

\mathcal{L}_{SOFT} only contains mass terms therefore the masses of the supersymmetric particles emerge from supersymmetry breaking.

2.2.3 R-Parity

The weak scale superpartners, which solve the SM hierarchy problem, have the side effect of violating the conservation of baryon and lepton numbers. The decay of a proton to a π^0 and e^- , which has not been detected so far, could be mediated by a squark. To get rid of this process one can introduce a new conserved quantity, the so called R-Parity:

$$R \equiv (-1)^{3B+L+2S} \quad (2.2.4)$$

B stands for baryon number, L for lepton number and S for spin. For all SM particles $R = 1$, for the superpartners $R = -1$. A very important consequence of R-Parity conservation is the stability of the lightest supersymmetric particles which cannot decay to SM particles [16].

2.2.4 Supersymmetry, Dark Energy and Dark Matter

The lightest neutral supersymmetric particle is a promising candidate for cold dark matter. In order to give mass to all fermions supersymmetric theories require two Higgs doublets: H_u which gives mass to all up-type fermions and H_d which is responsible for the masses of down-type fermions. These two Higgs bosons have a supersymmetric partner with spin 1/2 called Higgsino. Also for each SM neutrino there is a superpartner with spin 0, called sneutrino. Furthermore one is expecting a spin 3/2 gravitino, the fermionic superpartner of the graviton, which is considered to be a quantized gravitational wave. The fact that the graviton should have spin 2 is a consequence of General Relativity since there is an analogy between a particle of spin 2 and gravitational waves in linearized gravity, a linear approximation of the Einstein equation. The spin 1/2 bino and the neutral wino are the superpartners of the gauge fields B and W in electroweak unification that appeared in the previous section. Supersymmetry cannot be considered a good candidate to explain dark energy. Although SUSY breaking contributes to the energy density of the vacuum and therefore can reduce the fine tuning in the cosmological constant from 1 part in 120 to 1 part in 90 this is not sufficient to explain dark energy. To solve this problem a different approach is required [17, 16].

2.2.5 The MSSM and mSUGRA

The Minimal Supersymmetric Standard Model only extends the SM particle content at a minimal level. However, this theory introduces a large number of free parameters, since the mechanism of SUSY breaking is not known and therefore

Spin	U(1)	SU(2)	Downtype	Up-type	
2					Graviton
3/2					Gravitino
1	B	W_0			
1/2	Bino	Wino	Higgsino	Higgsino	Neutrino
0			H_d	H_u	Sneutrino

Table 2.2: The supersymmetric partners of neutral particles are considered to be candidates for dark matter [16].

is difficult to deal with. A version with only five free parameters at Grand Unification scale that induces electroweak symmetry breaking radiatively is called mSUGRA (which stands for Minimal Super Gravity). The free parameters are

- a universal scalar mass m_0
- a universal gaugino mass $m_{1/2}$
- a universal trilinear coupling A_0
- the Higgs vacuum expectation values $\tan(\beta)$
- the sign of the Higgsino mass mixing parameter μ

The mass parameters of the gauginos and the sfermions can be written as linear combinations of these free parameters. According to Eq. (2.2.5) the gluino mass cannot be much bigger than the squark mass:

$$M_{\tilde{g}} \lesssim 1.2m_{\tilde{q}} \quad (2.2.5)$$

The most promising way to discover SUSY is via missing energy and jets. If squarks and gluinos are existing and the phase-space allows it, high production rates are expected. The two lightest neutralinos $\tilde{\chi}_1^0$ and $\tilde{\chi}_2^0$ in mSUGRA show five main decay modes each, where the $\tilde{\chi}_2^0$ should produce a very clear signature that can be observed in inclusive searches [18, 19].

2.3 Beyond the Standard Model and Supersymmetry

There is a wide range of theoretical approaches extending the Standard Model and SUSY some of which will be presented in brief in the following section. A summary and references on theoretical approaches like New Vector Boson High Mass states or Heavy Majorana Neutrinos and right-handed bosons, not described here can be found in Ref. [19].

2.3.1 The Little Higgs Model of electroweak symmetry breaking

In contrast to the symmetry breaking mechanism of the SM the Little Higgs Model proposes a symmetry breaking mechanism that breaks a global (in contrast to a local in the SM) symmetry spontaneously. The light Higgs boson of

this theory is kept free from one-loop divergences that required an extension of the SM with supersymmetric particle content. However, by this process new heavy particles are introduced the lightest of which is a heavy quark singlet-state with charge $2/3$ called T . Its most important decay modes are:

$$T \longrightarrow th \quad (2.3.1)$$

$$T \longrightarrow tZ \quad (2.3.2)$$

$$T \longrightarrow bW \quad (2.3.3)$$

The channel $T \longrightarrow tZ$ is expected to provide a very clear signal.

2.3.2 Extra Dimensions and Black Holes

A good overview on this subject can be found in Refs. [20, 21, 19]. What follows is a summary of the concepts that are presented there in much more detail. Since 1914 there have been several approaches of unifying the fundamental forces by introducing spatial extra dimensions. Furthermore, extra dimensions at the TeV scale could provide a solution to the hierarchy problem and therefore they are an interesting topic of research. There are several competing concepts of extra dimensions providing distinct experimental signatures.

Large extra dimensions The so-called ADD model [21] introduces a certain number δ of extra dimensions which are all of the same scale in order to solve the hierarchy problem of the SM. It is assumed that gravitons can move freely through a $4+\delta$ dimensional world while the Standard Model particles are confined to the ordinary 4-dimensional spacetime, called “braneworld”. The extra dimensions are assumed to be compactified over a torus with radius R . For the Planck mass the theory arrives at the expression:

$$M_{Pl}^2 \approx R^\delta M_D^{\delta+2} \quad (2.3.4)$$

M_D stands for the quantum gravity scale of a theory with higher dimensions. One possible way of detection of ADD is the process of direct graviton emission which is accompanied by a jet or a photon like

$$q\bar{q} \longrightarrow G\gamma, \quad q\bar{q} \longrightarrow Gj \quad (2.3.5)$$

The graviton would appear as missing traverse energy since its coupling to matter in the Standard Model world is very weak. An interesting consequence of the ADD model is the existence of microscopic black holes. For a center of mass energy $\sqrt{s} \gg M_D$ a classical description of gravity could dominate over quantum description, a fact that could allow black holes. The Schwarzschild radius R_s of such a system could be larger than the one of an “ordinary” black hole due to its $4+\delta$ dimensionness. The produced black holes will evaporate immediately due to emission of thermal radiation (with an average lifetime of 10^{-26} to 10^{-27} seconds). The evaporation of such a black hole should produce spectacular events with a high total energy producing a bunch of SM particles being distributed in all directions of space.

Warped extra dimensions Warped extra dimensions are another approach to solve the SM hierarchy problem introducing a 5th dimension which is highly curved. The fifth dimension consists of two branes: the ultraviolet brane, where the graviton function has a peak, and a red-shifted ultraviolet brane. There are two decay-channels of the graviton in this model:

$$G \longrightarrow ee \quad (2.3.6)$$

$$G \longrightarrow \mu\mu \quad (2.3.7)$$

Universal extra dimensions The concept of universal extra-dimensions (UED) also allows SM particles to propagate in a bulk of extra-dimensions. The extra-dimensional momentum conservation leads to a new discrete symmetry called Kaluza-Klein (KK) parity. There is a mechanism that allows the pair production of first KK-excitations, the lightest state of which is predicted to be stable and therefore could be a candidate for dark-matter. KK-excitations are possible for all SM particles which propagate along extra dimensions. These excitations can have a mass depending on the compactification radius R^{-1} , a higher dimensional mass M_0 and the excitation mode m [22]. The compactification radius R^{-1} for these extra dimensions which describes their size is a free parameter. The remaining two free parameters of this model are ΔR , which is the number of KK levels present in the theory and m_H , which is a parameter of the Higgs sector without influence on the KK masses, apart from KK partners of the Higgs particles. At CMS the discovery potential has been investigated for four values of R^{-1} considering the final states 4μ , $4e$ and $2\mu 2e$, shown in Fig. 2.3.1. For a given R^{-1} the highest significance values are obtained by the muon channels.

2.3.3 Technicolor

Another alternative to the SM Higgs mechanism is Technicolor (TC) which introduces a new strong interaction that shows a similar dynamical behavior as spontaneous symmetry breaking. Technicolor introduces a new class of particles, the so-called technifermions at an energy scale that is similar to the weak scale and behaves like a QCD like force. Technifermion doublet states can condensate, producing pseudo-Goldstone bosons and a wide range of excited Technimesons. Furthermore, there is a color singlet sector including a TC pion, the π_{TC} with spin 0 and TC mesons with spin 1 like the ρ_{TC} and ω_{TC} . For the search for Technicolor the channel

$$\rho_{TC} \longrightarrow W + Z \quad (2.3.8)$$

is of particular interest since it has a final state of $3l + \nu$ that can be clearly distinguished from the background. The background consists of Standard Model processes which are involving W and Z bosons. The channel

$$\rho_{TC} \longrightarrow \pi_{TC} + W \quad (2.3.9)$$

is much harder to distinguish from the Standard Model background.

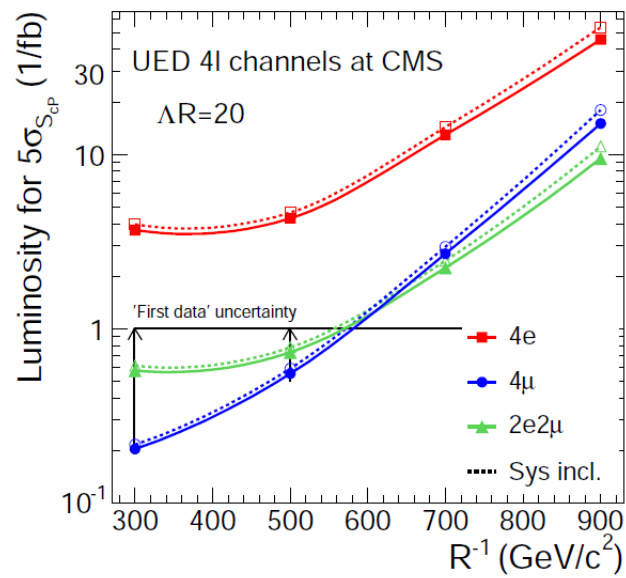


Figure 2.3.1: Discovery potential of universal extra-dimensions at CMS with the dotted lines showing the influence of experimental uncertainties [21].

Chapter 3

Experiments at the Large Hadron Collider

3.1 The LHC - Characteristics and parameters

The Large Hadron Collider (LHC) in Geneva is the most powerful particle accelerator that has been built so far. It will produce proton-proton or heavy ion collisions. The circular accelerator is installed in a tunnel with 27.6 km circumference, located on average 100 m below the surface. Along this ring there are four interaction points, where the counter-rotating beams can be brought to collision and the four LHC experiments are situated. At nominal design values, for proton-proton run the LHC can achieve center of mass energies of 14 TeV (7 TeV in each direction). For Pb-Pb collisions there will be a center of mass energy of $2 * 2,76$ TeV per nucleon available. However, until end of 2011 the LHC will only be operated at 7 TeV. For particle accelerators the luminosity plays a crucial role because it is closely related to the rate of interactions. If the interacting beams have a cross section σ , the reaction rate (number of collisions per unit time) is given by

$$N = \mathcal{L} * \sigma \quad (3.1.1)$$

where \mathcal{L} is called luminosity. According to Ref. [23] for LHC the luminosity is given by the expression:

$$\mathcal{L} = \frac{\gamma}{4\pi\beta^*} \frac{k}{k_0} \frac{N}{\varepsilon_n} \frac{N}{\Delta t} F_\phi \quad (3.1.2)$$

with N being the number of particles per bunch, Δt standing for the bunch interval and k standing for the number of bunches. ε_n stands for the normalized beam emittance. F_ϕ is a rather small correction factor due to the finite crossing angle ϕ were σ_x and σ_y are the rms lengths and widths of the bunches:

$$F_\phi = \frac{1}{\sqrt{1 + \left(\frac{\phi\sigma_x}{2\sigma_y}\right)^2}}$$

Number of bunches per beam	No	2808
Number of particles per bunch	k	$1.15 \cdot 10^{11}$
Bunch Occupation	k/k_0	0.797
Revolution Frequency	f	11.25 kHz
Bunch Interval	Δt	25 ns
γ		7463
Normalised Emittance	ε_n	$3.75 \mu\text{m}$
Crossing Angle	ϕ	$285 \mu\text{rad}$
rms Bunch Width	σ_x	$17 \mu\text{m}$
rms Bunch Length	σ_y	7.55 cm
beta at interaction point	β^*	0.55

Table 3.1: Parameters influencing the LHC luminosity [23, 24].

The LHC can provide luminosities of up to $10^{34} \text{ cm}^{-2} \text{ s}^{-1}$ which is about 10^2 larger than those achieved by Tevatron at Fermilab. Introducing the LHC parameters from Table 3.1 into the formula from above, this design luminosity can easily be obtained. Before a bunch enters the LHC, it has to undergo a series of pre-accelerators, starting with the LINAC 2 which reaches an energy of 50 MeV. The next step is the Proton Synchrotron Booster (PSB) which reaches 1.4 GeV. The PSB is followed by the Proton Synchrotron (PS), the oldest accelerator at CERN that is still operating, which accelerates the bunches to 26 GeV and injects them to the Super Proton Synchrotron (SPS) which reaches 450 GeV and is the last instance before the LHC. Figure 3.1.1 shows the CERN accelerator complex in detail. The SPS was the first collider that brought protons and anti-protons to collision. At the two SPS experiments UA 1 and UA 2 the W and Z bosons were discovered in 1983.

3.2 Summary of the different experiments and their goals

To have a wide range of experimental possibilities the LHC is equipped with four different experiments (Fig. 3.2.1), two of which (ATLAS and CMS) were designed as general purpose experiments. The other two pursue different, more specific goals.

ALICE (A Large Ion Collider Experiment)

Quantum Chromodynamics, the theory of the strong interaction, predicts a state of matter which is called “Quark Gluon Plasma”. It is assumed that the universe experienced this state for a very short time immediately after the Big Bang. Due to confinement this state, where quarks and gluons are considered to be asymptotically free, is very short lived. However, the deconfined state is a crucial prediction of QCD and therefore worth investigation. The ALICE detector is optimized to investigate leptons, hadrons and photons that are produced in the collision of heavy nuclei. The central feature of the detector is its huge time projection chamber with a diameter of about 5 meters.

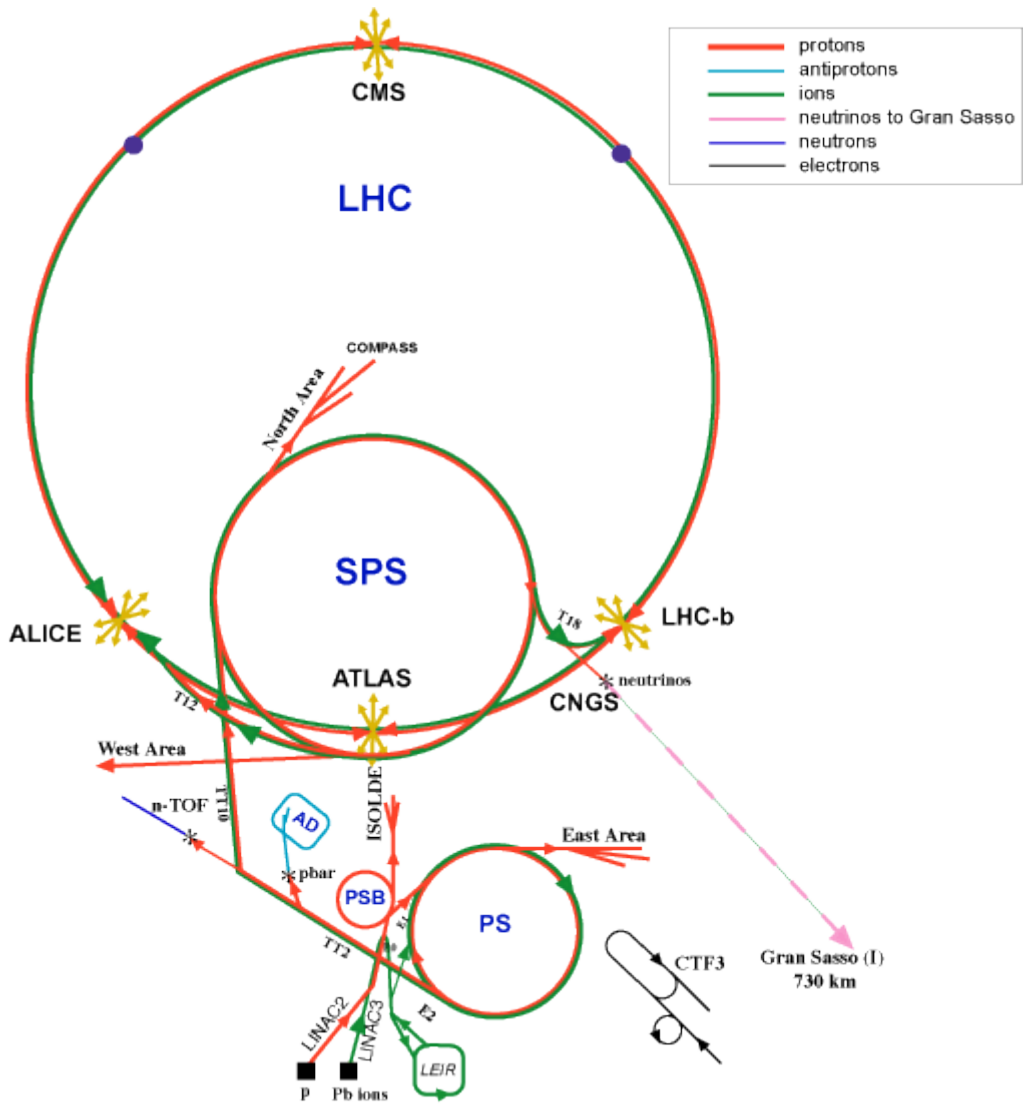


Figure 3.1.1: The CERN accelerator complex. (©CERN 2007)

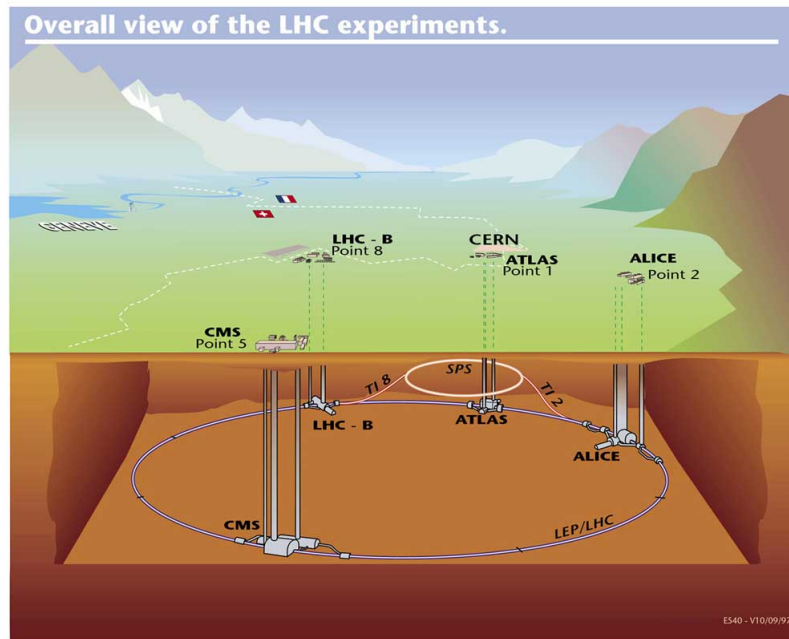


Figure 3.2.1: The Large Hadron Collider with its four experiments.

ATLAS

ATLAS, like CMS, is one of the two general purpose experiments, built to hunt the Higgs boson and discover new physics. Considering its diameter, it is the biggest LHC experiment. Its principal feature is the toroidal magnetic field.

LHCb

The purpose of LHCb is a detailed study of CP violation, investigating the decays of b-mesons (particles that contain b-quarks and anti b-quarks). Hints to an answer to the profound question why matter is dominant over antimatter in the universe are expected. Compared to the other experiments at the LHC, the LHCb detector was constructed asymmetrically and measurements only take place in forward direction. This design was chosen due to the fact that b-mesons, which have a relatively small mass compared to the total energies of the collisions at LHC, are traveling mostly in forward direction.

CMS

The Compact Muon Solenoid experiment is more compact than ATLAS and its key feature is the 4 Tesla solenoid magnetic field created by a single magnet. This strong magnetic field allows a very compact design of the muon spectrometer with a very good momentum resolution. The structure and properties of the CMS experiment will be described in more detail in the following chapters of this thesis.

Chapter 4

The Compact Muon Solenoid Detector

The CMS experiment was designed as a general-purpose detector. A summary of the CMS physics requirements to fully exploit the potential of the LHC is given in Ref. [25]:

- A central role is played by good muon identification and momentum resolution. The momentum resolution should be about 1% at 100 GeV and it should be possible to determine the charge of muons for momenta below 1 TeV unambiguously.
- The inner tracker should provide a good momentum resolution for charged particles.
- Furthermore, a good di-photon and di-electron mass resolution (also 1% at 1 GeV) with a wide geometric coverage, combined with good π_0 rejection and photon and lepton isolation is needed.
- CMS also has to provide a good resolution for missing transverse energy.
- A robust, flexible and efficient trigger system is required.

Due to these physics requirements, a strong magnetic field is needed to achieve a good energy and momentum resolution for charged tracks and muons. This 4 Tesla magnetic field is generated by a superconducting solenoid, which forms the core of the CMS detector. Its field configuration was optimized for the momentum measurement of muons produced in the collisions at LHC which requires a large bending power. The inner region of the detector (within the magnet) serves to identify photons, electrons and jets while muons are measured in both the inner and the outer regions of the detector, where the return field is strong enough to saturate 1,5 meters of iron which is interrupted by muon stations. The strength of the return-field is 2 Tesla. Four muon stations were integrated in the return yoke to provide a full geometric coverage. They consist of Drift Tubes (DT) in the barrel region, Resistive Plate Chambers (RPC) in the barrel and endcap regions and Cathode Stripe Chambers (CSC) in the endcap region. The inner tracker and the electromagnetic calorimeter are placed inside of the superconducting solenoid which has a inner diameter of 6 meters. The

electromagnetic calorimeter uses lead tungstate crystals (PbWO₄). In the barrel region there are avalanche photodiodes (APDs) to detect scintillation light which are combined with vacuum phototriodes in the endcap region. Muons can be detected in both the inner tracker and in the muon system, which improves the total resolution of their momentum. They are traveling through the detector on a helix-curve due to the opposite direction of the magnetic field in the return yoke with respect to the central field. To deal with the huge amount of data produced in each LHC collision, the CMS experiment is equipped with a powerful trigger system which will be described in Chapter 5. The rest of this chapter will mainly focus on the detector itself.

4.1 The CMS coordinate frame

The coordinate frame of the CMS experiment, valid for all sub-detectors and the trigger, is defined as follows [26]:

- The origin is the CMS collision point
- x: horizontal axis of the coordinate frame which is pointing towards the LHC center (southwards), CMS being located in the north of the LHC center
- y: the vertical axis which is pointing upwards
- z: points westwards in beam direction and is aligned parallel to the magnetic field of CMS
- ϕ is zero in the x-axis and 90 degrees in the y-axis
- The pseudorapidity η is zero in the x-y plane and infinity on the z-axis

The pseudorapidity η approximates the rapidity from special relativity for particles with unknown mass and momentum. The rapidity of a particle is defined as

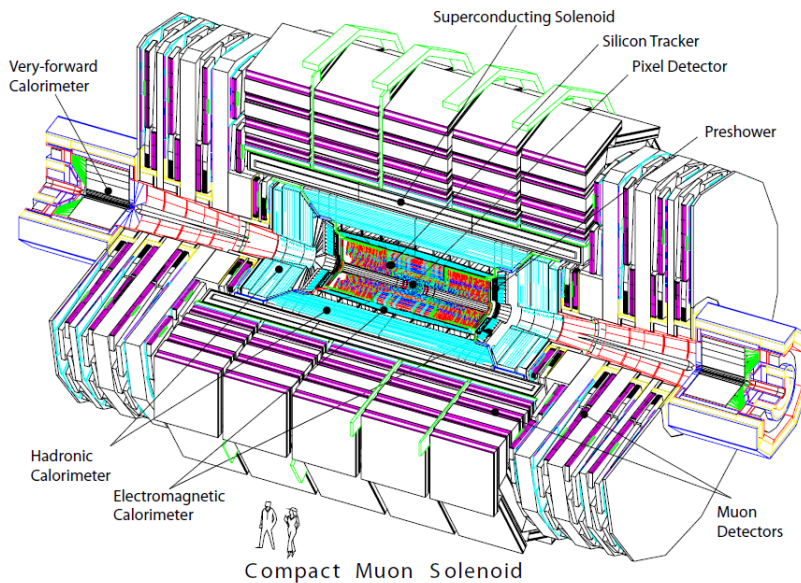
$$\tanh(y) = \frac{p_L}{E} \quad (4.1.1)$$

where p_L is the longitudinal momentum of the incident particle and E is the energy. An advantage of the rapidity compared to velocity is that rapidity values are easier to add since they are scalars and their differences are Lorentz invariant. The pseudorapidity can be defined as

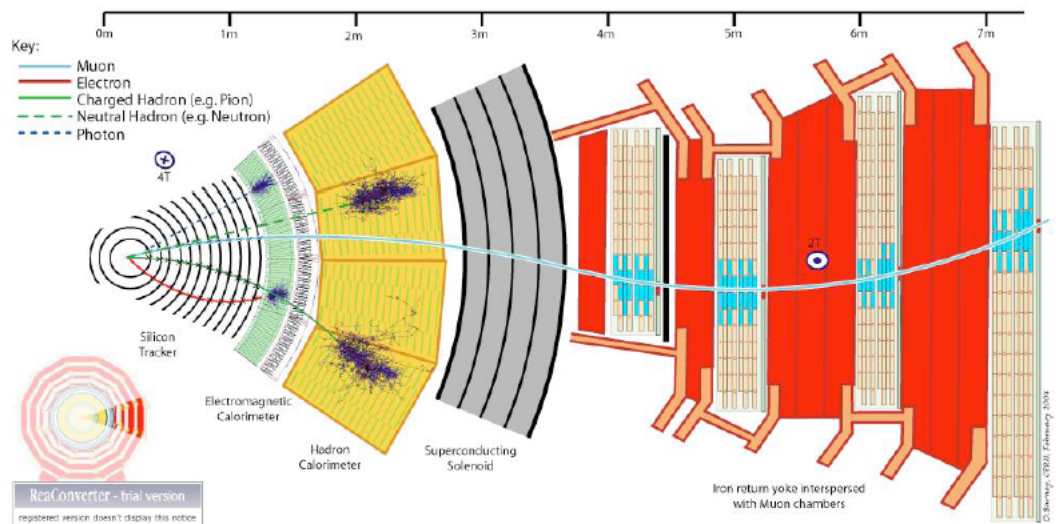
$$\eta = -\ln \tan \frac{\theta}{2} \quad (4.1.2)$$

θ is the polar angle of the considered particle relative to the beam. For high energies rapidity and pseudorapidity converge. It is convenient to consider the rapidity instead of the the polar angle θ as coordinate because the particle production can more or less be considered as a constant function of rapidity.

Figure 4.0.1: Design of the CMS detector [25].



Compact Muon Solenoid
(a) Scheme of the CMS detector.



(b) A slice of the CMS detector with a muon bend in both the calorimeter and muon system. Furthermore, an electron and a photon are seen in the electromagnetic calorimeter, while hadron showers are observed in the hadronic calorimeter.

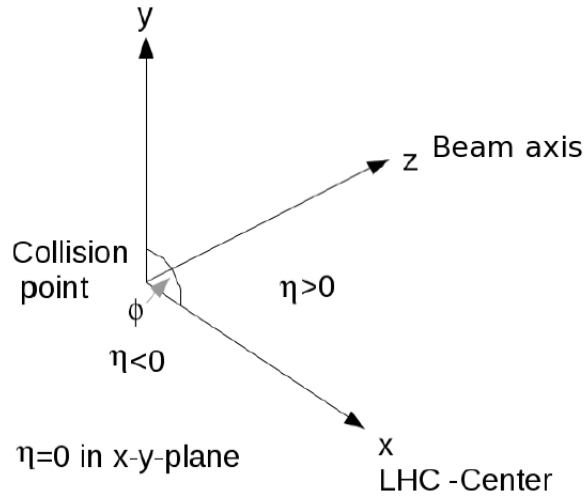


Figure 4.1.1: The CMS reference frame.

Length	12.5 m
Cold bore diameter	6.3 m
magnetic induction	4 T
Total Ampere-turns	41.7 MA-turns
Nominal current	19.14 kA
Inductance	14.2 H
Stored energy	2.6 GJ

Table 4.1: Parameters of the superconducting solenoid of the CMS experiment [25].

4.2 The Superconducting Solenoid

Compared to the magnets from previous high-energy physics experiments, the CMS solenoid provides three innovative features: due to the high number of ampere-turns required to produce a field of 4 T the winding consists of four layers instead of one to two that have been used at previous experiments (e.g. Aleph or DELPHI at LEP). Furthermore the conductor is made from a Rutherford-type cable co-extruded with pure aluminum and mechanically reinforced with an aluminum alloy. Its dimensions are much larger than those of the magnets of former experiments. Table 3 gives an overview of its general parameters [25].

4.3 The Tracking System

The CMS experiment is equipped with an inner tracking system, which allows the precise measurement of track parameters of charged particles and the identification of primary and secondary vertices. It has a length of 5.8 meters and a

diameter of 2.5 meters and surrounds the interaction point. When the LHC is operating at its design luminosity of $10^{34} \text{ cm}^{-2}\text{s}^{-1}$ there will be on average 1000 charged particles at each bunch crossing (i.e. every 25 ns) that are produced by more than 20 proton-proton collisions. Due to this large number of tracks a detector technology with high granularity and fast response is needed in order to attribute the tracks to the correct bunch crossing. To achieve this goal a high power density of on-detector electronics is needed, which requires an efficient cooling. On the other hand, the amount of material in the tracker should be kept to a minimum in order to minimize such effects as multiple scattering, bremsstrahlung, photon conversion or nuclear reactions. A compromise between these two requirements had to be found. Due to the intense particle flux also radiation damage has to be taken into account. These requirements led to a concept of a tracker design entirely based on silicon detector technology. The tracker is composed of a pixel detector and a silicon strip detector.

- The pixel detector consists of the barrel layers of radii 4.4 cm and 10.2 cm. It is the part of the tracking system that is placed closest to the interaction point. The endcaps of this system consist of two disks. The area covered in total by the pixel detector is 1 m^2 .
- The silicon strip tracker has 10 barrel detection layers which extend outwards up to a radius of 1.1 m.

The tracker has 48 million pixels in the barrel region and about 18 million pixels in the endcaps. Figure 4.3.1 gives insight into the architecture of the CMS tracker. The Tracker Inner Barrel and Disks (TIB/TID) are able to pursue up to four r - ϕ measurements using $320 \mu\text{m}$ thick silicon micro-strip sensors with strips parallel to the beam axis in the TIB and radial in the TID. At each of the two edges of each TIB three TIDs are attached. The Tracker Outer Barrel (TOB), surrounding the TIBs and TIDs has an outer radius of 116 cm and consists of six barrel layers in total. It performs another six r - ϕ measurements which have a single point resolution of $53 \mu\text{m}$ and $35 \mu\text{m}$ since it uses two different types of sensors with different resistivity. The Tracker Endcaps (TEC+, TEC- where the sign corresponds to the position with respect to the z -axis) cover a z range of $\pm 118 \text{ cm}$ and regions of $124 \text{ cm} < |z| < 282 \text{ cm}$ and $22.5 \text{ cm} < |r| < 113.5 \text{ cm}$. They are composed of nine disks each and perform up to nine ϕ measurements per trajectory which increase the acceptance of the tracker up to a pseudorapidity of $|\eta| < 2.5$ [25, 27, 28].

4.4 The CMS Calorimeters

Calorimeters at CMS are used to measure the energies of both electrically neutral and charged particles. While electrons, positrons and photons lose their energy already in the innermost part of the calorimeter, the electromagnetic calorimeter, hadronic jets are detected in the hadronic calorimeter which is located in the outer region.

4.4.1 The Electromagnetic Calorimeter

One of the most important criteria for the construction of the CMS Electromagnetic Calorimeter (ECAL) was the predicted decay of the Higgs boson into two

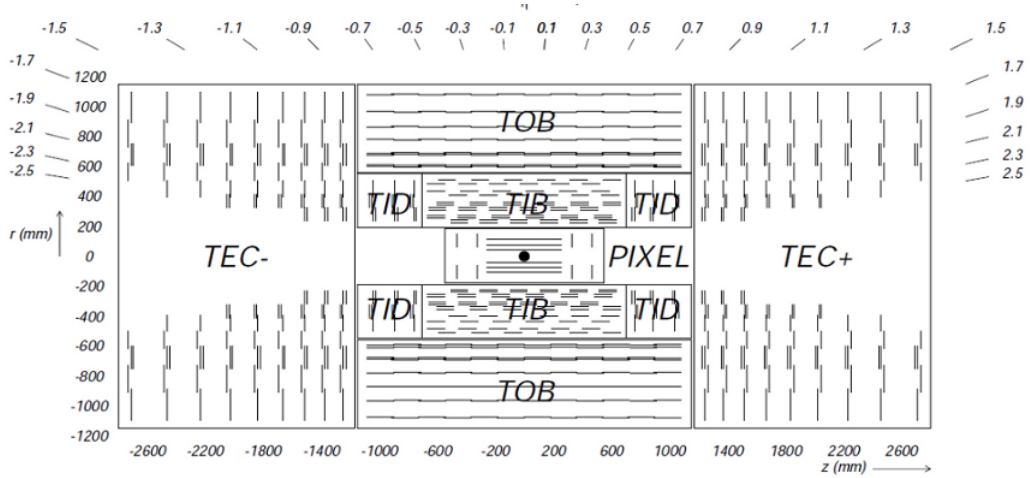


Figure 4.3.1: Schematics of the CMS tracker where each line represents a detector module.

photons. This decay produces a sharp peak over the background for a Higgs mass up to 140 GeV and requires a high resolution energy measurement, good angular precision and also a good pion/photon separation. The ECAL consists of a barrel section and two endcaps and is located between the outer Tracker and the Hadronic Calorimeter. In front of the endcaps a preshower detector is installed. The barrel section counts 61200 lead tungstate ($PbWO_4$) crystals while each endcap has 7324 crystals. Lead tungstate crystals were chosen for several reasons. They have high density (8.28 g/cm^3), short radiation length (0.89 cm) and a small Moliere radius (2.2 cm). Another important advantage is their fast scintillation decay time, which is of the order of magnitude of a LHC bunch crossing: they emit about 80% of their scintillation light within 25 ns. Their relatively low light output depends on the temperature, while their spectrum shows a broad maximum at 420 - 430 nm. The light emitted is collected by Avalanche photodiodes (APDs) in the barrel section and vacuum phototriodes (VPTs) in the endcaps. The barrel part of the ECAL (EB) covers a pseudorapidity range of $|\eta| < 1.479$ and is roughly 6 m long. The crystals in the barrels show a tapered shape and are slightly varying with position in η . The endcaps (EE) cover an η range of $1.479 < |\eta| < 3.0$ and the distance between the interaction point and the endcap is 315.4 cm. A shift towards the interaction point of 1.6 cm when the 4 T field is switched on has to be taken into account. Each endcap is divided in two halves, so-called Dees each of which contains 3 662 crystals which are structured in 138 standard SCs which are arranged in a x-y grid and 18 special partial supercrystals. Since the number of scintillation photons emitted and the amplification are both temperature dependent, the operation temperature of the entire system has to be kept constant (at nominally 291 K). Also the nominal temperature of the CMS ECAL is 291 K [29, 30, 25].

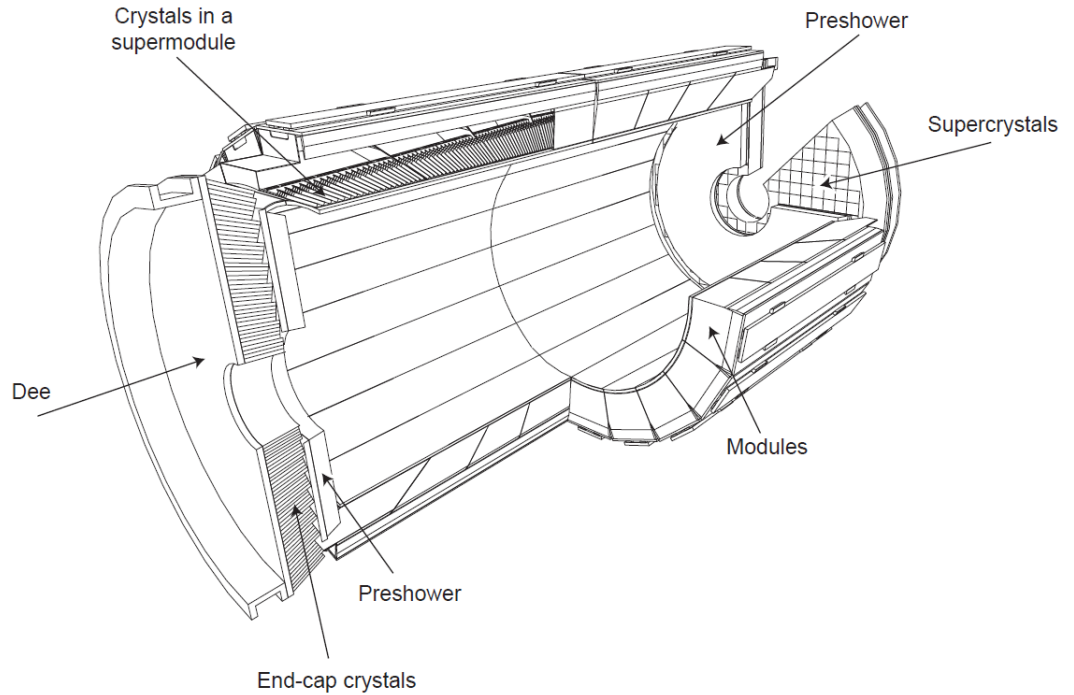


Figure 4.4.1: Schematics of the electromagnetic calorimeter at CMS.

4.4.2 The Hadron Calorimeter

The Hadron Calorimeter (HCAL) [31, 32] was optimized to study hadronic jets, to detect missing transverse energy that could come from ν or heavy exotic particles as predicted by SUSY for example. As the ECAL and Tracker, the HCAL barrel (HB) is placed inside the superconducting solenoid between the ECAL and the inner edge of the magnetic coil ($1.77 \text{ m} < R < 2.95 \text{ m}$). An outer hadron calorimeter was also installed outside the solenoid which completes the barrel calorimeter as can be seen in Fig. 4.4.2. The dotted line in this figure represents the η coordinate of the detector. Beyond $\eta = 3$ the forward hadron calorimeters with a distance of 11.2 meters from the interaction point extend the range of coverage. They use a Cherenkov-based, radiation-hard technology. Altogether the CMS hadron calorimeter covers an η range up to $|\eta| = 5.2$.

The hadronic barrel detector (HB) The HB is divided in two half sections and covers an η range of $0 < |\eta| < 1.3$. In total the HB consists of 36 identical independent units called wedges which are located in azimuthal direction. Each wedge consists of four ϕ sectors (also azimuthal). The scintillator in use is divided into 16 η segments which gives a total segmentation $(\Delta\eta, \Delta\phi) = (0.087, 0.087)$.

The endcaps (HE) The hadron calorimeter endcaps (HE) cover about 13.2% of the solid angle which corresponds to an η range of $1.3 < |\eta| < 3$, a region that contains about 34% of the final state particles. Due to the high

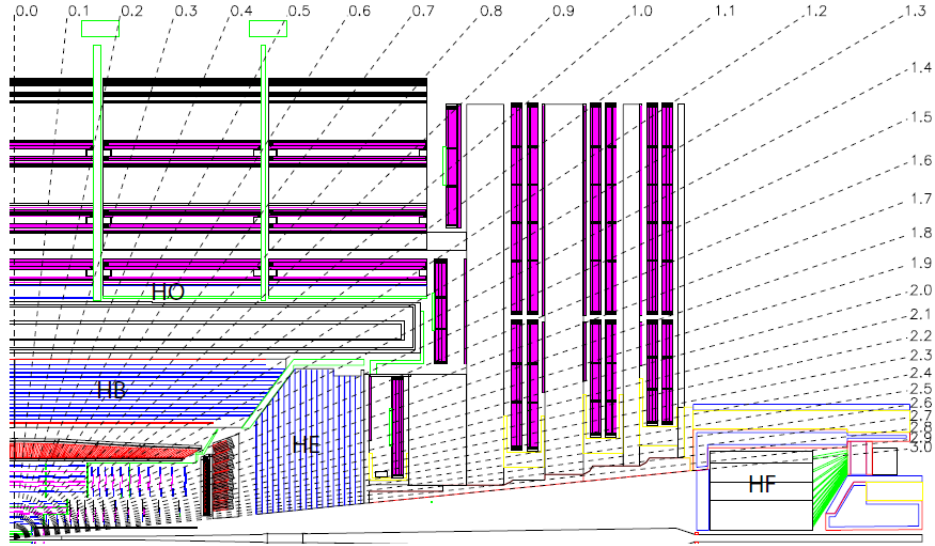


Figure 4.4.2: The Hadronic Calorimeter at CMS.

design luminosity of LHC the HE has to deal with high counting rates in the MHz range and has to provide a high radiation tolerance. Furthermore it has to be made of a non-magnetic material since it is inserted into the 4 T magnetic field. The main requirement to the absorber is to minimize the cracks between the HB and the HE. The scintillation light, produced by charged particles, is collected by wavelength shifting fibers (WSF).

The outer calorimeter design (HO) Since in the important pseudorapidity region $0 < |\eta| < 1.3$ the resolution of the combination of HB and EB is not sufficient for hadron showers these two systems are complemented by the outer calorimeter HO which is installed outside the solenoid. It uses the coil as additional absorber (equal to $1.4/\sin(\theta)$ interaction length) for both, measuring late beginning showers and the energy of showers after passing the HB. Outside the coil, the magnetic field is returned through an iron yoke that consists of five 2.536 m wide rings along the z-axis. The HO is integrated as first layer in each of these rings. Since at $\eta = 0$ the HB has its minimal absorber depth the central ring, corresponding to that position has two layers of HO scintillators on each side of a 19.5 cm thick piece of iron. The HO is geometrically constrained by the muon system.

The forward calorimeter (HF) The forward calorimeter has to deal with a huge particle flux, since for each collision about 760 GeV per proton-proton interaction will go to the two forward calorimeters which is quite high compared to 100 GeV that are deposited in the rest of the detector. The maximum of its energy, that is not distributed homogeneously, is expected for the highest rapidities. For this detector quartz fibers were chosen as active medium where

charged particles can produce Cherenkov light when traveling faster than the speed of light in this medium ($E > 190$ keV for electrons). Only a small fraction of the light that is produced will be captured. Since the HF is using Cherenkov light it is almost insensitive to neutrons and other low energy particles that are produced in decays of radio-nucleids.

4.4.3 The Muon system

Muon final states at CMS play a decisive role in the search for the Standard Model Higgs or supersymmetric particles, since muons are less affected by radiative losses in the tracker than electrons. Therefore a good 4-particle mass resolution is possible. The decays $H \rightarrow ZZ$ or $H \rightarrow ZZ^*$, for instance, are considered as gold plated if all four leptons in the final states are muons. The key requirements for the muon system therefore are:

- Unambiguous muon identification.
- A good muon momentum measurement. It should be within 8 to 15% in δ_{p_T}/p_T at 10 GeV and 20 to 40% at 1 TeV.
- A good muon trigger. It should allow to trigger on single and multi-muon events with well defined p_T thresholds.
- The charge assignment should be correct with 99% confidence up to energies of 7 TeV.
- Furthermore, the muon system should be resistant to the high radiation and interaction background produced by LHC.

Several processes contribute to the background. There are low energy radiative electrons which are produced by slow neutron capture near the muon capture. These neutrons emerge from hadronic cascades. The latter also can contribute to the background directly. Furthermore, there are muons that are produced by the π/K decay inside the central cavity.

The muon system at CMS consists of three different detector types all of which contribute to the L1-Trigger:

Drift Tubes (DT) In the barrel region drift tubes are used as tracking detectors because the expected muon rate is low and furthermore the strength of the magnetic field is also relatively low. The magnetic field is mostly uniform in that region. The DTs, consisting of standard rectangular drift cells, cover a pseudorapidity region $0 < |\eta| < 1.2$ and are organized in four stations. The first three stations together contain eight chambers that form two groups each of which is consisting of four cells. The first group measures the muon coordinate in the r - ϕ plane while the second group performs a measurement of the z -coordinate along the beam pipe. The fourth station is not equipped with z -measuring planes. The DTs contribute information for both, time and transverse momentum assignment to the L1-Trigger.

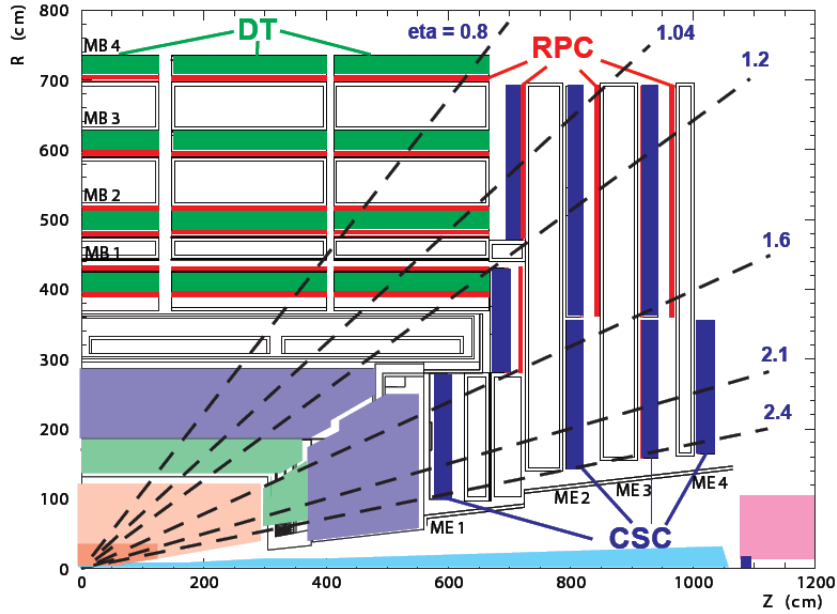


Figure 4.4.3: Scheme of the CMS Muon system [33].

Cathode strip chambers (CSC) In the endcaps, which have a higher event rate and background, cathode strip chambers are used covering $0.9 < |\eta| < 2.4$. In this region the magnetic field is strong and non-uniform. There are also four stations of this type perpendicular to the beam-pipe in each endcap. The cathode strips of each chamber are leading radially outward in z -direction and therefore perform a precision measurement within the r - ϕ plane. The anodes are more or less perpendicular to the cathode stripes and therefore can be used for a measurement of η and the beam crossing time of a muon.

Resistive Plate Chambers (RPC) There are resistive plate chambers located in both the barrel and endcap regions providing an independent high precision timing measurement which is needed by the trigger. Furthermore, they can also perform a coarse p_T measurement for the trigger. The RPCs consist of parallel plates filled with gas and provide a very good time resolution of about 1 ns and cover an η resolution up to 1.6. This results in a p_T resolution for muons of 15% in the barrel region and 25% in the endcaps for the L1-Trigger.

4.4.4 Forward detectors

4.4.4.1 Castor

The Centauro And Strange Object Research (CASTOR) is designed to look at the very forward regions in LHC collisions. Situated at a distance of 14.38 m from the interaction point, it covers an η range of $5.2 < |\eta| < 6.6$. Like HF also CASTOR is a Cherenkov-light based calorimeter and consists of layers of tungsten (W) plates as absorber and fused silica quartz (Q) plates as active

medium. These plates are installed at an angle of 45 degrees with respect to the beampipe.

4.4.4.2 Zero Degree Calorimeter

A set of two zero degree calorimeters (ZDC), covering a pseudorapidity of $|\eta| > 8.3$ to detect neutral particles, is located close to the two LHC beam pipes at a distance of about 140 m from the interaction point. Each ZDC consists of an electromagnetic and a hadronic calorimeter. It should be possible to detect heavy spectator neutrons with a resolution of 10 - 15%. Tests in 2007 at SPS gave an energy resolution for positrons with energies within 20 GeV to 100 GeV:

$$\left(\frac{\sigma}{E}\right)^2 = \left(\frac{70\%}{E}\right)^2 + (8\%)^2 \quad (4.4.1)$$

For pions with a positive charge and energies of 150 GeV to 300 GeV the energy resolution can be given according to a Landau fit:

$$\frac{\sigma}{E} = \frac{138\%}{\sqrt{E}} + 13\% \quad (4.4.2)$$

4.4.5 Trigger and Data Acquisition

The high collision rate of LHC combined with a huge number of readout channels of the CMS detector (about 55 millions) requires an elaborate Trigger and Data Acquisition (DAQ) system in order to collect and analyze the detector information available. Purpose of the trigger system is to select the data to be stored since due to the data size one cannot write all the data to the storage. It consists of two parts:

- The L1-Trigger system which will be described in more detail in the next section reduces the event rate from 40 MHz to a maximum of 100 kHz. Since a decision has to be taken within about 1 μ s a hardware based solution using FPGA chips has been chosen.
- The High-Level Trigger has to deal with a data flow of about 100 GByte/s from approximately 650 data sources, corresponding to the events which pass the L1-Trigger with an event rate of about 100 kHz. The HLT is part of the DAQ system and consists of commercial processors (for LHC startup 720 PC-nodes were foreseen). It has access to all the data recorded for a particular event and reduces the event rate by a factor of 1000 to 100 Hz.

The main tasks of the DAQ system can be summarized as

- distribution of events to worker nodes after the L1A accept
- performance of consistency and quality checks on data

The first storage of data takes place in the Front End Systems (FES) of the various sub-detectors which continuously store data in 40 MHz pipelined buffers, awaiting the decision of the L1-Trigger system. When the L1-Trigger sends an accept signal with a latency of 3.2 μ s the data will be extracted from the FES

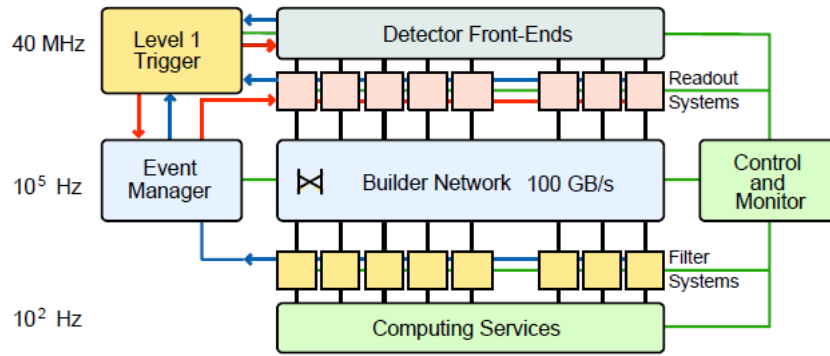
and moved to the DAQ system via the Front-End drivers (FED). The next step within the DAQ system are so-called front-end readout links (FRL) which are able to merge the data from up to two FEDs. The data is stored in 72 so-called super-fragments stored in memory buffers on Read Out Units (RU). The reconstruction of the entire event from the fragmented data is done by Builder Units (BU) of the event builder (Fig. 4.4.4).

Variations in the event rate and size might produce buffer overflows in the subdetectors front-end electronics which would lead to data corruption. To avoid this the Trigger Throttling System (TTS) was introduced which gives feedback from the front-ends of all subdetectors to the Global Trigger Processor and throttles the trigger if there is danger of buffer-overflow. This leads to some dead time at Level-1.

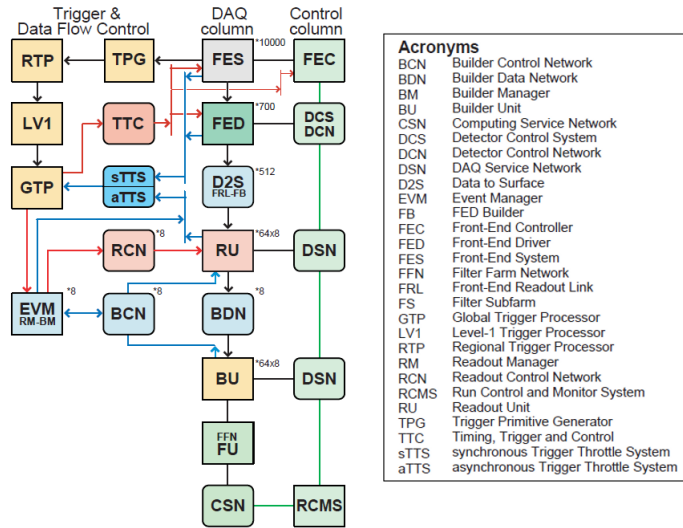
As a next step the data is processed by the High-Level Trigger. The HLT algorithms which decide whether an event is stored in the end are applied in so-called filter units (FU).

To have a fast way of evaluating the quality of the data taken, additional quality and integrity checks on the data are performed which are referred to as Data Quality Monitoring (DQM). The DQM provides a fast way to find problems of the detector at run time [25, 34].

Figure 4.4.4: The CMS Trigger/DAQ system.



(a) Schema displaying the different instances an event has to pass to be accepted.



(b) Schema of the CMS HLT and the DAQ system.

Chapter 5

The CMS L1-Trigger System

The physics that was taken as a guideline for the design of the L1-Trigger system of has been described in chapter 2. Figure 5.0.1 shows that the cross sections of processes to be investigated at LHC strongly vary in order of magnitude: while the production of $b\bar{b}$ has a cross section of about 1 mb, the cross section of the decay of the SM Higgs into four muons is only of the order of a few fb for the relevant mass range. This huge spectrum of cross sections requires a flexible and efficient L1-Trigger system for the CMS experiment in order to be able to select the interesting events among millions of background events. Its implementation will be described in this chapter. Figure 5.2.1 shows the overall architecture of the L1-Trigger system: the muon trigger and the calorimeter trigger build trigger objects which are evaluated in the Global Trigger according to requirements given in the L1 trigger menu.

5.1 Trigger objects

The following trigger objects [26] are built:

- μ - any muon (isolated or non-isolated)
- e/γ - electron/photon (isolated or non-isolated). This trigger only considers isolated electrons to avoid the huge background from QCD jets
- jet - a local energy cluster in the calorimeter (central and forward)
- τ - tau jets, corresponding to a narrow jet
- energy sums: E_T^{miss} (missing transverse energy), E_T^{total} (total transverse energy), H_T^{miss} (missing hadronic jet energy), H_T^{total} (total hadronic jet energy)

Combinations of the above trigger objects can also be built (2 μ , 2e, e μ , 2 jets, 3 jets, cross-object triggers).

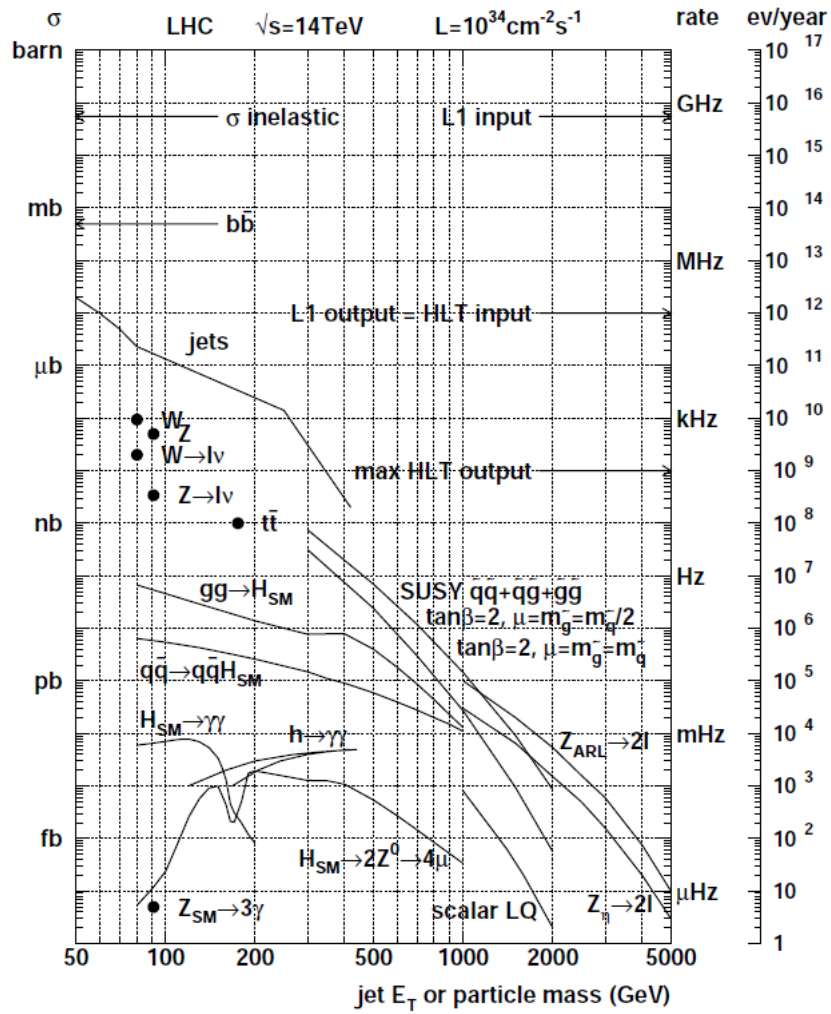


Figure 5.0.1: Cross section for basic physics processes defining the requirements for the CMS trigger [26].

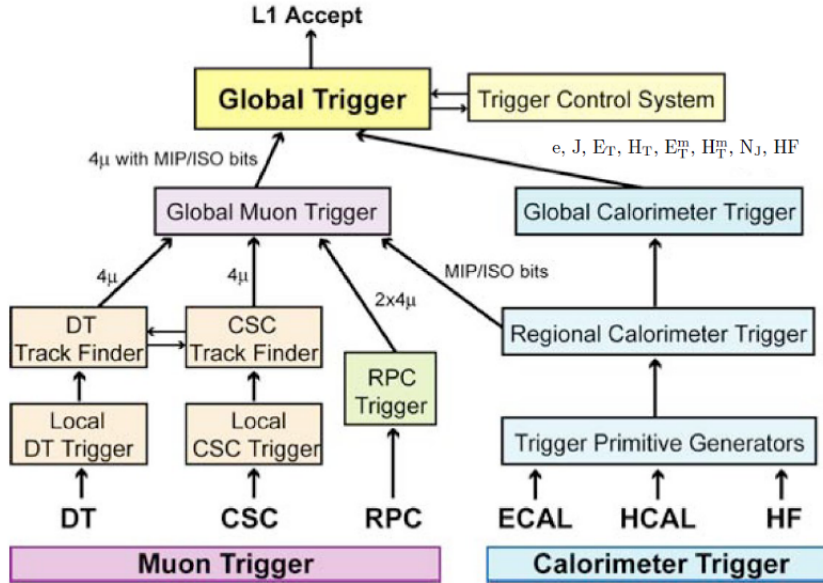


Figure 5.2.1: The L1-Trigger in overview.

5.2 Design of the L1-Trigger

5.2.1 The Calorimeter Trigger

The starting point for the calorimeter trigger at CMS are the trigger tower energy sums which are formed by the readout Trigger Primitive Generator (TPG) of the calorimeter detectors. A trigger tower is a defined (η, ϕ) - region within the detector. The cell size was chosen as a compromise between two requirements: the background of electron/positron triggers increases with the cell size. On the other hand, the number of trigger channels, proportional to the number of cells has to be kept small for cost reasons. The towers are organized in calorimeter regions each of which consists by 4 by 4 trigger towers, forming the basis for jet and energy triggers. For the HF regions, a calorimeter region consists only of one trigger tower. The trigger primitives are calculated from 40 MHz digital samples of the detector pulses, using TPG electronics. The most important task of this electronics is to assign a detector pulse to the correct bunch crossing since they can propagate through the detector several clock periods. The transverse energy sum is calculated for each tower separately. For different calorimeter regions different energy scales can be applied. The calculation of trigger primitives in the calorimeter trigger consists of

- the conversion to the correct transverse energy scale
- the calculation of the tower energy sums

The trigger primitives are forwarded via high-speed serial links to the Regional Calorimeter Trigger (RCT). The RCT determines electron and photon candidates for each region and calculates the sums of electromagnetic and hadronic

transverse energies for each tower. An important algorithm within the RCT is the electron/photon isolation algorithm. It is able to distinguish isolated e/γ from non-isolated e/γ within an η range $|\eta| < 3.0$. Furthermore, minimum-ionizing particle (MIP) and isolation (ISO) bits for muons are calculated by the RCT. Jets and τ s are defined by their transverse energy distribution in 3×3 calorimeter regions. Veto bits for the identification of jets from τ -decays (τ -jets) are set. In general they are narrower than quark or gluon jets. The τ -veto bit is set if there are more than two active ECAL or HCAL towers within a 4×4 region. The classification as a τ -jet is only possible for $|\eta| < 3.0$.

The Global Calorimeter Trigger (GCT) is the last part of the calorimeter trigger. It takes data from the RCT and sends a reduced amount of data to the Global Trigger. Its main task is to reduce the number of trigger objects that have to be considered by the GT. To achieve this, a rank is attributed to the RCT objects which is a criterion for sorting: only a defined number of objects with the highest rank is forwarded to the GT. After the sorting, up to four jets and four τ -jets from the central HCAL and four from HF can be sent to the GT. Furthermore, the total transverse energy vector and total missing energy vector are calculated in the GCT and also sent to the GT [25].

5.2.2 The Muon Trigger

At CMS three different muon systems (DT, CSC and RPC) contribute to the muon trigger. The good spatial precision of DT and CSC guarantees sharp momentum thresholds. The RPC system is dedicated to the trigger and provides an unambiguous bunch crossing assignment by its excellent time resolution. The muon trigger system consists of the following parts:

- a local DT and CSC muon triggers
- a regional DT and CSC trigger
- the Resistive Plate Chamber trigger
- the Global Muon Trigger

An overview of the components of the CMS Muon Trigger can be found in Refs. [25, 26]:

The Local Muon Trigger The Drift Tube local trigger is a four component electronic system: its ingredients are the Track Identifiers (BTI), Track Correlators (TRACO), Trigger Servers (TS) and so called Sector Collectors (SC). The BTIs search for aligned and coincident hits in four equidistant planes. The information on hits is used to determine track segments by position and angular direction. The TRACO tries to correlate track segments, measured in two ϕ type superlayers of the DT chambers. These correlations can be used to enhance the angular resolution and for producing a quality hierarchy. The TS performs a track selection based on TRACO data. The SC collects the trigger information (track quality, position, and transverse momentum) for each of the sixty 30° -sectors of CMS and sends it to the DT local trigger.

The Cathode Strip Chamber local trigger is responsible for the endcap region. There muons at a given p_T have a higher momentum than in the barrel

region which is challenging for the trigger since they produce more photons by Bremsstrahlung. For a better resolution the CSCs in the endcaps consist of six layers with cathode stripes and anode wires which can be correlated. The anode electronics is optimized to assign an event to the correct bunch crossing, while the cathode electronics was optimized to measure the ϕ coordinate. For both the cathodes and anodes coincident hits in at least four layers are required (the probability that a real muon hits at least four layers exceeds 99%). In the end, the track segments from the anode and cathode electronics are combined in so-called Local Charged Tracks (LCT), the best two of which are forwarded to the regional CSC trigger. The LCTs provide a high precision for the ϕ -coordinate in the bending plane, a rough η coordinate assignment and the bunch crossing number.

The Regional Muon Trigger The Regional Muon Trigger consists of two subsystems, the Drift Tube Track Finder in the barrel region and the Cathode Strip Chamber Track Finder in the endcaps.

The Drift Tube Trigger Track Finder has the main task to identify muons, determine their p_T , locations and quality. The candidate muons are sorted by a rank which is given by their p_T and quality information. The track finding mechanism (Fig. 5.2.2) is based on the principle of the extrapolation from a hit in a source segment in one certain muon station to a target segment in another station. This operation is performed using a pre-calculated trajectory with the vertex as origin. In case a compatible track segment is found it is linked to the source segment. A complete track is combined by a maximum number of track segments in the four muon stations. The DTTF works in two dimensions only. Nevertheless, a rough η assignment is possible. This job is done by 12 η assignment units that are referred to as Eta Track Finders (ETTF). The method which is used is a pattern matching method since the η information consists of patterns from the DT local trigger. In the regional trigger the DT chambers are arranged in wedges. There are twelve horizontal wedges in beam direction. Each wedge consists of six sectors with an angular width of 30 degrees in ϕ .

In contrast to the DTTF the CSC Track Finder (CSCTF), which is located in the endcaps works in three dimensions. Like for the DTTF its core components are twelve sector processors. There the consistency of almost all possible pairwise combinations of track segments with a single track is checked. Redundant tracks are canceled, while complete tracks are assembled from the extrapolation results. For each processor the best three muons are assigned quality and kinematic parameters.

In the region where DT and CSC chambers overlap ($\eta \approx 1$) the information from both systems can be used. For each wedge there are at most 12 muon candidates which are defined by transverse momentum, charge, η , ϕ and quality: This corresponds to two candidates per 30 degree sector. As next instance the so-called 12 Wedge Sorters (WS) perform a first sorting to at most 144 candidates per event by their p_T and their quality. Duplicate candidates are suppressed in this step. The final Barrel Sorter (BS) selects the best four candidates for the entire barrel region and forwards them to the Global Muon Trigger.

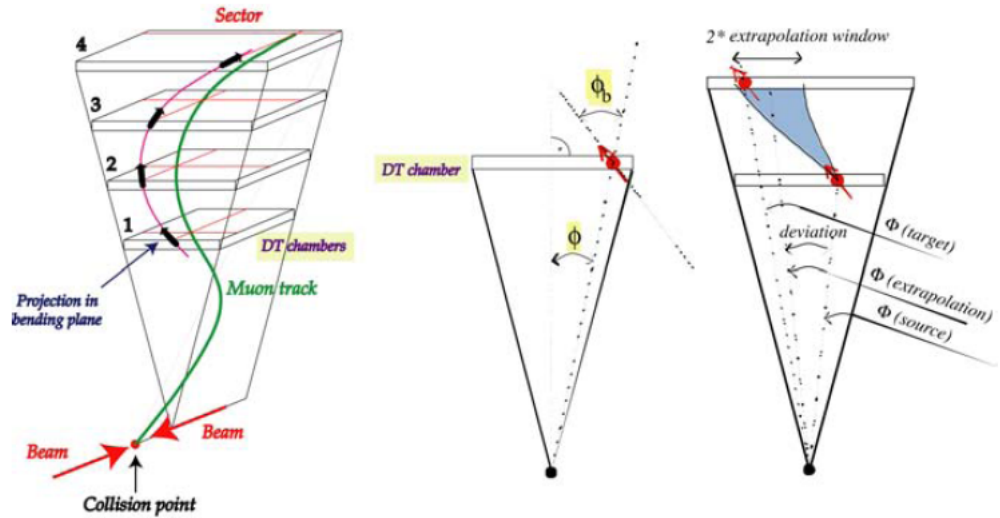


Figure 5.2.2: Scheme of the DTF track finding mechanism.

The Resistive Plate Chamber trigger The RPCs were designed as dedicated trigger detectors which have an excellent time resolution of about 1 ns that can be used for the bunch crossing identification. To measure the momentum of muons the ϕ coordinate is determined at several points along a track to get its bending which gives p_T of the muon. In the barrel region the stripes of the RPCs run parallel to the beam pipe while they run radially in the endcap region. Similar to the other systems described before, the RPC trigger is based on the evaluation spatial and temporal coincidence of muon hits in different layers. The Pattern Comparator Trigger (PACT) logic determines p_T and the electric charge of muon candidates. If their quality is low a HO confirmation is required. After sorting the candidates separately for the barrel and the forward region, the best four muon candidates of each region are sent to the Global Muon Trigger.

The Global Muon Trigger The Global Muon Trigger is the final part of the Muon Trigger. It improves the trigger efficiency making use of the redundancy of the three muon systems. For each bunch crossing it receives up to 16 Muon candidates, four from the barrel DT and barrel RPC and four from each subsystem in the endcap region (CSC and RPC). The p_T , η , ϕ , charge and quality is taken into consideration. Furthermore, the GMT evaluates isolation and minimally ionizing particle bits using information from the GCT for each calorimeter region. A muon is categorized as isolated if its energy loss in the calorimeter region it emerges from is below a certain threshold. First DT and CSC coordinates are matched with barrel and forward RPC candidates, comparing the spatial candidates. In case it is possible, their kinematic parameters are also merged. MIP and ISO bits are gained by back-extrapolation of candidate muon tracks through the calorimeter regions to the vertex.

For the overlap regions between barrel and endcaps, where muon candidates

can be detected by both the DT and the CSC, so-called cancel-out units reduce duplicate candidates. The redundant information from the DT and CSC trigger improves resolution and control: accidental coincidence of three or four background hits, for instance, could be identified as a real muon by the RPC. For the DT/CSC on the other hand this scenario is highly unlikely as it takes several planes in each station into account and therefore can be rejected as background. The combination of the two systems leads to an effective background rejection. There are two scenarios where a muon candidate is taken in any case:

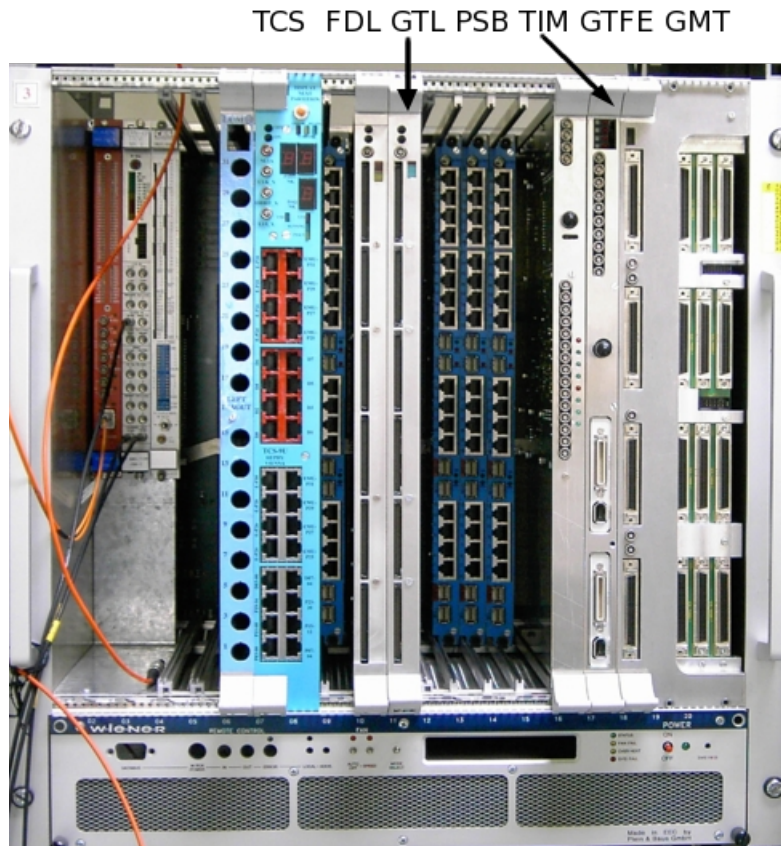
- it is seen by both DT/CSC and RPC. In this case the quality does not play a role
- if only one subsystem detects the muon its quality has to be high

Finally four muon candidates are forwarded to the GT, which are sorted by transverse momentum and quality [25, 26].

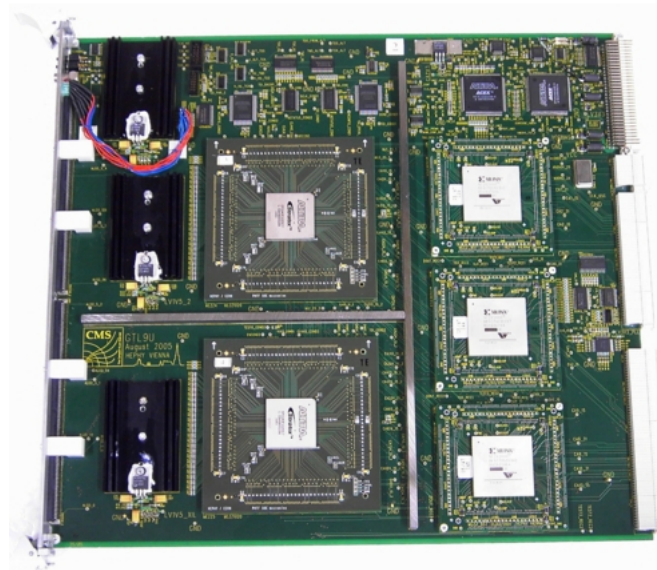
5.2.3 The Global Trigger

The Global Trigger (GT) is the last part of the L1-Trigger system at CMS. Its main task is to decide every 25 ns whether to accept or reject an event. Therefore it is implemented as a custom built electronic system. However, it not only applies energy and momentum thresholds, but can also deal with spatial information like azimuth and pseudorapidity and takes into account additional parameters like muon quality or MIP and ISO bits. Topological conditions can already be applied at the first trigger level, which is a big progress in this field: Collider experiments at Tevatron or LEP for example could not deal with spatial correlations at the first trigger level. The maximum input rate of the next level of the trigger system is 100 kHz. Therefore the thresholds at the L1-Trigger system have to be set in a way that this rate is not exceeded. The L1-trigger decision takes about $3.2 \mu s$ in total (equivalent to 128 bunch crossings) due to processing times of the hardware, the use of analogue pipeline memories by several sub-systems and an average distance of the Global Trigger electronics to the collision point of 90 m which was chosen to avoid radiation damage. The resulting propagation times of signals contribute to the latency. Drift times of muons in the DTs also account for a delay of up to 16 bunch crossing intervals. For the actual processing of an event by the L1-Trigger only $1 \mu s$ remains. Since the GT is the last instance within this chain the time remaining for its decision is a lot shorter, with only about a quarter microsecond. In the end a L1-Accept (L1A) signal is produced if a event was accepted. To be able to deal with these challenging requirements the GT has been implemented as a complex multi-component hardware system. Figure 5.2.3a shows the Global Trigger crate where the GT hardware is located together with the GMT. The most important hardware constituents of the GT are listed below and are described in more detail in Refs. [35, 36, 37].

Global Trigger Input The GT is fed by the Calorimeter Trigger and the Muon Trigger. From the GCT it receives the following input at its 24 input channels.:



(a) The order of the boards from left to right is TCS,FDL,GTL,PSB,TIM, GTFE and GMT.



(b) The GTL board. The two big chips are the condition chips, the three smaller ones the receiver chips.

Figure 5.2.3: The Global Trigger Crate.

- The total transverse energy E_T^{total} , the magnitude and the direction of the missing transverse energy E_T^{miss} , the total hadronic jet energy HTT and the magnitude and the direction of the missing hadronic jet energy HTM
- 4 non isolated and 4 isolated e/γ trigger objects
- 4 central and 4 forward jets
- 4 τ -jets

The objects are organized in quadruplets and sorted by their E_T within such a quadruplet. If an event contains fewer objects the channels reserved for lower E_T remain empty and only contain zeros.

The Global Muon Trigger, which shares a crate with the GT immediately sends the best four candidate muons to the GT. They are also sorted by rank defined by their p_T and quality. As already mentioned above the muons are defined by p_T , η , ϕ , a charge or sign bit, an isolation bit and three quality bits. The p_T threshold corresponds to five bits to which a non-linear scale can be applied.

The calorimeter data has to be delayed in order to arrive synchronously with the muon data.

Furthermore, the Global Trigger receives up to 64 “logical values” (true/false) called “external conditions” which can be combined with the trigger objects sent by GCT and GMT. In addition, the GT receives also up to 64 direct signals from various subsystems (BPTX, BSC, CSC, DT, HCAL, etc.) called “technical triggers” which are used directly for the Final-OR decision in the Final Decision Logic which is described later in this chapter.

The Timing Module (TIM) The TIM module is linked to the Trigger Timing and Control system (TTC) which is the common clock distribution system and provides the clock signal from the LHC and other fast control signals for the trigger crate. The timing for the trigger and the detector is defined by the LHC clock which has a frequency of 40 MHz. A Bunch Crossing Zero (BC0) signal which is sent by the LHC clock is used to synchronize the different parts of the detector electronics with respect to each other and to the LHC orbit pattern.

Pipeline Synchronizing Buffers (PSB) Pipeline Synchronizing Buffers (PSB) are used as input modules for the Global Trigger. They synchronize all calorimeter input channels to both the local 40 MHz clock and to the LHC orbit and also to each other. A PSB board contains four Infiniband connectors each of which can receive two streams of serial data which corresponds to 8 input channels in total. A serial data stream is converted back to 16 bit parallel data at 80 MHz by a DS92LV16 Serializer/Deserializer chip. A single PSB can receive up to four quadruplets of objects which are sent to the GTL through the crate backplane.

Central Trigger Control System (TCS) The main task of the trigger control system is to control the delivery of the L1A, taking into account the status of the readout electronics and the data acquisition. There are two ways to determine this status: on the one hand it is derived from local state machines

that emulate the occupation of the front-end buffers, on the other hand direct information can be used which is transmitted via a fast monitoring network. Precise trigger rules have to be applied in order to prevent buffer overflows in the readout and data DAQ chain. They limit the L1As for a certain number of bunch crossings. A typical example for a trigger rule would be: no more than 2 L1As per 625 ns or 25 bunch crossings. Furthermore, the TCS distributes the BC0 and Level-1 Reset commands to reset the trigger to the other subsystems. Two commands for a fast reset have been implemented: the Resync command enforces a re-synchronization of all subsystems and also involves the reset of readout buffers while the hard reset command performs a fast reconfiguration of frontend FPGA chips. The second command can be useful in case of electronic problems.

The GTL Board (GTL) The GTL board, the core of the Global Trigger, has 5 FPGA chips in total which can be seen at Fig. 5.2.3b. There are three receiver chips (called REC1, ..., REC3) which receive the 80-MHz input data via the backplane from the GMT and from the PSBs and adapt it to the board clock. These chips distribute the data to the two condition chips COND1 and COND2 where the actual processing of conditions and algorithms is done. Each of the two chips provides a capacity for 96 algorithms which would allow to calculate 192 algorithms synchronously in theory. However, only 128 bits are used for trigger algorithms at present: COND 1 exploits its nominal capacity of 96 algorithms while COND 2 only processes at maximum 32 algorithms. Since it is an exact copy of COND 1, COND 2 could also host up to 96 algorithms. Since the condition chips are based on FPGA technology they are largely programmable. The results are sent as parallel data via short flat cables to the FDL board.

The Final Decision Logic (FDL) Within the FDL board the trigger algorithms processed by the GTL and the technical triggers are organized in so-called slices which are independent. A slice consists of a prescale factor, a rate counter and the Veto Mask logic which is only available for the technical triggers. These concepts will be explained later in this section in more detail. For each of its 8 slices the FDL board provides a separate Final-OR circuit, therefore it has the capacity to calculate up to 8 Final-OR decision words independently, which are sent to the TCS board afterwards.

The Global Trigger Front End Module (GTFE) All relevant modules in the GT crate (FDL, TCS, GMT and PSB) contain buffers to keep trigger data until the Level-1 Accept signal arrives. When the readout signal arrives a readout processors (ROP) on the different boards collect the data and forward it as a record to the GTFE board. There the data from all boards are merged into a record and sent to the DAQ. Additionally data from the TCS and FDL is merged into an event record and forwarded to the DAQ Event Manager (EVM).

5.2.3.1 The logic processor

The core of the Global Trigger is its logic unit. As already mentioned before, it processes up to 128 trigger algorithms in parallel for each bunch crossing and

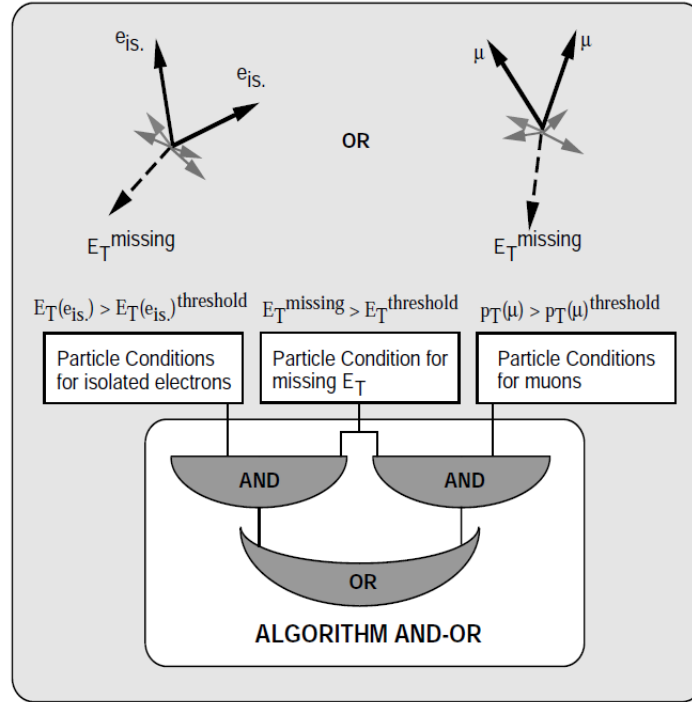


Figure 5.2.4: Algorithm to trigger on a SUSY slepton.

is highly programmable. An algorithm is a logical combination of conditions for trigger objects which can be joined by the three logical operator AND, OR and NOT. There is a set of “external conditions” available, which are delivered in binary format by different subsystems and can be used in algorithms like normal conditions. Possible examples are signals from the forward detectors or information about the presence of the beam by the LHC Beam-Pick-Up Timing Experiment (BPTX). The thresholds and spatial requirements for the trigger objects can be defined using discrete, configurable L1-Trigger scales. In a first step predefined conditions are applied to the trigger objects and thereby both, particle conditions between identical objects and correlation conditions between distinct objects are evaluated. For the conditions there are more possibilities. Considering the four input muons for example, different thresholds can be demanded for each of them, eg. a muon condition, taking into account four objects can have up to four different thresholds. A realistic use case would be the requirement of two muons being seen in the central region of the detector and two in the forward region, which could be achieved by the definition of windows in η and ϕ . A simple algorithm to trigger on a SUSY slepton is displayed in Fig. 5.2.4. The algorithm requires two muons exceeding a certain transverse momentum threshold or two electrons exceeding a certain transverse energy. Both objects are combined with a certain missing transverse energy. Generally it is intended to keep the algorithms at L1 as simple as possible whereas the HLT algorithms are more complex and have a better resolution as they have access to the whole event.

5.2.3.2 Trigger Partitioning and the Final-OR

The DAQ system at CMS provides eight separate partitions which correspond to the independent FDL slices in the hardware. When GTL has finished its job, Final-OR masks are applied by the FDL board to the 192 trigger bits (128 algorithm triggers and 64 technical triggers), combining all active triggers. The result of this Final-OR decision determines if there is a L1A signal for a particular DAQ partition. The Final-OR decision word can be influenced by several additional factors:

- For each of the trigger bits a prescale factor can be set to keep the trigger rate under control. Prescaling means an additional reduction of the rate of a bit that is defined by a given factor. That way it is possible to avoid that very common processes make the trigger rate exceed the maximum output rate of the Level-1. A set of prescale factors can be defined at the beginning of each run.
- Furthermore the output of the GTL can be masked to ignore certain bits which are not relevant for a particular run.
- There is also a Veto Mask Logic for technical trigger bits: if a certain technical trigger bit is defined as veto bit and that trigger fires, the event will be discarded in any case.

Eventually, if a event has fulfilled all criteria to be accepted, the L1-Accept signal is generated and sent via the Trigger Control System to the Trigger, Timing and Control (TTC) network which distributes it to all subsystems in order to save the data from the front-end buffers. In parallel it is sent to the Event Manager in order to start the CMS data readout. The modular organization of the TCS can be seen in Fig. 5.2.5: there are several different partitions, corresponding to components of different sub detectors. Furthermore, these partitions can be grouped at software level, whereupon each group corresponds to a DAQ partition [37].

5.3 The Level-1 Trigger Menu

A logical setup of requirements for trigger objects received by the Global Trigger is called Level-1 trigger menu. It can be considered as a combination of a set of algorithms (128 at present), 64 technical triggers, a set of physics scales, a set of definitions for external conditions and some additional, rather descriptive header information. The scales (which will be explained later in more detail) are especially important since they convert a pure hardware menu into a physics trigger menu. They are configurable but have to be kept constant for a particular trigger menu. Each trigger menu in use has to be available in four different representations in total. The basic one is the VHDL code which is the source for the firmware of the GTL condition chips. Furthermore, a trigger menu is stored in the CMS online database (OMDS) to be available for configuration and cloned from there to the CMS Offline Database (ORCON) in order to be available for data analysis. For back-up a trigger menu can also be exported to an XML file. What follows is a description of the possible ingredients of a trigger menu.

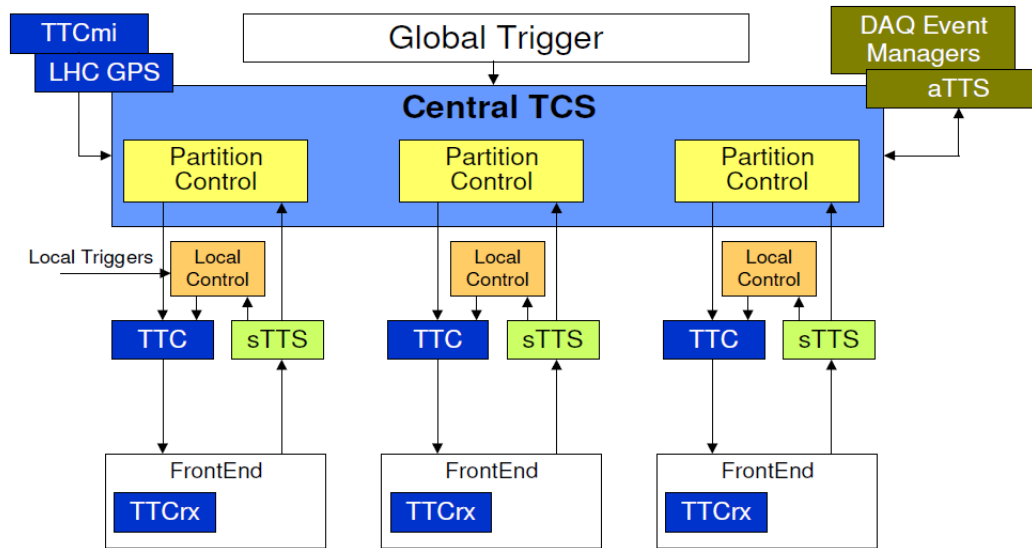


Figure 5.2.5: The Trigger Control System.

5.3.1 Condition types

A trigger menu can contain different types of conditions. They can be categorized in the following categories:

- Muon conditions for muons (CondMuon)
- calorimeter conditions for electron/gammas, jets and tau jets (CondCalo)
- Energy Sum conditions (CondEnergySum)
- Correlation Conditions which consider different objects with spatial correlation (CondCorrelation)
- HF bit counts
- HF ring Et sums
- External conditions (not evaluated in the GTL)

Muon Conditions Muon conditions consist of a set of templates that are compared against the four physical muons that arrive at the GT from the GMT. A single muon template is defined by the following parameters:

- The p_T threshold
- a Minimum Ionizing Particle (MIP) bit
- an isolation bit
- a η window
- a ϕ window

muon_data				condition bits			PT truth-table output	comments
PT equal high threshold	PT greater/equal high threshold	PT greater/equal high threshold	ISO_bit of muon	greater/equal selection	request_iso	enable_iso		
0	x	x	x	0	x	x	0	for tests
1	x	x	x	0	x	x	1	for tests
x	0	0	x	1	x	x	0	very low p_T muon
x	0	1	0	1	0	0	1	ignore isolation, take it
x	0	1	0	1	0	1	0	not isolated
x	0	1	0	1	1	x	0	not isolated
x	0	1	1	1	0	0	1	ignore isolation, take it
x	0	1	1	1	0	1	1	take isolated muon
x	0	1	1	1	1	x	1	take isolated muon
x	1	1	0	1	0	x	1	ignore isolation, take it
x	1	1	0	1	1	x	0 *)	requested but not isolated
x	1	1	1	1	x	x	1	take isolated muon
x	1	0	x	1	x	x	not used **)	must be inhibited by GUI

*) Because of request_iso = 1 do not trigger on a very high p_T , but non isolated muon.

**) Low-threshold for p_T must not be greater than high-threshold for p_T .

Table 5.1: p_T truth-table for muons [36].

- a quality bit

A muon condition can contain up to four templates for single muons. The number of templates that is contained by the condition defines its type. The simplest condition type only contains one single muon template (Type1s). The types Type2s, Type3s, Type4s and Type2wsc are also possible and contain the number of templates that is indicated by their names. The Type2wsc describes two single muon templates with additional spatial correlations. Differences in pseudorapidity $\Delta\eta$ and in azimuthal angle $\Delta\phi$ among the two trigger objects can be defined for these condition type. The comparison between the physical muons and the templates takes into account all possible permutations of the physical muons to find a combination that fits the template definitions in use (1234, 1243, 1324...). If fewer than four muons are required by a particular condition which means that their type is < Type4s the templates for the other muons are set to trivial values (e.g.: $p_T \geq 0$ GeV/c, $0^\circ < \phi < 360^\circ$ etc.). For conditions consisting of a single muon template a charge can be defined (positive, negative, ignored) while for conditions that contain more than one muon template a charge correlation is evaluated. The MIP bit requires a muon also having been seen by the calorimeter, the ISO bit is true for isolated muons. Table 5.1 illustrates the possible output for the different bits being set or unset and is valid for all muon condition types.

Calorimeter Conditions The structure of calorimeter conditions is similar to that of muons. A set of templates is applied to the calorimeter physics objects. There is also a maximum number of four templates per condition.

The available calorimeter objects are electron/gamma which can be isolated and non isolated, tau-jets and central and forward jets. According to the CMS naming convention these objects are called NoIsoEG, IsoEG, TauJet, CenJet and ForJet. The available condition types are Type1s, Type2s, Type3s, Type4s and Type2wsc like for muons. The parameters that are checked for a single calo template are:

- transversel energy $E_T \geq$ a threshold
- η window
- ϕ window

For conditions of Type2wsc a $\Delta\eta$ and a $\Delta\phi$ window can be defined.

Energy Sum conditions Total and missing transverse energy determined in the calorimeter trigger define their own condition category. Conditions for total E_T consist of a simple threshold comparator. For the missing transverse energy an additional ϕ window can be defined. The trigger objects that are available for this category are

- ETT is the total transverse energy
- ETM is the missing transverse energy. For ETM a ϕ window can be applied
- HTT is the total hadronic jet energy above a given threshold
- HTM is the missing hadronic jet energy. Also here a ϕ restriction can be defined

For the forward calorimeter (HF) separate energy sums and bit counts can be defined. In the L1 trigger menu they are categorized as:

HF bit counts A HF bit counts condition triggers on the number of HF towers within a certain HF subregion whose energy exceeds a threshold.

HF ring E_T sums HF ring E_T sums conditions also consider HF subregions but in a different way. They allow an E_T threshold for the entire subregion.

External conditions These bits are delivered by external sources (like the forward detectors CASTOR and ZDC or the BPTX experiment) and can be treated by GT algorithms like normal conditions. The assignment of these conditions to distinct input channels can be modified dynamically loading pre-defined database keys.

Correlation conditions For two different trigger objects it is possible to define correlations in η and ϕ . The η windows are important for example to find a trigger object in the barrel region of the detector and another of the same or a different type in the endcap region. It is possible to trigger on objects close or opposite to each other within programmable tolerance. To evaluate a correlation condition the $\Delta\phi$ and $\Delta\eta$ differences of all possible pairs of two

particle groups are evaluated. If muons are compared with calorimeter objects the muons which have a higher resolution have to be downscaled to calorimeter units. This is done in the hardware using lookup tables.

5.3.2 Algorithms

Trigger algorithms are logical combinations of different conditions. There are 128 algorithms at present which are distributed over two chips in the hardware. Algorithm bit 0–94 are located at condition chip 2 while algorithm bits 95–128 are located at chip 1. An algorithm consists of a logical expression, an algorithm name and an algorithm alias. The latter is not unique and therefore can be used for algorithms that are similar to each other in their physics goals but are implemented in a different way for example.

5.3.3 Scales

The trigger of CMS was designed in a way that independent trigger scales can be applied for each object type. Therefore there are in total 24 independent scales which are available in the online database. A trigger menu object is linked with a scales database key. The topic of the scales will be treated in more detail in the section about the L1 Trigger Menu Editor.

Chapter 6

Online Software at the CMS Experiment

Since operating an experiment of the dimensions and complexity of CMS by hand would be a hopeless enterprise it is essential to have a well organized software infrastructure which automatizes most of the operation and furthermore gives possibilities to monitor the detector performance. The part of the software that is dedicated to this is generally referred to as online software. The online software includes all software packages that are interacting directly with the detector or trigger hardware and will be described in brief in this chapter. Furthermore, most parts of the online software can be considered to be time-critical.

6.1 Basic systems for operation and data taking

6.1.1 Run Control and Monitor System

The Run Control and Monitor System (RMCS) [38] is responsible for monitoring and controlling the CMS experiment during data taking and consist of both hardware and software components. It allows the control and operation of the experiment from anywhere in the world since all the functionality is accessible via any web-browser. However, to be able to access the user interfaces by web-browser one has always to tunnel through a firewall for security reasons. The RMCS is organized hierarchically consisting of eleven branches (one per subsystem). The RCMS was implemented in Java and its applications are based on Java Server Pages technology. For the communication between the particular processes the Simple Object Access Protocol (SOAP) is used [39, 34].

6.1.2 Detector Control System

Purpose of the Detector Control System (DCS) is to control the auxiliary detector components like the cooling system or the power supplies and is implemented in a hierarchical way. At the uppermost level there are commands like “start” and “stop” which affect the whole detector and are forwarded to subsystems at lower hierarchy levels.

6.1.3 Cross-Platform DAQ Framework

The Cross-Platform DAQ Framework (XDAQ) [34] was designed as a platform independent environment that enables RCMS, DAQ and DCS to communicate with each other and allows configuration and control. Furthermore, it provides technology independent data storage. For the communication with the online configuration database (OMDS) the XDAQ framework provides an application called T-Store. The communication and data exchange with the T-Store is performed using SOAP messages.

6.1.4 Trigger Supervisor framework

The Trigger Supervisor (TS) [26, 39, 40] framework is a central part of the CMS online software. It was designed to configure, test and monitor the large number of trigger subsystems. Due to the complex architecture of the trigger, a simple and homogeneous client interface was needed, which allows the operation of several subsystems either simultaneously or in standalone mode. Furthermore, the TS is responsible for the information exchange with the RCMS. The main functional requirements the Trigger Supervisor framework has to fulfill are:

- The configuration of the entire trigger system. Important components to configure are FPGA firmware, LUT's, memories and registers. The complexity of the entire system should be hidden from the user.
- Provide an interface to test the trigger system. Self-tests and interconnection tests should be available.
- Synchronization of the HLT with the L1 trigger system. The HLT has to be up-to-date about the L1 configuration in order to ensure a proper operation of the full trigger system.
- A monitoring of the trigger to guarantee its proper functioning. For example, the spy memories of different hardware components can be monitored.
- Remote operation. A possibility to configure and operate the different components of the CMS trigger remotely since most scientists and experts involved are not be present at the experiment all the time.
- Error handling and logging. The TS has to provide logging mechanisms for troubleshooting. The error management has to provide a standard error format and has to provide remote error handling and notification mechanisms.
- The protocol of communication between the different subsystems should be the same for most subsystems and especially compatible with run control. Therefore SOAP and the Extensible Markup Language (XML) were chosen for data exchange.

The core entity of the Trigger Supervisor is the Central Node (which is also called Central Cell) which is responsible for Run Control and several sub-cells which communicate directly with the subsystems hardware. To each subsystem a separate, independent cell is assigned which is a TS node itself, with the same structure as the Central Node. These nodes for the different subsystems are also

referred to as TS leafes and each of them can be accessed independently. The framework shows a tree architecture (see Fig. 6.1.1) whereat all tree nodes are based on a common template, the control cell. It offers some basic functionality: first of all there is a Control Cell Interface (CCI) which is an external interface to the Cell. One possibility is HTTP but there could be others. The Access Control Module (ACM) has to guarantee that only authorized users or entities are accessing the cell. The Task Scheduler Module (TSM) is in charge of receiving the command requests and forwarding the replies. The Shared Resources Manager (SRM) coordinates the access to shared resources as the common database or other cells. Furthermore, an Error Manager (ERM) manages all errors that cannot be solved locally. There is a remote error handling mechanism based on the global CMS distributed error handling scheme. For the developer a cell provides three different ways of implementing functionality embedded in a graphical user interface. They are web browser based, using asynchronous java script (AJAX). However, the source code of all TS applications is written in C++ since the AJAX GUIs are created automatically, using the AjaXcell library [41]. Therefore the developer does not need to care about JavaScript. There are several different template types for user-interfaces available:

Cell Commands Cell Commands can be considered as simple executable procedures that can be defined for each cell. Commands are executed via SOAP. They can be started and instantiated via the cells proper GUI or via a SOAP message from another application within the TS network. Cell commands can be executed synchronously and asynchronously. In case they are executed asynchronously they go to a different thread and the main thread of the cell can still be used.

Cell Operations The Cell Operation interface can be used for complex control sequences for which the Cell Command might not be appropriate. It provides a Final State Machine (FSM) with the possible states “Halted” and “Configured”. If all subsystems reach the state “Configured” the state machine of the central node jumps to “Configured” and indicates the whole trigger is in a well defined state.

Cell Panels Cell panels provide a possibility to implement complex GUIs within the TS framework. They can be used for testing, configuration and monitoring of the different subsystem. Control panels can call commands via SOAP and use T-Store to communicate with the configuration database. They are web based using the AJAX cell which provides various classes to design a complex and efficient GUI. In fact a Control Panel consists of two applications, one on the server side, which is written on C++ and the AJAX GUI on the Client side. The communication between these two formally independently operating applications is performed via the CGI interface. The framework provides mechanisms to keep the communication between these applications synchronous.

6.2 Online configuration database

The online configuration stores parameters for all subsystems and is accessible via the TStore application of the XDAQ framework. This section only deals

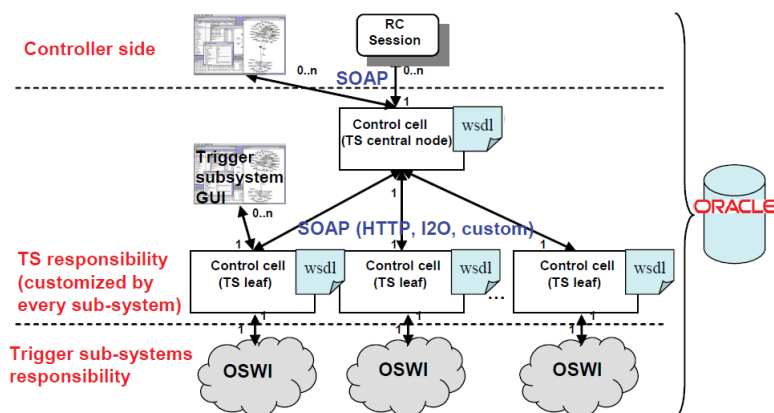


Figure 6.1.1: Concept of the Trigger Supervisor framework.

with a part of this huge database, the GT Trigger Menu Database, which will be needed later. The purpose of this database is to provide a central place to store L1 trigger menus. The tables store the information in a well-structured way. For the database an associative concept was chosen and there are only few keys the user has to deal with. To access a menu there are three possible keys:

- The Menu Interface key allows to access all technical triggers and algorithms and also their aliases (explained later). Menu interface names always have to start with the prefix `L1Menu_`: `L1Menu_Commissioning2010`. The Menu Interface therefore is the most abstract format for a menu.
- The Menu key points also to the L1 scales in use and gives implementation details of the particular algorithms. The names of Menu keys follow the convention:
`L1Menu_Commissioning2010/L1T_Scales_20080926_startup/Imp0`. `Imp0` in that case is the so-called algo implementation tag which allows a re-implementation of an algorithm pursuing the same physics goals.
- A complete menu can be accessed using the Menu Implementation key since it is also linked to all firmware specific implementation details of a trigger menu. The syntax of this key takes into account the firmware version number:
`L1Menu_Commissioning2009/L1T_Scales_20080926_startup/Imp0/0x1009`

Furthermore, it is also possible to access algorithms stand-alone, with a combination of an algorithm key and a scales key since algorithms are always implemented for a certain set of scales and cannot exist alone. Conditions, on the other hand, only get a physical meaning if they are linked to algorithms since there is no direct association between condition key and scales keys. The algorithm aliases mentioned above carry information of the HLT to keep it independent from implementation details of the L1-Trigger. A possible use case is a change of scales at first level. Then of course some algorithms would have to be re-implemented to pursue the same physics goals and get a new name in that case. If the HLT menus would point to these names they also would have

to be changed as a consequence. To avoid this the aliases were introduced since they can be kept constant despite of the names being changed.

Chapter 7

The L1 Trigger Menu Editor

The complexity of the Global Trigger at CMS including the trigger menus required a tool that makes it possible to generate new menus and edit existing ones without knowing details of the hardware implementation of the Global Trigger and the structure of the online database. Keeping this in mind the L1 Trigger Menu Editor (TME) was developed. In principle it could be considered as an interface between physics and hardware, that does not know anything about physics and scales. On the one hand it enables physicists to produce VHDL code, corresponding to a desired trigger menu, which is the source for GTL firmware without the need to program explicitly in VHDL, and on the other hand it saves the entire content of a trigger menu to the online database (OMDS). Performing these steps by hand without an integrated software solution that automatizes them would be a pretty time consuming and frustrating experience, the risk of errors would be extremely high. The Trigger Menu Editor hides a big share of the complexity of the task from the user and therefore allows him or her to focus on the essentials. It enables the user to develop a trigger menu from the initial idea until the VHDL code for FPGA chips on the GTL boards at one location. The actual firmware for the GTL board can safely be produced compiling the VHDL code using Altera QUARTUS, a commercial tool. Furthermore, it guarantees the consistency of this firmware with the database. From there the information can be read to reproduce a particular trigger menu and be copied to the CMS offline database where it serves as base for further data analysis. The TME was integrated in the existing CMS software infrastructure and uses existing functionality as far as possible in order to keep the project maintainable. A detailed description of the concept and the implementation of the L1 Trigger Menu Editor will follow in this section.

7.1 Requirements

7.1.1 Functional requirements

The principal functional requirements for the TME, some of which have already been mentioned before, are:

- to provide an easy way to create a new trigger menu from scratch or from an existing one. Possible changes of an existing menu, to be saved

eventually as a new menu are for example additional conditions and algorithms or changes of the header information, which also contains the cabling keys for external conditions and technical triggers or the removal of entire algorithms

- to produce the VHDL code which corresponds to a trigger menu on the fly, hiding all the implementation details of the code from the trigger expert who is using the tool
- to apply consistency checks while a menu is being processed
- to apply cross-checks on the consistency of all conditions and algorithms that are used by a local menu with the database
- to be able to deal with different sets of detector scales
- to store a trigger menu in the database and read it from there
- to generate new cabling keys for technical triggers from scratch or based on existing ones
- to generate condition names automatically following a defined convention in order to keep the configuration database as transparent as possible
- to provide a back-up format for development versions of trigger menus that have not been finalized and therefore cannot be written to the database

7.1.2 Non-functional requirements

- The Trigger Menu Editor should provide an intuitive user interface, which focuses on the essential inputs and guides the user through the production process
- There should be an easily accessible instance of the software which does not need to be set up by the person intending to use it
- The project should be integrated in the existing software infrastructure at CMS (for example, use existing tools for accessing the database or use some classes from CMSSW representing the L1 trigger menu)
- The project should be kept modular and easy to maintain

7.2 Concept and first steps

The requirements from the previous section were taken as guideline for the concept of the L1 Trigger Menu Editor. As a first step a language had to be chosen mainly between the two alternatives Java and C++. Despite Java seeming to offer some advantages like its platform independence the decision clearly fell in favor of C++ since major parts of the existing software infrastructure (online and offline) have already been written in C++. Therefore the use of C++ seemed to be a pre-condition for an optimal integration with existing software. In a next step the basic concept for the project was developed as it is illustrated

in Fig. 7.2.1. As framework for the L1 Trigger Menu Editor the Trigger Supervisor was chosen in order to have it at the same location as the rest of the trigger online software and to be able to share some functionality with it. The online software for the configuration of the GT is located in the GT Cell which has also been implemented as a TS Cell. A second pillar of the project are the trigger object classes from CMSSW, that are used by the L1 Trigger offline software. They were already representing a complete trigger menu with all its parameters and therefore provided an ideal base for the L1 Trigger Menu Editor. To be able to use them for a future implementation of the TME they had to be made accessible for the online software from TS. How this was realized in detail will be described below. The parts of the software which are responsible for writing the VHDL code for the FPGA chips of the Global Trigger were moved to a separate package which in theory could be operated stand-alone, only using a trigger menu object as input. This package was called VHDL Writer. It uses VHDL templates, defining the basic structure of the VHDL code as a seed for the VHDL output. The concept and framework of the VHDL code for the GTL was already existing before the TME project was started, yet it still was lacking the flexibility needed for a smooth operation of the GT. From the TME it can be used as a kind of plug-in and is accessible by a wrapper panel. Once the VHDL code has been written, it is compiled using Altera Quartus [42] which produces the actual firmware for the GTL that can be loaded to the condition chips. Of course the database plays a central role within that concept since it interfaces the TME and therefore the GTL firmware with the rest of the CMS experiment. Menus stored in OMDS are accessible for configuration by the GT Cell and are also transferred to the offline database where the information can be used for data analysis. Since the scales for the trigger objects can change they have to be taken from the database. After this short introduction the implementation of the concept will be illustrated in more detail in the next sections.

7.2.1 The TME as TS Cell

As framework for the TME the Trigger Supervisor was chosen since almost the entire online software for the L1 Trigger was implemented that way. Within this framework, the TME was implemented as a separate TS cell, which is in principle independent from the GT Cell and the GT Test Cell. However, it shares some functionality with the GT Cell. The implementation within the TS has the advantage that the TME Cell can be operated on a server within the CERN network and therefore is accessible via web browser. The user does not have to set up any software environment if he or she wants to design a trigger menu but just has to call the URL. From outside CERN a SSH tunnel has to be opened. Operating the Cell within the CERN network furthermore brings the advantage that there is a fast access to the OMDS database which is located in the CMS private network. This speeds up the operation of the GUI compared to a software instance that is operated from a remote place (e.g. Vienna) and accesses the database via a tunnel. On the other hand it was challenging to develop a GUI of the complexity which was required to design a trigger menu using the ajax classes provided by the TS which just had freshly been developed when the development of the TME started. The main problem was the refresh time of several objects that made the GUI slow in situations where a big amount of content had to be reloaded. However, this problem almost disappeared with

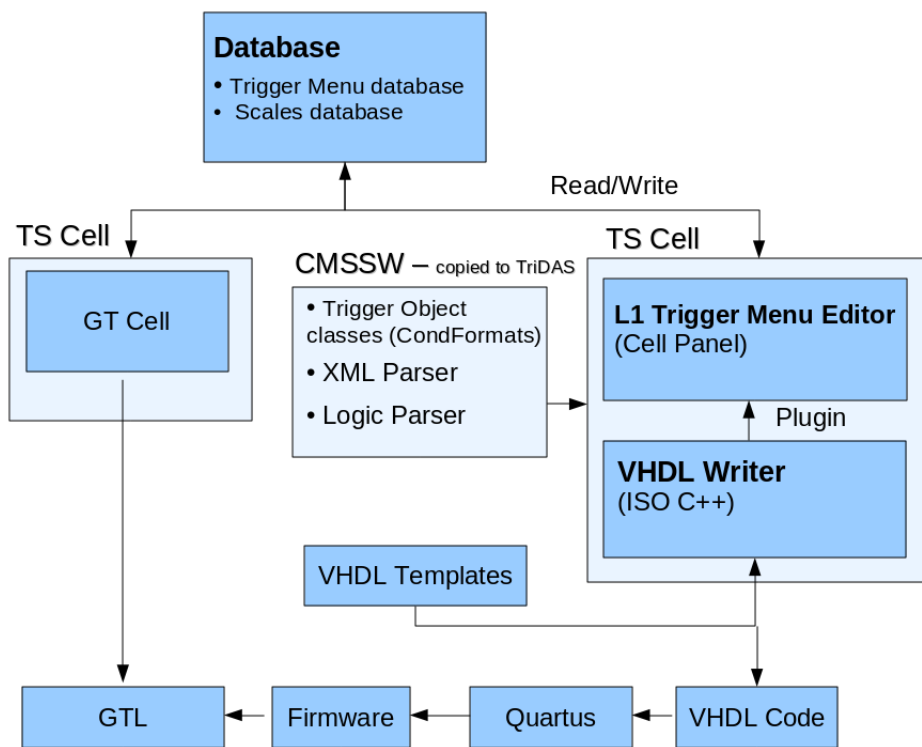


Figure 7.2.1: Integration of the L1 Trigger Menu Editor with the CMS software infrastructure.

more recent versions of the framework and the increasing speed of web browsers.

7.2.2 Integration of the CMSSW Classes

Since there were already classes for the L1 trigger menu existing in CMSSW these classes were chosen as base for the TME, which has the advantage that there is only one representation in the trigger software (both online and offline). Changes, if necessary, can be done at just one spot. The classes used by the TME are all part of the Level-1 Global Trigger offline software, used also by the L1 GT emulator software. The classes that are used by the TME were taken from three different packages:

- L1TriggerConfig/L1GtConfigProducers: From this package the L1GtXmlParser was taken. It can parse a complete trigger menu in XML format
- Cond Formats/L1TObjects: This package contains the trigger object classes which represent a trigger menu. The top of hierarchy class is the L1GtTriggerMenu which provides two maps as container for the trigger objects: L1GtAlgorithm and L1GtCondition. The L1GtCondition is a base class for the more specific template classes: L1GtCaloTemplate, L1GtMuonTemplate etc.
- Data Formats/L1GlobalTrigger: The only class taken from this package is the L1GtLogicParser which checks the syntax of logical expressions of L1GtAlgorithms.

However, the classes from CMSSW could not be used directly for the online software since they were located in a different CVS repository than the online software. Several ways to make them accessible were discussed: one way would have been to link the TME directly to the CMSSW library to make the required functionality available. This proceeding would have had the big disadvantage that CMSSW had to be installed on each machine operating TME, which could have led to complications. Therefore it was decided to copy the classes from the CMSSW CVS repository to the TriDAS CVS repository. This procedure was automatized using a shell script (`sync-with-cmssw.sh` in `../extern`) which checks out a defined tag of the CMSSW classes and synchronizes the local TriDAS environment with the recently checked-out version. After testing whether TME is working properly the updated classes can be checked-in to the TriDAS CVS repository manually. Most of the CMSSW classes which are used by TME are by purpose free of the CMSSW framework. Therefore they compiled in TriDAS immediately without any problems. The XML-parser, however, is using the CMSSW logger and thus would not compile in TriDAS without modifications. Therefore the script modifies this class automatically and forwards the stream originally dedicated to the CMSSW logger to a buffer, which can be dealt with from TriDAS.

7.2.3 Shared features with the GT Cell

The GT Cell is responsible for configuration and monitoring of the GT hardware. Therefore it needs read access to the online database where all relevant information for the configuration and a representation of the trigger menu is stored. During the configuration process the GT Cell also takes into consideration the information on the trigger menu, cross-checking the power-up values of

the energy thresholds in the firmware which are accessible via VME addresses with values stored in the database. Therefore it is able to read the trigger menu information from there. In order to avoid the use of duplicate code it was decided to use this functionality from the GT cell within TME.

7.3 VHDL Writer and the VHDL code for the GTL

The VHDL code for the GTL board in principle consists of two packages. There is a static package containing definitions that are constant as long as the requirements do not change. A possible introduction of new condition types for example would lead to a modification of this package. The second part of the VHDL code contains all definitions of conditions and trigger algorithms that are processed by the GTL. As these definitions are dependent on the trigger menu in use this package has to be produced dynamically and changes with every new trigger menu. As already mentioned in the overall description of the concept, the parts of the L1 Trigger Menu Editor that are responsible to produce the variable parts of the VHDL code form a sub-unit of the TME: the VHDL Writer was written in ISO C++ and was kept free of from both, the TS framework and CMSSW. At the beginning of the development the “VHDL Writer” was available in both, the TriDAS and the CMSSW CVS repository, however, maintaining both branches was to much effort and therefore it was not further maintained in CMSSW. The VHDL Writer uses a set of templates to produce the VHDL code. They are available in a human-readable format and can be modified with any text editor. As long as the structure of the output keeps constant and no files are added, the VHDL code simply can be changed by editing the templates without touching the source code of VHDL Writer. There are templates of two different categories which are referred to as “VHDL templates” and “internal templates”. The VHDL templates show the structure of a VHDL file containing substitution parameters of the format \$(substitution_parameter). The internal templates on the other hand contain string constants which can be used as content of the substitution parameters. Their syntax is illustrated here. Apart from the definition of string constants it allows the use of comments.

```

%% *****
%% -----This is an internal template-----
%% *****

%% I'm a comment

#PARAMETER_NAME
This is a parameter
##

%% Here the body starts
VHDL code

```

A class for VHDL templates To be able to deal with the templates in an optimized way a class has been developed which provides a set of basic needed routines. It is called `L1GtVhdlTemplateFile.cc` and supports both the standard format of VHDL templates as well as the more specific format of the internal templates. The most basic features are:

- to open a VHDL template file
- to save a file from the buffer under a new filename
- a simple routine to fill a substitution parameter with string content
- a routine to replace a substitution parameter with the content of another file
- a routine to append lines to a file
- a routine to append another file at the end of a file
- a routine that returns a list of all substitution parameters from a template file.

For opening an internal template a flag has to be set in the constructor. Then the set of string constants defined in that template are parsed and are available in a separate map. Internal templates also can have a body that consists of normal VHDL code.

The VHDL output The VHDL output is produced for the two condition chips independently in separate subdirectories which are created automatically. The class writing the output, using the `L1GtVhdlTemplateFile` as a tool is, the core class of the project, the `L1GtVhdlWriterCore.cc`. As input a map of conditions and algorithms filled with CMSSW trigger objects is taken. Then the templates are filled based on the content of this input. The two condition chips are processed independently. What follows is a short description of the output files.

cond_chip.vhd The `cond_chip.vhd` is the top of hierarchy file which contains the instantiation of all conditions. A mapping between condition names and a unique integer index is defined in that file which is used for the whole VHDL Code. The `cond_chip.vhd` is the only spot within the VHDL where condition names show up as strings. The mapping is also dumped to a simple text file in each output directory.

algo_and_or.vhd contains the definitions of the trigger algorithms with the condition names being replaced by numerical indices. The same indices are also used for the other files.

The setup files The setup files with file names ending with `_setup.vhd` are used to define the lookup tables in the firmware. At the moment LUTs are used for η , ϕ and the spatial correlations $\Delta\eta$, $\Delta\phi$. LUTs cannot be accessed via the VME and therefore only can be changed by creating a new firmware.

def_val_pkg.vhd The `def_val_pkg.vhd` stores power-up values for all parameters that are stored in VME registers in the firmware and can be modified via VME bus. The necessary addresses are stored in the database and additionally dumped to a simple text file for debugging.

algo_and_or.vhd The `algo_and_or.vhd` contains the definitions of all trigger algorithms for a specific chip. The names of conditions used by these algorithms are replaced by their firmware integer indices in the logical expressions. Due to internal definitions of the VHDL code the condition indices in this file differ by one from the rest of the VHDL code and start by 1 instead of 0.

7.4 Lookup tables in the VHDL code and mirror operations

An import process during the generation of the VHDL code is the calculation of the lookup tables for spatial parameters and correlations. Although this section might be a little bit technical it can be very useful for understanding the VHDL output. For the VHDL code the bitmasks that are displayed as clickable scales by the TME GUI have to be mirrored, which generally leads to some confusion. Therefore the mirror operations, performed by the VHDL Writer, will be explained in this section in all detail. The way such a TME bitmask is translated to VHDL code can be seen in Fig. 7.4.1. To understand the reason for this mirror operations let us consider a 16 bit LUT for example. Each bit in this LUT has its unique address starting at 0000 for bit 0 and 1111 for bit 15. Let us now consider a symmetric hardware scale that consists of 14 bins. The bin indices are: $\{-6, \dots, -0, +0, \dots, +6\}$. In the real implementation of the firmware such a scale for example is used for η of calorimeter objects. In the VHDL code these hardware bin indices are translated to the binary addresses for bits of the LUT. Bin $\{-4\}$ would be assigned to the address "1100" with the MSB defining the minus sign (provided the scale in use is a η scale this bin would correspond to the range $[-1.7399 ; -1.3920]$). The addresses of all negative hardware bins are listed in the following table:

Bin	Address (binary)
-6	1110
-5	1101
-4	1100
-3	1011
-2	1010
-1	1001
-0	1000

We observe that the lowest bin $\{-6\}$ of our hardware scale has the highest address 1110 corresponding to LUT bit 14. For the negative bins the rule is that the lower its index is the higher is its address within the LUT. This is no magic but simply due to the fact that the function `bin -> address` uses the MSB for the minus sign of negative differences. For the bins $\{0, \dots, 6\}$ there is no such

TME Bin	HW Scale	Physics scale
#0	-6	[-3 ; -2.172]
#1	-5	[-2.172; -1.74]
#2	-4	[-1.74; -1.392]
#3	-3	[-1.392; -1.044]
#4	-2	[-1.044; -0.696]
#5	-1	[-0.696; -0.348]
#6	-0	[-0.348; 0]
#7	+0	[0; 0.348]
#8	+1	[0.348; 0.696]
#9	+2	[0.696; 1.044]
#10	+3	[1.044; 1.392]
#11	+4	[1.392; 1.74]
#12	+5	[1.74; 2.172]
#13	+6	[2.172; 3]

Table 7.1: The mapping between a hardware scale, a TME bitmask and a physics scale.

inverse order since the MSB is always zero. The higher the bin index the higher is their address:

Bin	Address (binary)
+6	0110
+5	0101
+4	0100
+3	0011
+2	0010
+1	0001
+0	0000

It is said that the negative bins are mirrored which means that the address of the highest negative bin follows that of the highest positive bin and the lowest negative bin gets the lowest address within the LUT (there can be a gap in-between, depending on the size of the LUT). The addresses 7 and 15 are not used in this schema. After understanding the principle all mirror operations performed by VHDL Writer will be listed in this section for the sake of convenience. A possible mapping between our sample hardware scale, a TME bitmask and a physics scale is given in Table 7.1. As example for the physics scale a calo η scale has been chosen that fits that schema.

This principle basically is valid for all mirror operations that are performed by the TME. However, the length of the TME bits and the LUT can vary for the different cases. For convenience all mirror operations performed by TME can be found in Appendix A in all detail.

7.4.1 VME Addresses

Since the thresholds and some other parameters in the firmware can be set via VME bus, VME addresses for these parameters have to be calculated during

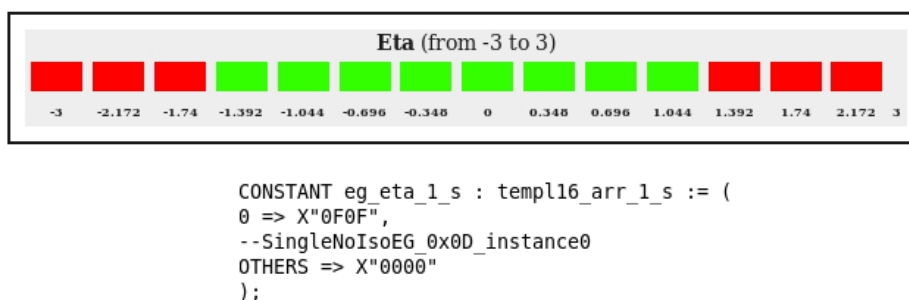


Figure 7.4.1: Example for a TME η input mask translated into VHDL code.

the firmware production process, which is done by the so-called VME Writer. The addresses for a condition are influenced by several parameters which are the condition category, the object type and the condition chip index of a condition (0 or 1). For conditions that consist of more than one template each object has its independent set of addresses. Therefore the object index influences the VME addresses as well. Last but not least the unique condition integer index, which is calculated by the VHDL Writer for each condition has to be taken into account. The VME Writer dumps a simple text file containing the VME addresses of all conditions in the output directory for each chip for debugging purposes and furthermore stores them in maps that can be written to database.

7.5 Scales

In the firmware implementation of a trigger menu, its thresholds and other parameters only consist of bitmasks, while the parameters carrying the spatial restrictions or correlations are implemented as look-up tables. Therefore the firmware does not know anything about physics scales. On the other hand, of course, a physicist, using the TME wants to understand the physical meaning of the bit masks and hardware thresholds he or she is dealing with. Therefore TME has to deliver their physical interpretation and operate as a kind of bridge between hardware and physics. Thereby it is especially important to have the possibility of different sets of scales since the scales available can change with time. The calorimeter scales, for example, can be defined in the GCT.

7.5.1 Available scales

The implementation of the L1 Trigger at CMS provides a high flexibility in the use of scales. Scales can be defined by the GCT and the GMT. The GCT allows independent scales for all calorimeter object types: each of them can use its own scales for the energy threshold, η and ϕ . Therefore for conditions of the category CondCalo, 15 scales in total exist. The objects from CondEnergySum (ETM, ETT, HTT, HTM) are allowed to use independent energy scales. The types ETM and HTM are additionally equipped with two independent ϕ scales.

For muon conditions there are independent η , ϕ and p_T scales. The HF Ring Et Sums have a scale for their E_T sum threshold.

7.5.2 Scales management

Due to this large diversity of scales it was important to find a reliable way to keep an overview of the scales available in general and, more specifically, which scales are in use for a particular trigger menu. Therefore it was decided to define the scales in the online database to have them at a location which is generally accessible. Each trigger menu is associated with a specific scales key, which corresponds to a set of scales in the database. When loading a menu or creating a new one, the trigger menus are always coupled with such a scales key. A trigger menu cannot exist standalone. Within TME there exists an interface that can be initialized from such a scales key, and once this is done these scales are available and in use until a new menu is loaded.

7.5.3 Scale-dependent implementation of algorithms

Changing the scales in use leads to some complications concerning algorithms since the naming convention for algorithms usually uses a physics threshold in the name of a L1 algorithm (e.g. L1_SingleJet10). If scales change this algorithm would suddenly get a completely different meaning, which is potentially dangerous since the name still implies its old implementation. With the database content increasing that would have definitely led to some confusion. There were several possible approaches to avoid that trouble. One possible approach was just to leave out the physics thresholds of the algorithm names, which would have made the DB much less human readable. The way that was chosen was a different one: to solve the problem the database scheme was extended in a way that it allowed to implement an algorithm independently for each set of scales by introducing another instance for algorithms the, the abstract algorithms which are connected with the actual algorithms via a association table. That way the algorithm L1_SingleJet10 can be implemented for each set of scales key independently, which keeps the database a lot more transparent and does not have any restrictions in functionality.

7.5.4 Interpretation of hardware differences of spatial correlations

Another problem concerning scales that had to be solved was to find the correct interpretation of the hardware differences calculated by the trigger for the spatial correlations of two objects, $\Delta\eta$ and $\Delta\phi$. To illustrate the matter let us consider what happens if the hardware calculates a difference in ϕ between two calorimeter objects. The ϕ scale for each participating calo object has 20 bins at the moment. Taking two ϕ scales and considering the possible differences between two objects in hardware bins there is a minimal difference of zero bins and a maximum difference of twenty bins. However, since there is no preferred direction in the hardware for the calculation of the differences at maximum ten bins are relevant for $\Delta\phi$: a difference of 20 bins, for example would be equivalent to a difference of 0 bins due to this symmetry, which is consistent with the fact that the maximum relevant physical difference is 180° . Therefore differences of

0,20, 1,19 ... 10,10 bins are considered to be identical. Figure 7.5.1 shows how the hardware differences can be interpreted from a physics point of view: The fact that both objects are seen in the same bin ($\Delta_{HW} = 0$) means that they can have a minimum difference of zero (they coincide) and a maximum difference in ϕ of 20 degrees (if they are seen close to the borders of the ϕ segment). If the objects are located in two segments next to each other ($\Delta_{HW} = 1$) their minimum difference is also 0 degrees (if both objects are located very close to the inner border of the two ϕ segments) and their maximum difference can be 40 degrees applying the same argumentation. The biggest difference of $\Delta_{HW} = 9$ in theory would show a difference of 160 to 200, however, of course 200 for the hardware is the same as 160 because of the symmetry described above. Therefore the physical interpretation of the last bin of the $\Delta\phi$ scale is 160 - 180. The situation gets even a little bit more complicated if the ϕ scales of the two compared objects show a translation. At the moment that is the case for correlations between calo objects and EnergySums for example (The calo ϕ scale starts at 350 while the scale for EnergySums starts at 0 degrees). In that case the translation of the scales has to be added, which for example would increase the interval for bin 0 from [0;20] to [0;30]. The last bin would be [170;180] in that case, following the strain of thought from before. For $\Delta\eta$ the situation is also more complicated, since the η scales per definition are not linear. In the case of ϕ only the absolute difference of bins is relevant: If two particles are discovered in neighboring segments their maximum difference in ϕ will always be 40 degrees (apart from the exceptions described before). In contrast, for η eg. the difference of the neighboring bins 2 and 3 differs from that of the two neighboring bins 6 and 7 due to the non-linearity of the η scales. Considering a difference of two bins, using the present set of scales one can get differences from [0 ; 0.696] to [0 ; 1.26]. In the GUI the TME only displays the maximum possible difference for a bin, as a rough guideline. However, it is always possible to produce the matrix from Fig. 7.5.2 on the fly to look up the exact meaning of a hardware difference. The lines which are parallel to the diagonal and marked in a color symbolize a constant difference in hardware bins. However, the physical interpretation varies on these lines depending on the η segments that are subtracted from each other. One can could optimize the η resolution, restricting the compared objects in η . Considering the example from above it would be possible to achieve the better resolution of [0 ; 0.696] by additionally defining a narrow η window for the two objects which only allows the desired difference in η .

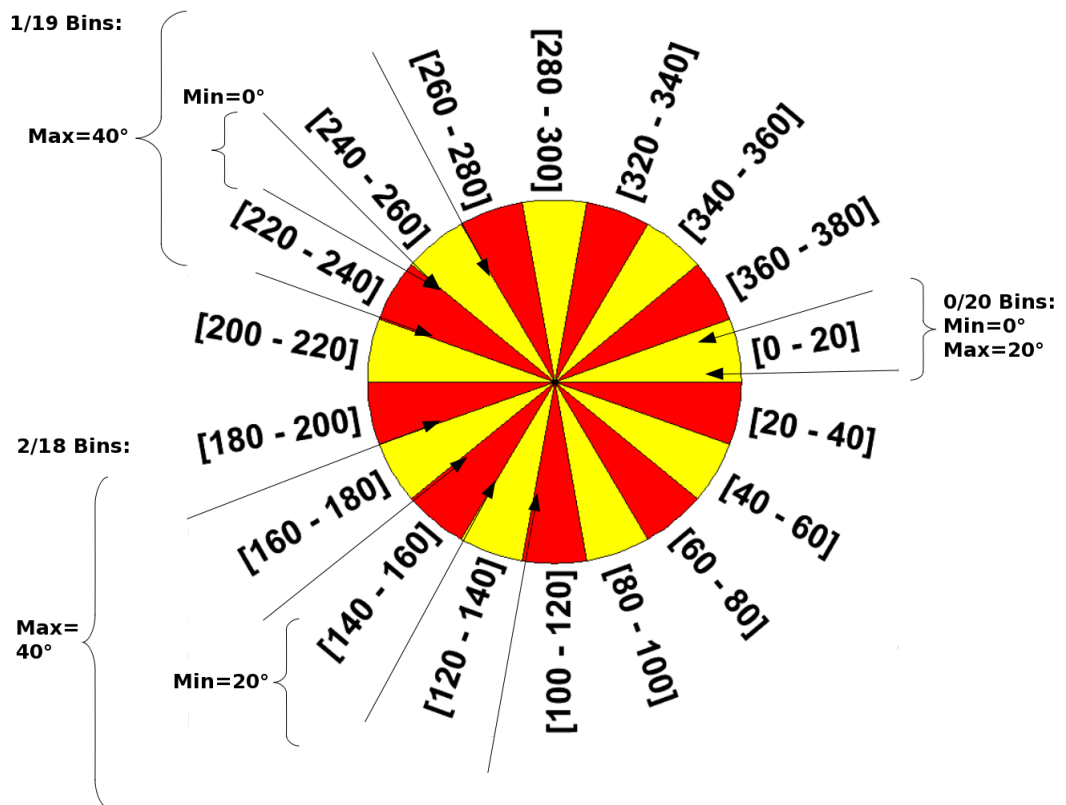


Figure 7.5.1: Illustration of the transformation from hardware differences to physics differences for $\Delta\phi$.

Delta Eta

Eta Scale	[-3;-2.172]	[-2.172;-1.74]	[-1.74;-1.392]	[-1.392;-1.044]	[-1.044;-0.696]	[-0.696;-0.348]	[-0.348;0]	[0;0.348]	[0.348;0.696]	[0.696;1.044]	[1.044;1.392]	[1.392;1.74]	[1.74;2.172]	[2.172;3]
[-3;-2.172]	HWI: 0 [0 ; 0.828]	HWI: 1 [0 ; 1.26]	HWI: 2 [0.432 ; 1.608]	HWI: 3 [0.78 ; 1.956]	HWI: 4 [1.128 ; 2.304]	HWI: 5 [1.476 ; 2.652]	HWI: 6 [1.824 ; 3]	HWI: 7 [2.172 ; 3.348]	HWI: 8 [2.52 ; 3.696]	HWI: 9 [2.868 ; 4.044]	HWI: 10 [3.216 ; 4.392]	HWI: 11 [3.564 ; 4.74]	HWI: 12 [3.912 ; 5.172]	HWI: 13 [4.344 ; 6]
[-2.172;-1.74]	HWI: 1 [0 ; 1.26]	HWI: 0 [0 ; 0.432]	HWI: 1 [0 ; 0.78]	HWI: 2 [0.348 ; 1.128]	HWI: 3 [0.696 ; 1.476]	HWI: 4 [1.044 ; 1.824]	HWI: 5 [1.392 ; 2.172]	HWI: 6 [1.74 ; 2.52]	HWI: 7 [2.088 ; 2.868]	HWI: 8 [2.436 ; 3.216]	HWI: 9 [2.784 ; 3.564]	HWI: 10 [3.132 ; 3.912]	HWI: 11 [3.48 ; 4.344]	HWI: 12 [3.912 ; 5.172]
[-1.74;-1.392]	HWI: 2 [0.432 ; 1.608]	HWI: 1 [0 ; 0.78]	HWI: 0 [0 ; 0.348]	HWI: 1 [0 ; 0.696]	HWI: 2 [0.348 ; 1.044]	HWI: 3 [0.696 ; 1.392]	HWI: 4 [1.044 ; 1.392]	HWI: 5 [1.392 ; 2.088]	HWI: 6 [1.74 ; 2.436]	HWI: 7 [2.088 ; 2.784]	HWI: 8 [2.436 ; 3.132]	HWI: 9 [2.784 ; 3.48]	HWI: 10 [3.132 ; 3.912]	HWI: 11 [3.564 ; 4.74]
[-1.392;-1.044]	HWI: 3 [0.78 ; 1.956]	HWI: 2 [0.348 ; 1.128]	HWI: 1 [0 ; 0.696]	HWI: 0 [0 ; 0.348]	HWI: 1 [0 ; 0.696]	HWI: 2 [0.348 ; 1.044]	HWI: 3 [0.696 ; 1.392]	HWI: 4 [1.044 ; 1.74]	HWI: 5 [1.392 ; 2.088]	HWI: 6 [1.74 ; 2.436]	HWI: 7 [2.088 ; 2.784]	HWI: 8 [2.436 ; 3.132]	HWI: 9 [2.784 ; 3.912]	HWI: 10 [3.216 ; 4.392]
[-1.044;-0.696]	HWI: 4 [1.128 ; 2.304]	HWI: 3 [0.696 ; 1.476]	HWI: 2 [0.348 ; 1.044]	HWI: 1 [0 ; 0.696]	HWI: 0 [0 ; 0.348]	HWI: 1 [0 ; 0.696]	HWI: 2 [0.348 ; 1.044]	HWI: 3 [0.696 ; 1.392]	HWI: 4 [1.044 ; 1.74]	HWI: 5 [1.392 ; 2.088]	HWI: 6 [1.74 ; 2.436]	HWI: 7 [2.088 ; 2.784]	HWI: 8 [2.436 ; 3.216]	HWI: 9 [2.868 ; 4.044]
[-0.696;-0.348]	HWI: 5 [1.476 ; 2.652]	HWI: 4 [1.044 ; 1.824]	HWI: 3 [0.696 ; 1.392]	HWI: 2 [0.348 ; 1.044]	HWI: 1 [0 ; 0.696]	HWI: 0 [0 ; 0.348]	HWI: 1 [0 ; 0.696]	HWI: 2 [0.348 ; 1.044]	HWI: 3 [0.696 ; 1.392]	HWI: 4 [1.044 ; 1.74]	HWI: 5 [1.392 ; 2.088]	HWI: 6 [1.74 ; 2.436]	HWI: 7 [2.088 ; 2.868]	HWI: 8 [2.52 ; 3.696]
[-0.348;0]	HWI: 6 [1.824 ; 3]	HWI: 5 [1.392 ; 2.172]	HWI: 4 [1.044 ; 1.74]	HWI: 3 [0.696 ; 1.392]	HWI: 2 [0.348 ; 1.044]	HWI: 1 [0 ; 0.696]	HWI: 0 [0 ; 0.348]	HWI: 1 [0 ; 0.696]	HWI: 2 [0.348 ; 1.044]	HWI: 3 [0.696 ; 1.392]	HWI: 4 [1.044 ; 1.74]	HWI: 5 [1.392 ; 2.088]	HWI: 6 [1.74 ; 2.52]	HWI: 7 [2.172 ; 3.348]
[0;0.348]	HWI: 7 [2.172 ; 3.348]	HWI: 6 [1.74 ; 2.52]	HWI: 5 [1.392 ; 2.088]	HWI: 4 [1.044 ; 1.74]	HWI: 3 [0.696 ; 1.392]	HWI: 2 [0.348 ; 1.044]	HWI: 1 [0 ; 0.696]	HWI: 0 [0 ; 0.348]	HWI: 1 [0 ; 0.696]	HWI: 2 [0.348 ; 1.044]	HWI: 3 [0.696 ; 1.392]	HWI: 4 [1.044 ; 1.74]	HWI: 5 [1.392 ; 2.172]	HWI: 6 [1.824 ; 3]
[0.348;0.696]	HWI: 8 [2.52 ; 3.696]	HWI: 7 [2.088 ; 2.868]	HWI: 6 [1.74 ; 2.436]	HWI: 5 [1.392 ; 2.088]	HWI: 4 [1.044 ; 1.74]	HWI: 3 [0.696 ; 1.392]	HWI: 2 [0.348 ; 1.044]	HWI: 1 [0 ; 0.696]	HWI: 0 [0 ; 0.348]	HWI: 1 [0 ; 0.696]	HWI: 2 [0.348 ; 1.044]	HWI: 3 [0.696 ; 1.392]	HWI: 4 [1.044 ; 1.824]	HWI: 5 [1.476 ; 2.652]
[0.696;1.044]	HWI: 9 [2.868 ; 4.044]	HWI: 8 [2.436 ; 3.216]	HWI: 7 [2.088 ; 2.784]	HWI: 6 [1.74 ; 2.436]	HWI: 5 [1.392 ; 2.088]	HWI: 4 [1.044 ; 1.74]	HWI: 3 [0.696 ; 1.392]	HWI: 2 [0.348 ; 1.044]	HWI: 1 [0 ; 0.696]	HWI: 0 [0 ; 0.348]	HWI: 1 [0 ; 0.696]	HWI: 2 [0.348 ; 1.044]	HWI: 3 [0.696 ; 1.476]	HWI: 4 [1.128 ; 2.304]
[1.044;1.392]	HWI: 10 [3.216 ; 4.392]	HWI: 9 [2.784 ; 3.564]	HWI: 8 [2.436 ; 3.132]	HWI: 7 [2.088 ; 2.784]	HWI: 6 [1.74 ; 2.436]	HWI: 5 [1.392 ; 2.088]	HWI: 4 [1.044 ; 1.74]	HWI: 3 [0.696 ; 1.392]	HWI: 2 [0.348 ; 1.044]	HWI: 1 [0 ; 0.696]	HWI: 0 [0 ; 0.348]	HWI: 1 [0 ; 0.696]	HWI: 2 [0.348 ; 1.128]	HWI: 3 [0.78 ; 1.956]
[1.392;1.74]	HWI: 11 [3.564 ; 4.74]	HWI: 10 [3.132 ; 3.912]	HWI: 9 [2.784 ; 3.48]	HWI: 8 [2.436 ; 3.132]	HWI: 7 [2.088 ; 2.784]	HWI: 6 [1.74 ; 2.436]	HWI: 5 [1.392 ; 2.088]	HWI: 4 [1.044 ; 1.74]	HWI: 3 [0.696 ; 1.392]	HWI: 2 [0.348 ; 1.044]	HWI: 1 [0 ; 0.696]	HWI: 0 [0 ; 0.348]	HWI: 1 [0 ; 0.78]	HWI: 2 [0.432 ; 1.608]
[1.74;2.172]	HWI: 12 [3.912 ; 5.172]	HWI: 11 [3.48 ; 4.344]	HWI: 10 [3.132 ; 3.912]	HWI: 9 [2.784 ; 3.564]	HWI: 8 [2.436 ; 3.216]	HWI: 7 [2.088 ; 2.868]	HWI: 6 [1.74 ; 2.52]	HWI: 5 [1.392 ; 2.172]	HWI: 4 [1.044 ; 1.824]	HWI: 3 [0.696 ; 1.476]	HWI: 2 [0.348 ; 1.128]	HWI: 1 [0 ; 0.78]	HWI: 0 [0 ; 0.432]	HWI: 1 [0 ; 1.26]
[2.172;3]	HWI: 13 [4.344 ; 6]	HWI: 12 [3.912 ; 5.172]	HWI: 11 [3.564 ; 4.74]	HWI: 10 [3.216 ; 4.392]	HWI: 9 [2.868 ; 4.044]	HWI: 8 [2.52 ; 3.696]	HWI: 7 [2.172 ; 3.348]	HWI: 6 [1.824 ; 3]	HWI: 5 [1.476 ; 2.652]	HWI: 4 [1.128 ; 2.304]	HWI: 3 [0.78 ; 1.956]	HWI: 2 [0.432 ; 1.608]	HWI: 1 [0 ; 1.26]	HWI: 0 [0 ; 0.828]

Figure 7.5.2: Physical interpretation of the hardware differences in η (non-linear).

7.6 Implementation details of the L1 Trigger Menu Editor TS Cell

For the implementation of the L1 Trigger Menu Editor a modular project architecture was chosen to keep things maintainable. The trigger menu classes from CMSSW could be considered as a kind of skeleton of L1 TME since they were already providing all features and parameters that were needed. The big challenge was to transform this skeleton into a construction kit a physicist can play with. In the CMSSW there was already existing a VHDL parser that allowed to produce a trigger menu object from a XML file. This feature was used very intensely at the beginning of the development process of the TME and is still available as a possible backup for unfinished trigger menus. However, it was decided not to use the XML file as interface between VHDL writer, offline software and TME since this would require more than one software representation of the L1 trigger menu. Instead the CMSSW classes were chosen as central representation for a trigger menu and all functionality was built around them. The TME on the one hand provides a graphical user interface for filling them, and on the other hand, they can be used as input for the VHDL writer or the database writer, a class which writes a trigger menu to OMDS. This way of implementation allows a certain back-end independence.

7.6.1 The user interface

The main objective during the development of the graphical user interface of TME was to provide an intuitive GUI which is more or less self-explaining on the one hand, and on the other hand prevents the user by a sophisticated infrastructure of cross-checks of all inputs from creating inconsistent trigger menus. In general TME is usable by non-expert users for browsing through existing trigger menus, however, the crucial features, that should only be used by experts require a password authentication as described below. All GUIs within the Trigger Supervisor were implemented as Cell Panels using the existing TS infrastructure for GUIs. Figure 7.6.1 shows the layout of the TME TS page. A scheme of the classes involved can be found in Appendix B.

Trigger Supervisor

- Commands
- Default
- Operations
 - Create
 - Destroy
- Control
- Control Panels
 - L1TriggerMenuEditor
- Monitoring & Alarms
- Hotspot
- Peers
- DB

New TM, Load XML, 2 XML, Load DB, 2 DB, New Algo, New Cond, Copy Cond, Header, VHDL, Help, Drop-down Lists, Tree, Connect, Restore GUI

Menu Interface: *L1Menu_Commissioning2009_vme*, Scaleskey:*L1T_Scales_20080926_startup*, Tag: *No tag applied!*, DB: *Depends on environment*

Calorimeter Condition *SingleCenJet_0x0F_Barrel_instance0*

Add object descriptions: Obj 0: Update Name

Condition Type: **Type1s: 1 single object**
Object Type: **CenJet: central jet**
Condition Chip: **2**
Algos using this condition: **L1_SingleJet30**

Delete Condition Change chip Remove DB Lock! Quit

CenJet 0

Energy threshold: [GeV]

Phi Range:

Phi range in degrees (starts at 350, Increment: 20)

350	30	70	110	150	190	230	270	310	350
-----	----	----	-----	-----	-----	-----	-----	-----	-----

Eta Range:

Eta (from -3 to 3)

-3	-2.172	-1.74	-1.392	-1.044	-0.696	-0.348	0	0.348	0.696	1.044	1.392	1.74	2.172	3
----	--------	-------	--------	--------	--------	--------	---	-------	-------	-------	-------	------	-------	---

Algorithms

- 1::L1_MinBias_HTT10
- 2::L1_SingleHFBitCountsRin
- 3::L1_SingleHFBitCountsRin
- 4::L1_SingleHFRingETSumsF
- 5::L1_SingleHFRingETSumsF
- 6::L1_SingleHFRingETSumsF
- 7::L1_SingleHFRingETSumsF
- 8::L1_DoubleHFBitCountsRin
- 9::L1_DoubleHFBitCountsRin
 - HFBitCounts_Ind2_0x1_i
 - HFBitCounts_Ind3_0x1_i
- 10::L1_DoubleHFRingETSum
- 11::L1_DoubleHFRingETSum
- 12::L1_DoubleHFRingETSum
 - HFRingETSums_Ind2_0x3
 - HFRingETSums_Ind3_0x3
- 13::L1_DoubleHFRingETSum
- 15::L1_SingleJet6
 - SingleCenJet_0x03_Barr
 - SingleCenJet_0x03_End
 - SingleForJet_0x03_Insta
 - SingleTauJet_0x03_Barr
 - SingleTauJet_0x03_End
- 17::L1_SingleJet20
- 18::L1_SingleJet30
 - SingleCenJet_0x0F_Barr**
 - SingleCenJet_0x0F_End
 - SingleForJet_0x0F_Insta
 - SingleTauJet_0x0F_Barr
 - SingleTauJet_0x0F_End
- 19::L1_SingleJet40
- 20::L1_SingleJet50
- 21::L1_SingleJet60
- 30::L1_SingleTauJet10

Support | About TS v1.9.0

Figure 7.6.1: Layout of the TME central panel. The tree on the left hand side is produced by the TS framework and can be used to create an instance of the central panel.

The central panel The central panel which is displayed right at startup and never disappears does not provide functionality itself and rather operates as a container for all functional panels and the trigger object panels. It consists of three independent sections each of which fulfills a different purpose. At the very top the panel displays the main navigation task bar that contains links to all important sub-panels and allows a fast access to them. It also displays the most important header information about the trigger menu in progress like its interface name and the scales key. The right quarter of the central panel is reserved for a tree that allows to browse through all algorithms and conditions in use. For displaying algorithms, conditions and the functional panels which are described below the content plane of the central panel can be used, for which the most space of the central panel is reserved and which can be filled dynamically.

Functional panels This class of panels can be accessed via the main menu of the central panel. In total there are ten of these panels, fulfilling different tasks.

- The first panel allows to create a new trigger menu from scratch. It is possible to define its name and select a scales key, which are the most important steps to begin the production process.
- There are two separate panels that allow the user to load a trigger menu from a XML file and export menus to that format. The panel to load a menu contains a browser for the local file system that enables the user to search for the desired file quite comfortably.
- There are also two database panels. The first one contains all read functionality. It is possible to import whole menus, standalone algorithms or even single conditions. The database writer panel has two purposes. If TME is operated in public mode it displays the password query to enable the write access (to database and local file system). Once enabled it is possible to write trigger menus to database, after writing their firmware. All parameters of the menu have to be in a well defined state before writing it to database and the panel only acts as wrapper for the `TmDatabaseWriter`.
- For setting the header parameters of a trigger menu the header panel (Fig. 7.6.2) can be used. The header information consists of a Menu Interface name, descriptions for Menu interface, Menu and Menu implementation, a firmware version which can be generated automatically by the panel and designer name and date. Furthermore a technical triggers cabling key and an external conditions cabling key for the trigger menu being processed have to be defined in this panel. Also the Algo Implementation Tag can be used by this panel.
- The firmware panel was written as a wrapper for the Vhdl Writer. Having defined all conditions and algorithms before and set the header information the user can produce the VHDL output for his trigger menu pressing a single button. Only a parent folder for the output directory has to be defined, the output directory, including all its sub directories will be created automatically.



Figure 7.6.2: The header panel as example for a functional panel.

- The naming convention in use:
output_L1Menu_NAME_L1T_Scales_SCALESKEY_ImpTAG_FWVERSION
- Last but not least there is a panel for adding new conditions to a menu. It guides the user to the desired condition in three steps. The first thing to be chosen is the condition category and chip followed by condition type and object and an optional suffix for the condition name in the last step.
- A panel to generate technical triggers cabling keys from scratch or from existing keys is also available. The panel allows to load a technical triggers cabling key from the database, modify it and write it back to database providing some useful features like an input mask to swap two bits or drop down lists with all available technical triggers.

The condition and object parameter panels These panels are providing GUIs to edit conditions and the objects they consist of. Their implementation schema more or less follows the structure of the CMSSW classes for conditions. There, like in the hardware, muon and calo conditions can contain up to four objects which are represented by so-called templates. In CMSSW the class L1GtCondition therefore was chosen as base class for the more specific templates. These derived templates are available for all different condition types and contain structures which represent the parameters of the different objects, so-called object parameters. In the TME a similar concept was used. There are condition panels for the distinct condition types are operating as containers for object parameter panels. These are displayed within the condition panels in a tab container. The panel for muon conditions can contain up to four object parameter panels for muons. The same can be stated for calorimeter conditions. The panel for correlation conditions can contain object parameter panels of two different types as it is required by this condition category. Figure 7.6.3 shows the representation of a muon object parameter in TME.

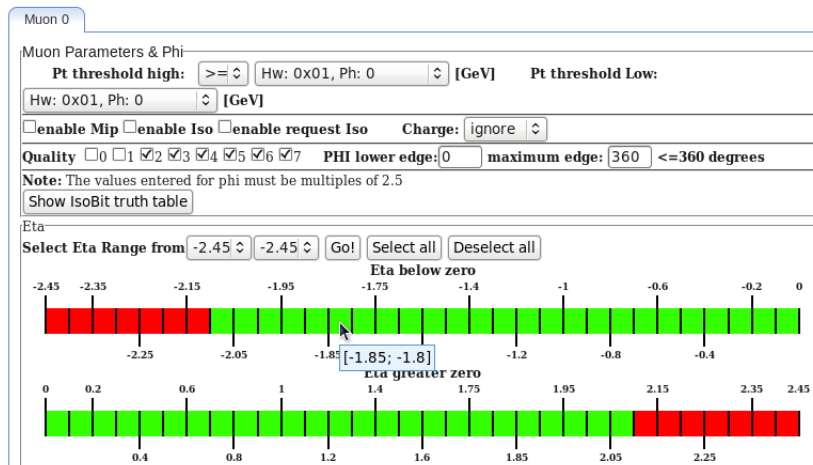
The algorithm editor panel The algorithm editor panel (Fig. 7.6.4) allows the user to add new algorithms to a menu and edit and delete existing ones.

Muon Condition *SingleMu_0x01_Open* + -

Add object descriptions: Obj 0:

Condition Type: **Type1s: 1 single object**
 Object Type: **Mu: muon**
 Condition Chip: **2**
 Algos using this condition: **L1_SingleMuOpen**

(a) The common header of all condition panels. The condition name is generated automatically apart from some optional object description that can be added manually.



(b) Example for a object parameter of a muon condition.

Figure 7.6.3: The implementation of conditions in the L1 Trigger Menu Editor.

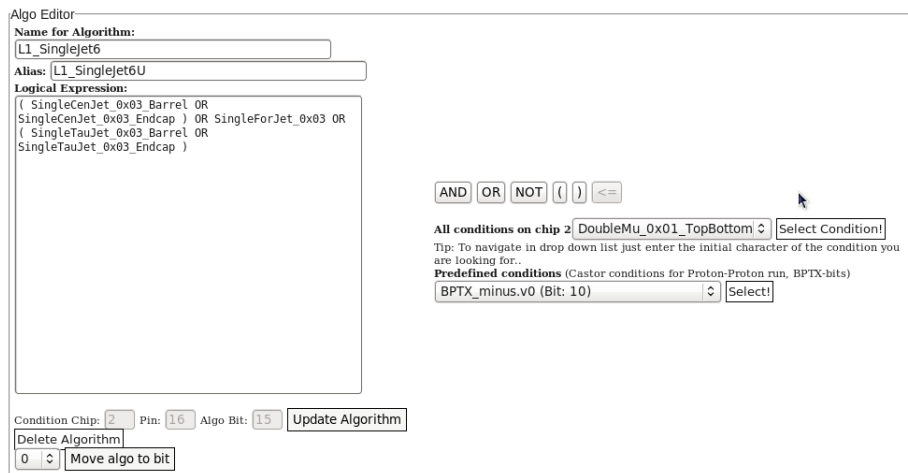


Figure 7.6.4: The algorithm editor panel.

Logical expression can be entered in human readable format combining condition names with the operators AND, OR and NOT. A syntax check for the user input is performed by the L1GtLogicParser from CMSSW. To increase the level of convenience there are drop down lists with available condition names which allow the users to select the conditions they want to use for their logical expression. The first list displays all conditions at the chip of the algorithm, the second one the available external conditions together with the bit they are assigned to by the cabling key in use. The logical operators can be added by pressing the helper buttons, which saves the users the effort of typing them by hand. At the bottom of the panel there is an input mask to change the algorithm bit. It is also possible to move algorithms between the two condition chips applying this feature.

The navigation tree The algorithm tree at the right border of the GUI is the most important utility to browse through a trigger menu. At the first level it shows the algorithms in use, ordered by their bits. Expanding the algorithms one can directly access all conditions that are used by the expanded algorithms. If desired the tree can be replaced by a set of drop-down lists which shows two separate, alphabetical list of conditions and algorithms.

7.6.2 Non - visible classes

The L1 Trigger Menu Editor core class This class is a base class for the L1TriggerMenuEditor.cc, which is implemented as a Cell Panel within the Trigger Supervisor framework. It contains basic features that are required to edit a trigger menu like copying or deleting conditions or generating their names automatically. The functionality was moved to this ISO C++ class to keep it independent from the Trigger Supervisor framework.

The XMLWriter This class which was also kept independent from the TS framework, can generate a XML file from a trigger menu. Thereby it uses the

tag definitions from the CMSSW XML parser, which has the advantage that these definitions are kept at one location. Like this the format of the XML file can simply be changed by modifying these tag definitions.

7.6.3 Automatic condition name generation

During the development process of TME it was decided to relieve users of the burden of choosing condition names manually due to the fact that this procedure turned out to be tedious, as a consequence of the naming convention for conditions: in contrast to algorithms, which have a physics threshold in their name, for conditions a naming convention was chosen such that they should carry their hardware thresholds in their names, for example “Double_Mu_0xFF”. The reason behind this convention is that in the database schema there is no direct connection between conditions and scales, which means that standalone conditions that do not occur in combination with an algorithm do not have a physical relevance. Therefore condition names should be independent from the scales. The convention in use at present is as follows:

- If all thresholds in a condition are equal it gets the name “Double_Mu_0xFF”
- If the thresholds differ the name looks like “Double_Mu_0xFF_0xFA”
- Additional descriptions for each object are allowed
“Double_Mu_0xFF_first_0xFA_second”

Of course the automatically generated names are always cross-checked with the database. If an identical name is discovered the user has two options: either he imports the existing condition from database or renames his local condition.

7.6.4 Consistency checks

To avoid mistakes during the operation of the trigger a series of sophisticated checks was implemented within the TME, intended to keep the produced output consistent and to minimize the number of possible errors.

External Conditions Cabling Key Changing the external conditions cabling key requires a consistency check with the algorithms that are currently in use. If one or more algorithms use external conditions that are not part of the cabling key, it cannot be used. If this case occurs the user will be informed that the desired key cannot be used for the menu. Therefore it has to be checked whether a selected cabling key is compatible with all local algorithms before it can be applied.

Algorithm names Due to the database schema algorithm names have to be unique. Therefore it is checked for each new algorithm, and also if an algorithm is renamed, if the desired name is already used either in the database or in the local development menu. Furthermore it is checked whether the names start with “L1_”, which is required by the naming convention for algorithms. On the other hand, algorithm aliases need not be unique within the database.

General checks on conditions and algorithms For conditions several cross-checks have been implemented which are listed below:

1. Database consistency: as already mentioned before there is a synchronous cross-check with the database. If the name of a local condition coincides with one of the conditions in the database the user is asked to either rename the condition or import it from database. That feature prevents any discrepancy between the local workspace and the database.
2. Cross-check with algorithms: since conditions are always used as parts of algorithms an additional cross check is required. If a local algorithm was imported from the database the conditions it uses have to be locked in the local workspace. Otherwise it would be possible to modify an algorithm from the database locally, which would mean that the local menu is inconsistent with the database. However, there is an easy way out of this dilemma. If the algorithm is renamed locally (of course the new name must not be used in the database) the conditions used by it can be changed without danger.
3. Conditions can only be deleted from the local workspace if they are not used by any algorithm. Otherwise the produced firmware would be faulty.
4. Due to the two condition chips available in hardware and software it has to be ensured that an algorithm can only use conditions that are available on its own chip.
5. Forbidden characters in condition names: Since condition names occur as indices in the VHDL code they must not contain characters the Quartus compiler cannot deal with.
6. The name prefixes have to be consistent with naming conventions, which is also checked by DB constraints. If a menu contains conditions that are violating this convention it cannot be written to the database.
7. The import feature for algorithms checks if an algorithm is implemented for the current set of scales. In case it is not is has to be re-implemented for the set of scales in use and therefore cannot be imported from the database.

Menu Interface name The Menu Interface name always has to start with “L1Menu_”. Otherwise it would also violate a database constraint.

Firmware version Since the firmware version in general has to be unique it has to be checked. When designing a new trigger menu there is no possibility to choose a firmware version that is already in use. An exception is the VME mode, which allows to associate a new trigger menu with an existing firmware (with severe restrictions, of course). In that case the version of the firmware the new menu has to be associated with has to be used. In that case it even cannot be changed.

Synchronization checks between the condition chips

1. Due to the fact that the trigger menu class uses two condition chips and single conditions can be used on both chips at a time, there has to be a consistency check since the conditions are formally independent on the different chips. If a condition is modified on chip 1, it has to be ensured that the changes are applied to its copy on chip 2 and vice versa.
2. If an algorithm is moved from one chip to another it has to be ensured that all conditions are physically present at the destination chip. In case a condition is missing, it has to be copied together with the algorithm.

7.6.5 The Trigger Menu HTML file

Each time when the VHDL code for a trigger menu is produced, an additional HTML file is written to the output directory, which contains all relevant information about the trigger menu in a human readable, very compressed format. The scales in use are also printed. Furthermore the bitmasks are equipped with a mouse-over effect which is showing the physical interpretation of the bins to improve legibility. The naming convention for the filename is:

L1Menu_Debug_21042010_v3_L1T_Scales_20080922_Imp0_0x0001.html

In the output directory can also be found a bash-script which uploads the entire output to a public web space, which is a fast and easy way to make the HTML file publically accessible.

7.6.6 Database access

Preprocessing of a trigger menu to produce multiple condition instances The GTL firmware stores the energy thresholds for all condition types and several other parameters in VME registers. At the same time the L1 Trigger Menu Editor allows the use of one condition in more than one algorithm, which has the unpleasant side effect that modifying the thresholds of such a condition might affect more than one algorithm. In most cases that effect would be rather inconvenient and it would be more desirable to have a unique VME address each time a particular condition occurs in an algorithm. For this purpose the concept of multiple instances of a condition was developed: before writing the VHDL code for a menu is preprocessed. During this process additional instances of conditions that are used by more than one algorithm are introduced. In case the algorithms L1_A and L1_B shared condition COND_C before the preprocessing algorithm L1_A uses COND_C_instance0 and L1_B uses COND_C_instance1. Considering their parameters COND_C_instance0 and COND_C_instance1 are exact copies of the original COND_C of course. With respect to their implementation in the firmware, however, the two freshly created instances are independent and therefore have independent VME addresses.

The Database Writer After producing the firmware for a menu, the menu can be written to database. Creating the firmware before writing a menu to the database is necessary in order to get the VME addresses for the VME parameters which are calculated during this process. In order to keep the database slim only new conditions and algorithms are written. If algorithms and conditions of the menu that has to be written are detected in the database, the existing version of

them will be linked to the new menu. For the actual writing process the TStore tool provided by the XDAQ framework is used.

7.6.7 The VME mode

Due to the fact that the GTL firmware stores particular parameters in VME registers these parameters can be modified via VME bus without creating new firmware. Therefore a VME mode in TME was implemented in which only these parameters, mainly the thresholds, are editable. When everything is modified the menu can be written back to the database as a new menu which uses an existing firmware key. However, a frequent use case for the VME mode is the following: If the only thing that has to be changed for a menu in use is the technical triggers cabling key this can comfortably be done with the VME mode. Of course, no thresholds have to be modified in that case. The menu is just loaded, activating the VME mode check box (see Fig. 7.6.5a), then the Technical Triggers Cabling key can be changed in the header panel, and finally the menu is written back to database. Also a new menu interface name has to be selected.

If one also wants to change the thresholds for a given menu, the following steps have to be undergone in order to guarantee that the modified menu is consistent with both the firmware version and the database.

1. The menu has to be loaded with the VME mode checkbox activated.
2. A new name for the menu has to be chosen in the header panel. The firmware version in that case cannot be changed.
3. Since algorithm names have to be unique, the algorithms to be changed have to be renamed. Once renamed, a drop down list with all thresholds of the algorithm appears and these can be modified.
4. The conditions the thresholds belong to will be renamed automatically. Here the user cannot interfere in the VME mode.
5. Once the changes are completed the menu can be written to database. If the hardware is configured with the new key that has been created the new thresholds will be set in the desired way.

The way a algorithm is displayed in the VME mode can be seen in Fig. 7.6.5b.

7.6.8 Operation of the L1 TME on a server and password protection

To make the TME easily accessible it was decided to have an installation on a server within the CERN network. To avoid unauthorized write access to the database and the local file system, an additional password protection mechanism was introduced. In the public mode all features providing write access to the database or producing output are disabled. What is not allowed in public mode is

- to store a trigger menu as a XML file on the local file system
- to produce VHDL code

Load Trigger Menu...

Available Menus:
 L1Menu_Commissioning2009_philipp2/L1T_Scales_20080926_startup/Imp0/0x101f


VME Mode
 (Only VME parameters can be edited and the menu can be written to Database as a new one **without** firmware being created before!)

Import algorithm to current menu...
 Available Algorithms (implemented for current scales):
 L1_BscHighMultiplicity

Available Algo Bits:
 14

Import condition to current menu...
 Available Conditions:
 Import the list below(Just copy and paste the names from the list into the text area, each condition a line)

(a) The VME mode can be activated checking the VME Mode check-box below the menu interface name in the database loader panel.



Menu Interface: *L1Menu_Commissioning2010_v0_vmeModified*, Scaleskey:L1T_Scales_20080926_startup, Tag: No tag a environment, VME Mode: active

Alias:

Logical Expression:
 QuadCenJet_0x03_0x04_0x03_0x04 OR QuadForJet_0x04 OR QuadTauJet_0x04 OR (TripleCenJet_0x04 AND (SingleForJet_0x04_VMEx0 OR SingleTauJet_0x04_VMEx0)) OR (TripleForJet_0x04 AND (SingleCenJet_0x04_VMEx0 OR SingleTauJet_0x04_VMEx0)) OR (TripleTauJet_0x04 AND (SingleCenJet_0x04_VMEx0 OR SingleForJet_0x04_VMEx0)) OR (DoubleCenJet_0x04 AND DoubleForJet_0x04_0x03) OR (DoubleCenJet_0x04 AND DoubleTauJet_0x04) OR (DoubleForJet_0x04_0x03 AND DoubleTauJet_0x04) OR (DoubleCenJet_0x04 AND SingleForJet_0x04_VMEx0 AND SingleTauJet_0x04_VMEx0) OR (DoubleForJet_0x04_0x03 AND SingleCenJet_0x04_VMEx0 AND SingleTauJet_0x04_VMEx0) OR (DoubleTauJet_0x04 AND SingleCenJet_0x04_VMEx0 AND SingleForJet_0x04_VMEx0)

Condition	Obj 1	Obj 2	Obj 3	Obj 4
DoubleCenJet_0x04	Hw: 0x04, Ph: 8 <input type="button" value="v"/>	Hw: 0x04, Ph: 8 <input type="button" value="v"/>		
DoubleForJet_0x04_0x03	Hw: 0x04, Ph: 8 <input type="button" value="v"/>	Hw: 0x03, Ph: 6 <input type="button" value="v"/>		
DoubleTauJet_0x04	Hw: 0x04, Ph: 8 <input type="button" value="v"/>	Hw: 0x04, Ph: 8 <input type="button" value="v"/>		
QuadCenJet_0x03_0x04_0x03_0x04	Hw: 0x03, Ph: 6 <input type="button" value="v"/>	Hw: 0x04, Ph: 8 <input type="button" value="v"/>	Hw: 0x03, Ph: 6 <input type="button" value="v"/>	Hw: 0x04, Ph: 8 <input type="button" value="v"/>
QuadForJet_0x04	Hw: 0x04, Ph: 8 <input type="button" value="v"/>	Hw: 0x04, Ph: 8 <input type="button" value="v"/>	Hw: 0x04, Ph: 8 <input type="button" value="v"/>	Hw: 0x04, Ph: 8 <input type="button" value="v"/>
QuadTauJet_0x04	Hw: 0x04, Ph: 8 <input type="button" value="v"/>	Hw: 0x04, Ph: 8 <input type="button" value="v"/>	Hw: 0x04, Ph: 8 <input type="button" value="v"/>	Hw: 0x04, Ph: 8 <input type="button" value="v"/>
SingleCenJet_0x04_VMEx0	Hw: 0x04, Ph: 8 <input type="button" value="v"/>			
SingleForJet_0x04_VMEx0	Hw: 0x04, Ph: 8 <input type="button" value="v"/>			
SingleTauJet_0x04_VMEx0	Hw: 0x04, Ph: 8 <input type="button" value="v"/>			
TripleCenJet_0x04	Hw: 0x04, Ph: 8 <input type="button" value="v"/>	Hw: 0x04, Ph: 8 <input type="button" value="v"/>	Hw: 0x04, Ph: 8 <input type="button" value="v"/>	
TripleForJet_0x04	Hw: 0x04, Ph: 8 <input type="button" value="v"/>	Hw: 0x04, Ph: 8 <input type="button" value="v"/>	Hw: 0x04, Ph: 8 <input type="button" value="v"/>	
TripleTauJet_0x04	Hw: 0x04, Ph: 8 <input type="button" value="v"/>	Hw: 0x04, Ph: 8 <input type="button" value="v"/>	Hw: 0x04, Ph: 8 <input type="button" value="v"/>	

(b) A algorithm with its thresholds in the VME mode.

Figure 7.6.5: The VME Mode.

- to write a trigger menu to the database
- to export standalone algorithms to database.

To enable these features the user has to authenticate with the database credentials. Once authenticated these features are available during the whole session. However, it is possible to read menus from the database or load them from a XML file also in public mode.

7.6.9 Firmware deployment

When the VHDL writer has finished its job, the commissioning process for the firmware can start. First the VHDL output has to be compiled using the Quartus compiler. This can be done executing a shell script. As a next step the firmware will be tested on a test crate which is an exact copy of the trigger crate at CMS and is physically located next to it. For testing the Global Trigger, there is a sophisticated test framework, the so called TestCell which has been developed within the TS. Getting into this in detail would be beyond the scope of this thesis, however, the principle of the tests is easy: Pattern files are created and used as input for both the GT Hardware and for the L1 Trigger Emulator. If everything is working fine the output of these two systems should be identical. In case there is a mismatch, the situation has to be investigated since there is either a bug in the GT hardware/firmware or in the L1 Trigger Emulator (if bugs in the TestCell and Pattern Test Writer can be excluded).

Chapter 8

Performance and Basic Rates Analysis

So far more than thirty different L1 trigger menus have been designed, consisting of both menus for the operation of CMS and menus that were only used offline for Monte Carlo simulations. This chapter is dedicated to some basic analysis of trigger rates for the menu L1Menu_Commissioning2010_v4 for a better understanding and optimization of the performance of the trigger. A list of all algorithms used in this menu can be found in Appendix C. Furthermore, a first physics result of the CMS experiment will be presented at the end of this chapter.

8.1 Analysis of trigger rates and trigger correlations

For a better comprehension and optimization of the performance of the L1-Trigger it is important to understand both the total post-deadtime L1 trigger rate and the rates of particular triggers together with the dependence of these quantities on the luminosity. One has to be able to adapt the prescale factors for a given menu in order to keep the L1 rate below the limit of the HLT input rate. Due to the non-linear relationship between luminosity and trigger rate one needs a tool that allows a systematic analysis. Such a tool should provide three basic features:

- It should be able to extrapolate the total L1 rate from the data and also simulate how this rate changes, given a modified set of prescale factors
- It should be able to extrapolate the rates of single triggers from the data in order to understand their contribution to the total rate
- It should allow to investigate the correlations between particular triggers to highlight redundancies

The basic idea was to implement this tool within ROOT [43], the data analysis framework used at CERN, as macros that can be operated standalone on a tree produced with CMSSW. ROOT is an object orientated data analysis framework

used extensively in high energy physics. It is using CINT, a C++ interpreter as a command line script processor which allows the ROOT macros being coded in C++. It can also compile the C++ macros using aCLiC compiler. The data to be dealt with is usually stored in ROOT trees or more basic ntuples, which are both implemented as C++ classes. Ntuples store the data in a tabular format, where each event corresponds to a separate row of a well defined length. ROOT trees on the other hand are much more flexible since they can store C++ objects and therefore their structure can get much more complex than that of ntuples. Provided the relevant data of one or more CMS runs is already available as ntuple or tree one could write a macro that analyzes these trees under the desired aspects. A second task was to find a way to create these trees in a more or less automatized way, which will be described at the end of this section. In total two macros have been developed to do the required analysis and rate predictions. The L1PrescalesSimulator focuses on the analysis of the total trigger rate and its dependency on the luminosity while, the L1RatesAnalyzer investigates trigger correlations and the rates of particular triggers.

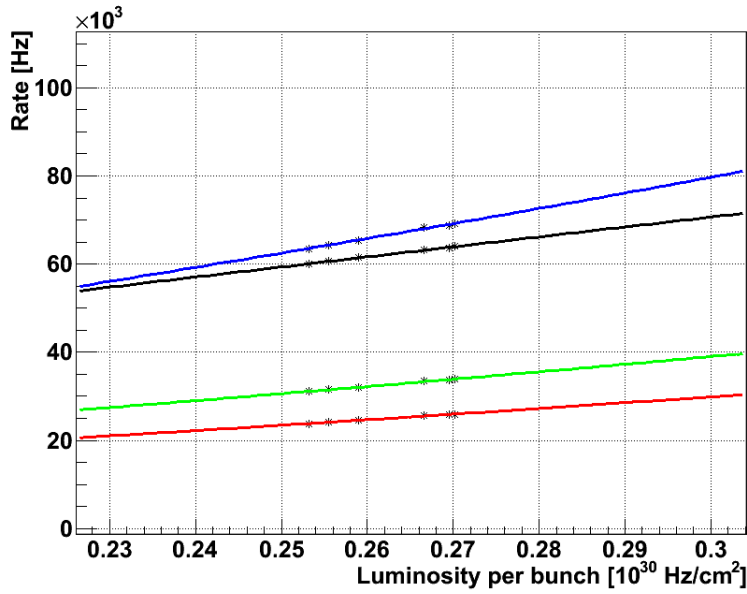
8.1.1 The total trigger rate versus luminosity

With an increasing luminosity of the LHC, the pre-scaling of the L1 triggers has to be adapted in order to keep the total L1 rate under control. Since during LHC operations the luminosity increases quite frequently a way was needed to analyze this dependency and make systematic rate evaluations for different sets of prescale factors. The input data is taken from the Nano DST data stream that provides a reduced event format optimized for the requirements of L1 trigger analysis. Especially important for this chapter is the L1 trigger word that is needed to reconstruct the trigger rates to be investigated. The events from this stream are an unbiased sample of events selected by the L1-Trigger, prescaled by a factor (currently 10) to get a reasonable rate. To get the post TCS dead-time rates from the data, one simply can loop over the available events since each event contains the GT trigger word which consists of 192 bits (the 128 L1 algorithms and the 64 technical trigger bits) and carries the information which triggers fired on that event. However, the decision word is written in the GT payload after prescaling but before the trigger masks (used to compute the Final-OR) are applied by the FDL. Therefore the Final-OR mask has to be applied to get the triggers that effectively fired on the particular event. One counts then how many events have been accepted for a given luminosity section. A luminosity section at the LHC is a well-defined data taking unit of 23.31 s for which the luminosity can be considered to remain constant. There is a well-defined mapping between luminosity section index and luminosity. This is in principle everything that is needed to plot the total trigger rate versus the luminosity. To predict the behavior of the L1 rate with increasing luminosities the data is fitted with a 2nd order polynomial due to the non-linear relationship between L1 rate and luminosity. To evaluate a modified prescaling based on the data basically the same loop can be used. However, events have to be ignored artificially with a frequency that is given by the desired prescaling. The curve obtained in that way is a good prediction how a modified prescaling influences the total L1 Rate. At the moment the prescale factor that is applied for the Nano DST stream is 10, therefore every 10th event is taken without bias. Due to the large number of events (about 100k) available per luminosity section the

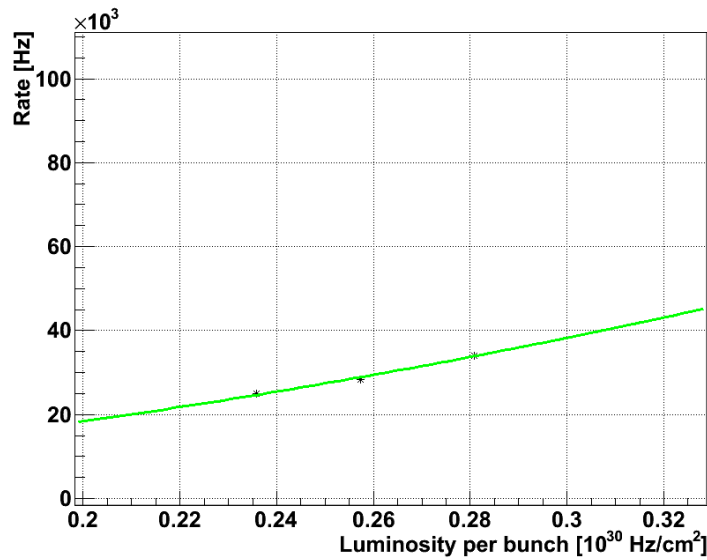
statistical uncertainty for the total trigger rate is small ($<1\%$). The systematic uncertainty on luminosity as measured at the LHC now is around 11% . One aims to improve it in the future to about 5% . The statistical error for the luminosity was estimated to be about 1% (Appendix C). Therefore, for luminosity the systematical uncertainty is dominant. For the rates analysis it is convenient to consider the luminosity per bunch for several reasons:

- During a fill the number of the circulating bunches keeps constant. However, due to losses within a particular bunch the luminosity per bunch and therefore also the trigger rate decreases during a run: it depends on the luminosity per bunch.
- For the moment the LHC is being operated with a bunch density of $1.1 * 10^{11}$ particles per bunch for proton-proton runs (which will not change until the end of 2010).
- If the number of bunches in a fill increases, the trigger rate can be extrapolated for the new number of bunches simply by stretching the curve by the factor N_{New}/N_{Old} if the dependence for N_{Old} is known and the rate is plotted against the luminosity per bunch, assuming the same bunch density. More bunches only means more collisions with the same luminosity per collision, therefore there is a direct proportionality.

Figure 8.1.1a shows the results of an evaluation of prescaled trigger rates for different fill schemes of the LHC, based on data of selected luminosity sections of run 143953. The purpose of this exercise was to find suitable prescale factors for a predictable increase of the number of bunches in an LHC orbit, keeping the L1 Rate in the region of 40 kHz. The effective trigger rate as it was reconstructed from data is represented by the black line in this plot. The rate plotted as a red line was extrapolated from the original rate, simulating a certain set of prescale factors being applied. The green line is an extrapolation of the prescaled rate to a fill schema of 47 colliding bunches, the blue line to a schema of 96 colliding bunches. Fig. 8.1.1b shows the total trigger rate versus luminosity per bunch for run 146511 with 47 colliding bunches in the LHC orbit. For this run the same prescale factors have been used online as for the previous prediction. Therefore it should be equivalent to the green line in Fig. 8.1.1a. At the first glance the two curves look quite similar but in fact the result obtained from the data slightly differs from the predicted curve. For a range of the luminosity per bunch from 0.2 to 0.3 the maximum difference between the predicted and the measured rate is about 3 kHz, which gives a deviation of 8 %, taking into account that the total rate is about 40 kHz for that particular case. This deviation can be explained by several factors like the non-linear dependence on the luminosity and an additional influence of beam parameters on the luminosity per bunch that might vary from run to run, especially during commissioning. In any case, the rate prediction should be always good enough for the purpose to estimate the prescale factors for a change in LHC luminosity with a precision of about 10%. In Appendix C a plot of the predicted rate from Fig. 8.1.1a and the measured rate from Fig. 8.1.1b can be found in the same plot together with the numeric dependences for both plots.



(a) Predicted, prescaled trigger rates for different fill schemes of the LHC with 47 and 96 colliding bunches, based on data from run 143953. The black line is the total trigger rate of this run. For the rate prediction six selected luminosity sections were used.



(b) The extrapolated trigger rate for run 146511 based on data from three selected luminosity sections.

Figure 8.1.1: Analysis of trigger rates and prediction of prescale factors.

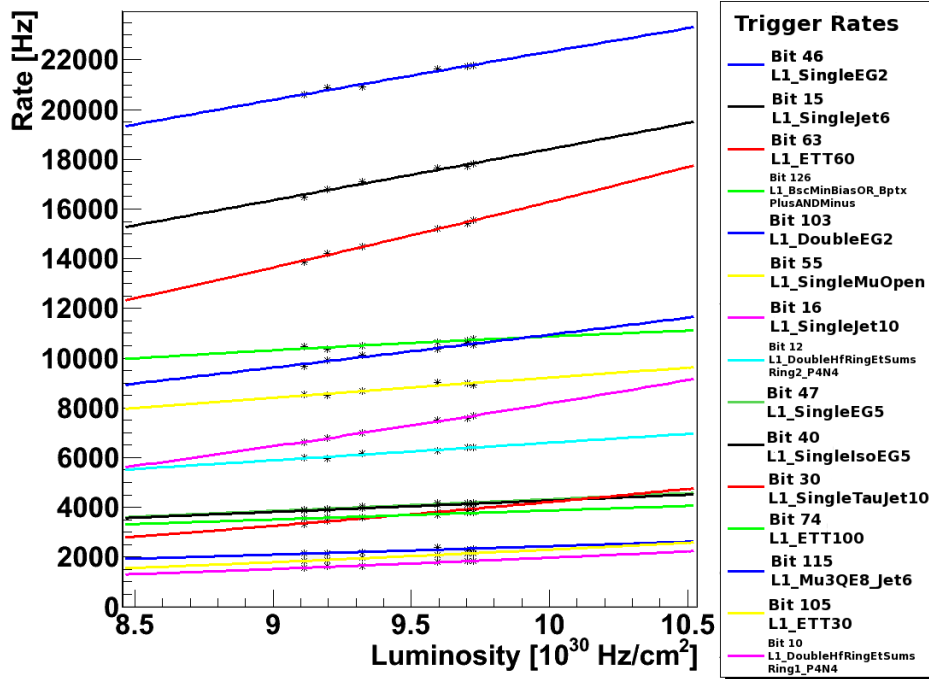
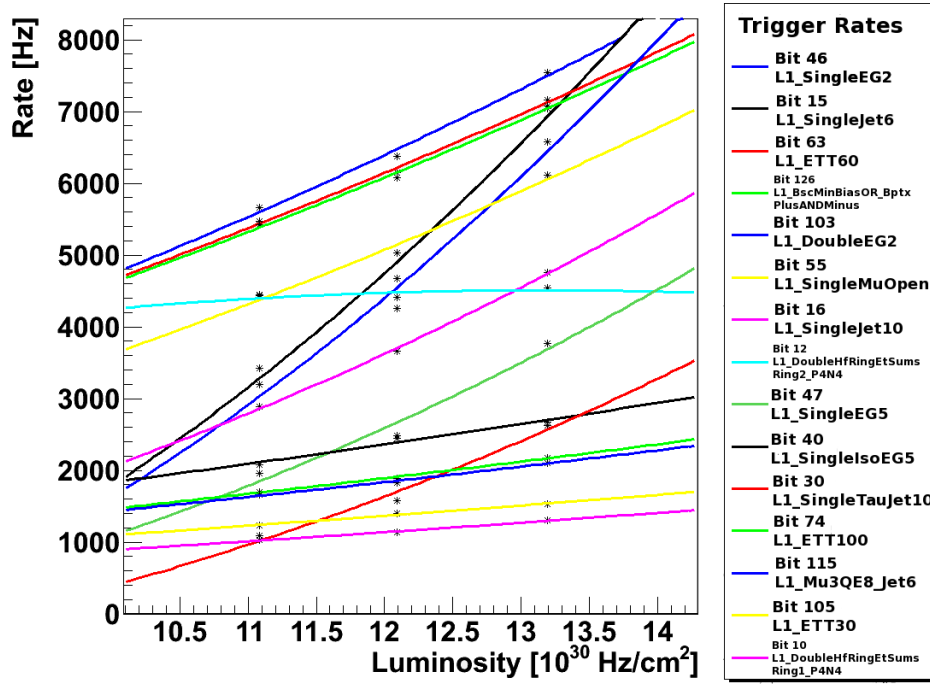


Figure 8.1.2: The 15 highest trigger rates for menu L1Menu_Commissioning2010_v4.

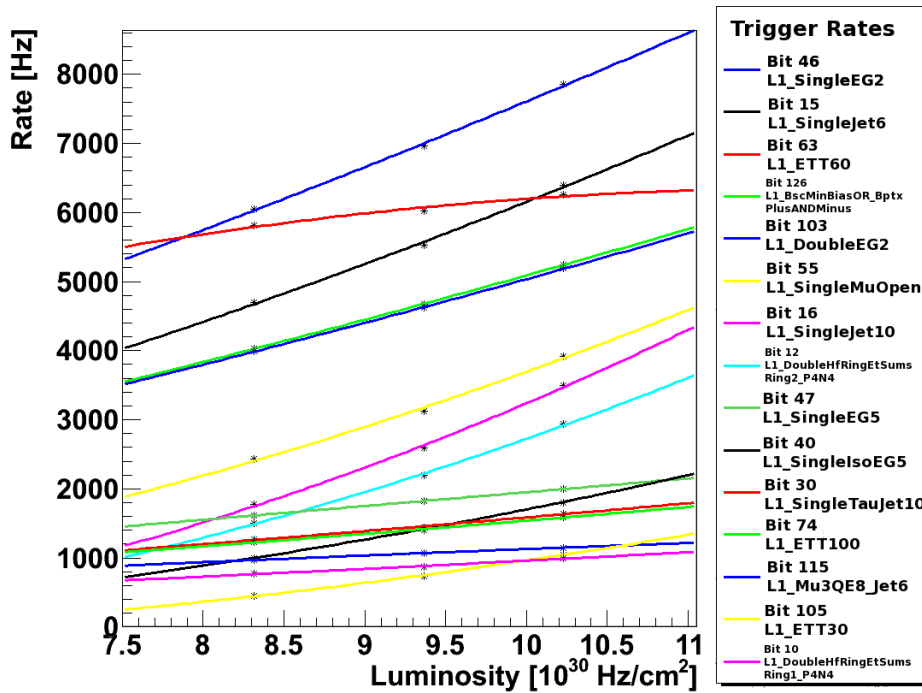
8.1.2 The rate of particular triggers versus luminosity

In addition to the total L1 rate, one also needs the contribution of each particular trigger to the total rate. The proceeding is very similar to that from before, however, now the different bits have to be taken into consideration separately. This time an event is only counted by the loop if the bit of interest has triggered on that event. Therefore one gets the rate for a certain algorithm or technical trigger. The L1RatesAnalyzer plots the trigger rates of the 15 most frequent bits and their dependence on the luminosity in one and the same histogram. The number is pretty arbitrary and can easily be modified via configuration. Figure 8.1.2 shows the rates of the unrescaled triggers for a luminosity region from about $8.5 - 10.5 \text{ Hz cm}^{-2}$. The rates of these top triggers cover a range from about 20 kHz (algorithm L1SingleEG2) to about 2 kHz (algorithm L1_DoubleHfRingEtSumsRing1_P4N4). It can be concluded that the triggers with dominant contributions to the L1 Rate are rather commissioning triggers than physics triggers, the rate of which stays in the region of 2 kHz.

Figure 8.1.3a considers the most significant trigger rates for a luminosity range from 10 to 14 Hz cm^{-2} based on selected luminosity sections for run 146511 from LHC fill 1366, which has been one of the most stable LHC fills so far. Comparing this plot to Fig. 8.1.2 the effect of the newly defined prescale factors gets visible which keep the peak rate below 10 kHz. The factors that were applied are the same as those which have been used for the prediction



(a) The rates of the 15 triggers with the highest rates have been analyzed for run 146511 from LHC fill 1366.



(b) The rates for run 146514 which was the last run of LHC fill 1366 with lower luminosities.

Figure 8.1.3: The highest trigger rates for two different runs at different luminosities.

performed before.

8.1.3 Correlations between different triggers

Another subject of investigation is the correlation between different triggers. Here the `L1RatesAnalyzer` also considers the 15 most frequent bits and draws a simple correlation table for them. The different fields in Fig. 8.1.4 describe the percentage of all events at which two triggers triggered synchronously. The diagonal shows auto-correlations of a certain trigger which are equivalent to the percentage of all events a trigger fired at. Of course, the correlation table is symmetric at its diagonal. Comparing the two plots in Fig. 8.1.4 it strikes out that the correlations generally increase with the luminosity. Furthermore, it is also clearly visible that some triggers got prescaled between the two Runs. The highest correlation in the unprescaled setup for run 143953 can be observed for the two algorithms `L1_SingleEG2` (bit 46) and `L1_DoubleEG2` (bit 103) which are triggering together in 8.20 percent of all events.

8.1.4 The work flow from the raw data to the root trees

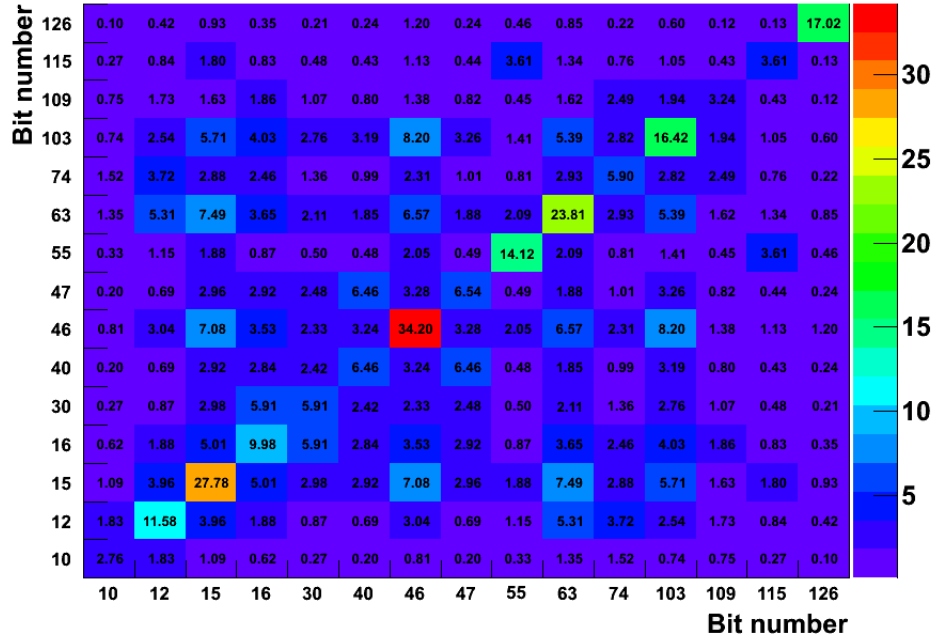
The workflow to create the ROOT tree used for rate predictions will be described in the following. Two steps are required in preparation for an analysis:

1. A ROOT tree from the NanoDST data has to be produced
2. A ROOT ntuple containing the luminosity information for the considered Runs has to be generated

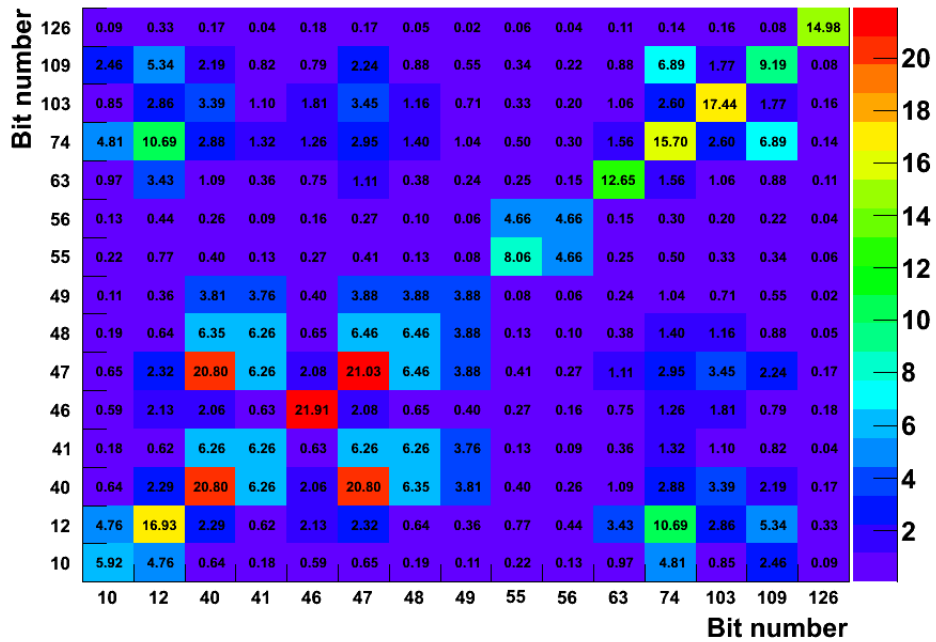
For step 1 two different approaches are possible: either the data tree is directly produced from the streamer files at CASTOR storage, where the raw data is stored; a more sophisticated solution is to use the CMS Remote Analysis Builder (CRAB) which starts a distributed GRID job. In the first case the CMSSW executable `cmsRun` is called directly with a python script that parses a configuration file. The preparation for both solutions is the same since both use a JSON configuration file as input which has to contain the following parameters:

- The run IDs to be considered
- Selected luminosity sections for each run

Retrieving the luminosities also involves the JSON file mentioned above, meaning that the analysis can be done from a single starting point. To obtain the luminosities CMSSW already provides a tool, the Python script `lumiCalc.py` which is used for that purpose. Here the work flow is as follows: A Python script parses the JSON file, calls `lumiCalc.py` with the run numbers as parameters and finally fills the obtained mapping between luminosity section and luminosity into a ROOT ntuple.



(a) Run 143953 with peak luminosities of about $10 \times 10^{30} \text{ cm}^{-2} \text{ sec}^{-1}$.



(b) Run 146511 with peak luminosities of about $16 \times 10^{30} \text{ cm}^{-2} \text{ sec}^{-1}$.

Figure 8.1.4: Correlation table for the 15 bits with the highest rates for two different runs.

8.2 A first result of the CMS experiment

In September 2010 the CMS collaboration published first results on angular correlations for charged particles which are emitted at different center-of-mass energies. The data was taken for proton-proton collisions at energies of 0.9, 2.36, and 7 TeV. In total two related studies have been performed one of which investigates short-range correlations in data collected with a minimum bias trigger for a $|\Delta\eta| < 2$ at all the three of the energies mentioned above. The second study focuses on the long-range structure ($2.0 < |\Delta\eta| < 4.8$) of two particle correlation functions, depending on the particle transverse momentum and the charged particle multiplicity at 7 TeV center-of-mass energy. In order to study high multiplicity events a special high multiplicity trigger was implemented at both levels of the CMS trigger system. At L1 a very simple algorithm was used, demanding the total transverse energy to exceed a 60 GeV threshold (L1_ETT60). For the HLT a more complex online vertexing algorithm has been applied. Fig. 8.2.1 shows a plot of the two particle correlation function at 7 TeV for both ordinary minimum bias and high multiplicity events. For high multiplicity events at a p_T range of $1 < p_T < 3$ GeV/c (Fig. 8.2.1d) a “ridge”-like structure emerges with an extension in $|\Delta\eta|$ of at least 4 units that has never been observed for pp or $p\bar{p}$ collisions. Also Monte Carlo simulations did not predict this effect. However, the effect shows similarities to structures which have been observed at heavy ion experiments such as PHOBOS at Relativistic Heavy Ion Collider (RHIC) [44]. Carefully applied cross-checks could exclude the effect being an interplay of systematic errors in the detector, the trigger and the analysis code. The statistic uncertainty of the analysis is considered to be negligibly small. To find a physical explanation for these new two particle correlations at high multiplicity further efforts will be needed due to the small dimensions of the effect and the complex environment being involved [45]. This is an example of how a very flexible and performant trigger system (L1 and HLT) allows an efficient selection of data for physics analysis.

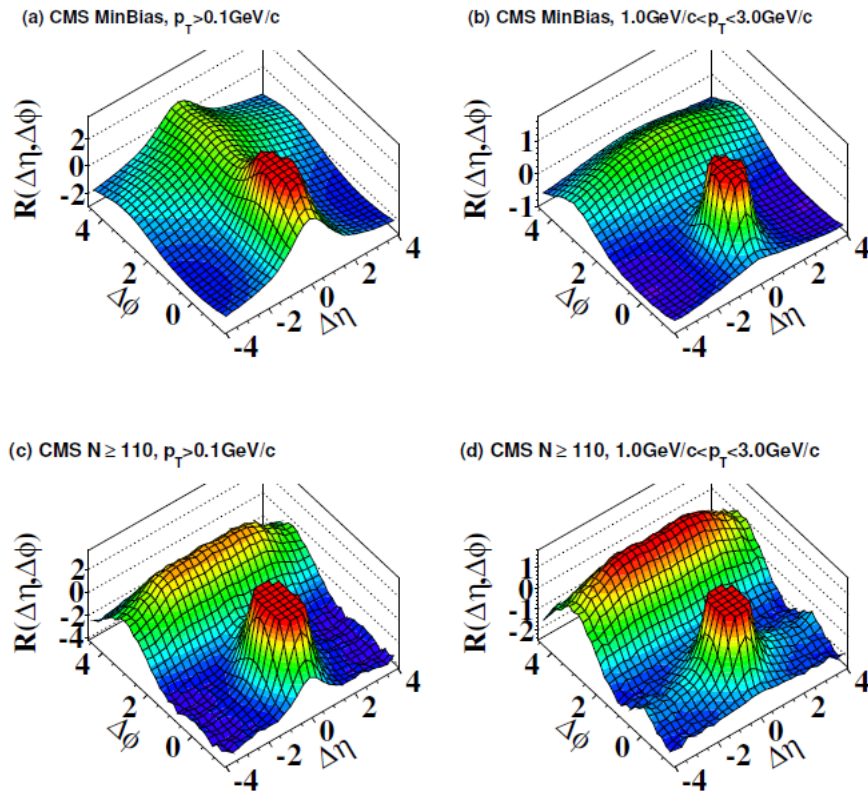


Figure 8.2.1: Correlation plot of the 2 - particle correlation observed at CMS for high multiplicity events (right plot). The ridge-like structure emerges in (d).

Chapter 9

Summary and Perspectives

The principal goal of this thesis, to provide an efficient and integrated solution for the production of L1 trigger menus at CMS has been achieved. Many of features of the L1 Trigger Menu Editor has already been used and tested during operation of the trigger. Furthermore, function tests have been performed which showed that the GT hardware operates in good agreement with the GT emulator and therefore proved the consistency between online and offline software of the trigger. So far various different menus for commissioning, data taking and simulation have been produced. Some of them were designed under considerable time pressure, proving that it is possible to produce and validate a new L1 trigger menu at CMS within a day, if needed. At the time of writing this summary, it is possible to generate a physics menu from scratch, write it to the online database and afterwards create the VHDL code for the firmware of the GTL condition chips at one single location. The compilation of the firmware, its testing and its deployment still involve several distinct steps. Here certainly one could think of the development of a more integrated work flow for the future. However, in combination with the available documentation, it is already possible to produce and deploy a L1 trigger menu in a safe, fast way, therefore integrating the other steps would complicate unnecessarily the L1 Trigger Menu Editor.

The trigger rates analysis, forming the second part of this thesis, can be considered to be in a very basic prototype status at the moment. Here it was demonstrated how one could use the available environment to perform such an analysis and the results achieved could be used to estimate the prescale factors for the increase of the number of circulating bunches in the LHC from 36 to 47. Very recently further predictions have been done for higher luminosities. With the LHC luminosities further increasing the analysis of trigger correlations will gain importance. However, more complex analysis tools like for exclusive rates of particular triggers and a better integration of the tools with the software environment or a higher level automatization are possible extensions for the future. One could also think to integrate similar features into the Online Data Quality Monitoring (DQM).

Almost one year after the LHC started its regular operation one can conclude that the CMS experiment is operating smoothly and can be considered to be well prepared for the search for new physics. The LHC meanwhile has reached its foreseen center-of-mass energy of 7 TeV and has already achieved one of the

main goals for 2010: a luminosity of $10^{32} \text{ cm}^{-2}\text{s}^{-1}$. Whatever will be seen at CMS during the next months and years, it will be interesting.

Acknowledgments

First of all I would like to thank Claudia-Elisabeth Wulz for making this thesis possible within the challenging environment of the CMS Trigger Project and giving me the opportunity to come to CERN several times during my work what gave me an impression of the great atmosphere at this laboratory. The stays at CERN were an important experience for me and were always very motivating and inspiring for my work. I want to thank her also for her support in writing and finishing this thesis.

Furthermore, I want to thank Vasile Mihai Ghete, the scientific supervisor of the thesis, for his great support in getting into and dealing with such a complex project, to which this thesis is only a tiny contribution and in the same way I want to thank him for his countless worthy inputs for this thesis, many times beyond normal working times. Without his thorough revision it definitely would not look like it looks now.

An important role for this thesis played also Herbert Bergauer. Without his expertise on VHDL code and his countless explications on this subject I would have been really hard to deal with that matter and get the thing working.

I would like to thank Ivan Mikulec, Christian Hartl, Manfred Jeitler, Anton Taurok, Marc Magrans de Abril and Luigi Guiducci for the great collaboration and precious help in integrating the software at its final destination, the CMS experiment at CERN. Talking about this the countless coffee breaks with many interesting and exhilarating conversations come up to my mind. I really enjoyed working in the CMS Trigger team.

Financial support from HEPHY Vienna made the work for this diploma possible.

Last but not least I want to thank my brother and my family for their support and my great friends in Vienna and Barcelona, who will know that they are addressed to, for making the last years of my life a wonderful and unforgettable time.

Bibliography

- [1] G. Brianti, et al., *The Large Hadron Collider - Conceptual Design*. CERN/AC/95-05(LHC), 1995.
- [2] J. Ellis, *Physics at LHC*. hep-ph/0611237v1, 2006.
- [3] Giacomelli G.; Giacomelli R., *The LEP legacy*. arXiv:hep-ex/0503050v2, 2004.
- [4] D. Griffiths, *Introduction to elementary particles*. John Wiley & Sons, Inc., 1987.
- [5] B. M. Walter Greiner, *Gauge theory of weak interactions*. Springer Verlag, 2000.
- [6] A. Pich, *The Standard Model of Electroweak Interactions*. arXiv:0705.4264v1 [hep-ph], 2007.
- [7] e. a. The CDF, the D0 Collaborations: T. Aaltonen, *Combination of Tevatron searches for the standard model Higgs boson in the $W+W-$ decay model*. arXiv:1001.4162v3 [hep-ex], 2010.
- [8] I. Tsukerman, *Discovery potential at the LHC: channels relevant for SM Higgs*. arXiv:0812.1458v1 [hep-ex], 2008.
- [9] J. L. R. Michael Gronau, *Determining the Weak Phase γ From Charged B Decays*. arXiv:hep-ph/9509325v1, 2000.
- [10] Attila Krasznahorkay Jr. for the ATLAS and CMS collaborations, *Outlook for b Physics at the LHC in ATLAS and CMS*. University of Debrecen - Dept. of Experimental Physics, 2000.
- [11] A. M. Bogdan A. Dobrescu, Patrick J. Fox, *CP violation in B_s mixing from heavy Higgs exchange*. arXiv:1005.4238v1 [hep-ph], 2010.
- [12] G. 't Hooft, *Recent developments in gauge theories*. Proceedings, held in Cargèse, Corsica, August 26 - September 8, 1979, (1980), pp. 135-157, ISBN 0-306-40479-6, 1979.
- [13] C. Kounnas, *Grand unification with and without supersymmetry and cosmological implications*. World Scientific Publishing Co Pte Ltd., 1984.
- [14] J. S. Gianfranco Bertone, Dan Hooper, *Particle Dark Matter: Evidence, Candidates and Constraints*. arXiv:hep-ph/0404175v2, 2004.

- [15] S. P. Martin, *A Supersymmetry Primer*. arXiv:hep-ph/9709356v5, 2008.
- [16] J. L. Feng, *Supersymmetry and cosmology*. arXiv:hep-ph/0405215 v2, 2004.
- [17] H. S. Thomas Borne, Georges Lochak, *Nonperturbative Quantum Field Theory and the Structure of Matter*. Kluwer Academic Publishers, Dordrecht, Netherlands, 2001.
- [18] CMS Collaboration et al, *Search for MSSM/mSUGRA at DØ*. Springer-Verlag, 2003.
- [19] CMS Collaboration et al, *CMS Physics Technical Design Report Volume II:Physics Performance*. CERN/LHCC 2006-021, 2006.
- [20] L. Benucci, *Searching for extra-dimensions at CMS*. Journal of Physics: Conference Series 171 012090, 2009.
- [21] M. Kazana, *Discovery potential for Universal Extra Dimensions signals with four leptons in the final state*. CMS CR 2006/062, 2006.
- [22] E. Papantonopoulos, *The invisible universe: dark matter and dark energy*. Springer Heidelberg New York, 2007.
- [23] K. H. K. Eggert and A. Morsch, *Luminosity Considerations for the LHC*. CERN AT/94-04 (DI) LHC Note 263, 1994.
- [24] F. Ruggiero, *Nominal LHC parameters*. Phys. Rev. C75 (2007) 054913, 2003.
- [25] CMS Collaboration, “The CMS experiment at the CERN LHC,” *Journal of Instrumentation*, vol. 3, no. 08, p. S08004, 2008.
- [26] CMS Collaboration, *CMS TriDAS project : Technical Design Report; Volume I, The Level-1 Trigger*. CERN-LHCC-2000-038, 2000.
- [27] CMS Collaboration, *The CMS tracker system project: technical design report*. CERN-LHCC-98-006, 1998.
- [28] F. Hartmann and the CMS Tracker Collaboration, *Construction of the CMS Tracker*. doi:10.1016/j.physletb.2003.10.071, 2006.
- [29] CMS Collaboration, *The electromagnetic calorimeter project: technical design report*. CERN-LHCC-97-033, 1997.
- [30] CMS Collaboration, *Changes to CMS ECAL electronics: addendum to the technical design report*. CERN-LHCC-2002-027, 2002.
- [31] CMS Collaboration, *The Hadron Calorimeter Technical Design Report*. CERN/LHCC 1997-31, 1997.
- [32] CMS Collaboration, *The CMS tracker: addendum to the technical design report*. CERN-LHCC-2000-016, 2000.
- [33] CMS Collaboration, *CMS Physics Technical Design Report, Volume I: Detector Performance and Software*. CERN/LHCC 2006-1, 2006.

- [34] CMS Collaboration, *CMS TriDAS project : Technical Design Report; Volume II, Data Acquisition and High-Level Trigger*. CERN-LHCC-2002-26, 2002.
- [35] M. Jeitler et al., *The level-1 global trigger for the CMS experiment at LHC*. JINST 2 P01006, 2007.
- [36] HEPHY, *The Global Trigger Hardware Web Page*. <http://wwwhephy.oeaw.ac.at/p3w/electronic1/GlobalTrigger/GlobalTrigger.htm>, 2007.
- [37] CMS Trigger and DAQ group, J. Varela (ed.), *CMS L1 Trigger Control System*. CMS NOTE 2002/033, 2002.
- [38] M. Gulmini et al., *Run Control and Monitor System for the CMS Experiment*. arXiv:cs/0306110v1 [cs.DC], 2003.
- [39] I. Magrans de Abril, *The CMS Trigger Supervisor: Control and Hardware Monitoring System of the CMS Level-1 Trigger at CERN*. PhD thesis, Departament d' Electrònica, Universitat Autònoma de Barcelona, 2008.
- [40] Magrans de Abril, I.; Wulz, C.-E.; Varela, J., *Conceptual design of the CMS trigger supervisor*. IEEE Trans. Nucl. Sci. 53 474-483, 2006.
- [41] I. Magrans de Abril, M. Magrans de Abril, *Enhancing the User Interface of the CMS Level-1 Trigger Online Software with Ajax*. 15th Real Time Conference, Fermi National Accelerator Laboratory in Batavia, IL, USA, 2007.
- [42] Altera Corporation, *Quartus II Handbook Version 10.0 Volume 1: Design and Synthesis*. The Altera Quartus web page, 2010.
- [43] The ROOT team, *The ROOT Users Guide (v. 5.26)*. <http://root.cern.ch/>, 2009.
- [44] PHOBOS Collaboration, *Cluster Properties from Two-Particle Angular Correlations in pp Collisions at $\sqrt{s} = 200$ GeV and 410 GeV*. 2007.
- [45] The CMS Collaboration, *Observation of Long-Range, Near-Side Angular Correlations in Proton-Proton Collisions at the LHC*. CERN-PH-EP/2010-031 2010/09/22, 2010.
- [46] C.-E. Wulz, *Concept of the First Level Global Trigger for the CMS experiment at LHC*. Nucl. Instrum. Methods Phys. Res., A 473 (2001) 231-242, 2001.
- [47] The LEP Collaborations: ALEPH Collaboration, DELPHI Collaboration, L3 Collaboration, OPAL Collaboration, the LEP Electroweak Working Group, *Precision Electroweak Measurements and Constraints on the Standard Model*. arXiv:0712.0929v2 [hep-ex], 2007.
- [48] A. Taurok, H. Bergauer, M. Padrta, *Implementation and Synchronisation of the First Level Global Trigger for the CMS Experiment at LHC*. Nucl. Instrum. Methods Phys. Res., A 473 (2001) 243-259, 2002.

- [49] J. Erö et al., *The CMS Drift Tube Trigger Track Finder*. 2008 JINST 3 P08006, 2008.
- [50] N. A. et al., *Calorimeter trigger synchronization in the CMS experiment*, vol. 568. Nucl. Instrum. Methods Phys. Res., A 568 (2006) 634-641, 2006.
- [51] V. M. Ghete, *The CMS L1 Trigger emulation software*. Journal of Physics: Conference Series 219 (2010) 032009.
- [52] K. Potter, *Large Hadron Collider (LHC) project of CERN*. LHC Project Report 36, 1996.
- [53] R. Assmann, M. Ferro-Luzzi, M. Giovannozzi, W. Herr, J. Jowett, M. Lamont, E. Shaposhnikova, *BEAM PARAMETERS AND MACHINE PERFORMANCE TO BE REACHED IN 2010*. <http://lhc-commissioning.web.cern.ch/lhc-commissioning/>, 2010.
- [54] R. E. Marshak, *Conceptual foundations of modern particle physics*. World Scientific Publishing Co. Pte. Ltd., 1993.
- [55] G. D. Nima Arkani Hamed, Savas Dimopoulos, *The Hierarchy Problem and New Dimensions at a Millimeter*. arxiv:hep-ph/9803315, 2008.

List of Figures

2.1.1	The experimental data fits the predicted Breit-Wigner curve for only three generations of light neutrinos existing.	10
2.1.2	Example of a charged weak current with the coupling $\frac{-ig_w}{\sqrt{2}}\gamma^\mu\left(\frac{1-\gamma^5}{2}\right)$	11
2.1.3	The potential $V(\phi)$. Because of its characteristic shape it is often called mexican hat potential.	13
2.1.4	$\Delta\chi^2$ plotted vs probability. From experimental evidence and this fit it follows that $114.4 \text{ GeV} \leq m_H \leq 158 \text{ GeV}$. Tevatron excluded the Higgs for a mass range from 158 - 175 GeV.	15
2.1.5	The branching ratios of the Higgs particle versus its mass.	17
2.2.1	One loop correction to m_H^2 by the coupling of a fermion to the Higgs field.	18
2.3.1	Discovery potential of universal extra-dimensions at CMS with the dotted lines showing the influence of experimental uncertainties [21].	24
3.1.1	The CERN accelerator complex. (©CERN 2007)	27
3.2.1	The Large Hadron Collider with its four experiments.	28
4.0.1	Design of the CMS detector [25].	31
4.1.1	The CMS reference frame.	32
4.3.1	Schematics of the CMS tracker where each line represents a detector module.	34
4.4.1	Schematics of the electromagnetic calorimeter at CMS.	35
4.4.2	The Hadronic Calorimeter at CMS.	36
4.4.3	Scheme of the CMS Muon system [33].	38
4.4.4	The CMS Trigger/DAQ system.	41
5.0.1	Cross section for basic physics processes defining the requirements for the CMS trigger [26].	43
5.2.1	The L1-Trigger in overview.	44
5.2.2	Scheme of the DTF track finding mechanism.	47
5.2.3	The Global Trigger Crate.	49
5.2.4	Algorithm to trigger on a SUSY slepton.	52
5.2.5	The Trigger Control System.	54
6.1.1	Concept of the Trigger Supervisor framework.	61
7.2.1	Integration of the L1 Trigger Menu Editor with the CMS software infrastructure.	66

7.4.1	Example for a TME η input mask translated into VHDL code. . .	72
7.5.1	Illustration of the transformation from hardware differences to physics differences for $\Delta\phi$	75
7.5.2	Physical interpretation of the hardware differences in η (non-linear). . .	76
7.6.1	Layout of the TME central panel. The tree on the left hand side is produced by the TS framework and can be used to create an instance of the central panel.	78
7.6.2	The header panel as example for a functional panel.	80
7.6.3	The implementation of conditions in the L1 Trigger Menu Editor.	81
7.6.4	The algorithm editor panel.	82
7.6.5	The VME Mode.	87
8.1.1	Analysis of trigger rates and prediction of prescale factors.	92
8.1.2	The 15 highest trigger rates for menu L1Menu_ Commissioning2010_ v4.	93
8.1.3	The highest trigger rates for two different runs at different luminosities.	94
8.1.4	Correlation table for the 15 bits with the highest rates for two different runs.	96
8.2.1	Correlation plot of the 2 - particle correlation observed at CMS for high multiplicity events (right plot). The ridge-like structure emerges in (d).	98

Appendix A

The VHDL Writer Mirror Operations

η in calo conditions For η of calorimeter objects (with the exception of forward jets) a 16 - Bits LUT is used in the firmware. Due to the η resolution of the L1-Trigger in the TME GUI in total 14 segments for η are available that can be enabled or disabled. A sample scale from the scales key L1_Scales is used to illustrate the physical interpretation of the particular bins. The next table shows how the actual LUT is filled from the bitmask from the example from before. The mapping used now is from TME bin to LUT index. In the following unused bits are always indicated by x:

LUT index	0	...	6	7	8	...	14	15
TME Bin	#7	...	#13	x	#6	...	#0	x

For forward jets the situation is a slightly different one: For η of forward jets there are in total 8 segments which correspond to four η towers in positive and four in negative direction of the beam. In the hardware they are also represented in a 16 -bits LUT, the transformation schema from GUI to LUT is more or less equivalent to the one described before:

LUT index	0	...	3	4	...	7	8	...	11	12	...	15
TME Bin	#4	...	#7	x	...	x	#3	...	#0	x	...	x

ϕ for calorimeter conditions For ϕ of calorimeter conditions a 32-bit LUT is used. At the moment the resolution of the L1-Trigger allows 18 segments for ϕ , which in contrast to η are not mirrored in the firmware.

LUT index	0	1	2	...	16	17	18	...	31
TME Bin	#0	#1	#2	...	#16	#17	x	...	x

Bits 18 to 31 are not used.

$\Delta\eta$ for calorimeter objects For $\Delta\eta$ the firmware calculates the expression $|\eta_1 - \eta_2|$. Therefore the η values are converted to a positive range, using a conversion table which is part of the static VHDL code. This is done due to the

reason that the hardware scale for η contains the bins -0 and +0. Calculating the difference is a lot easier with hardware scales of the format $\{0, \dots, 13\}$. After this conversion, the subtraction can be performed. The negative differences of $\{-1 \dots -13\}$ hardware segments are mirrored before they are written to the LUT for the reason described above. The resulting 32-bit LUT is filled from the GUI as follows:

LUT index	0	...	13	14	...	50	19	...	63
TME Bin	#0	...	#13	x	...	x	#13	...	#1

The TME bin #0 only occurs once because the difference of zero does not have a sign.

$\Delta\eta$ for forward jets is following the same rules as the other calorimeter objects with the only difference that there is a available range from 0 ... 7:

LUT	0	..	3	4	..	15	..	21	22	..	43	..	49	50	..	61	..	63
TME	#0	..	#3	x	..	#15	..	#21	x	..	#21	..	#15	x	..	#3	..	#1

$\Delta\phi$ for calorimeter objects $\Delta\phi$ for calorimeter objects is calculated in a similar way. The available LUT has 32 bits. The largest difference in ϕ that makes sense from a physicist's point of view is the opposite alignment of the considered objects (180 degrees). Therefore the TME shows only the GUI segments #0...#9 despite the hardware providing the possible differences of $\{0, \dots, 128\}$. The reduction to 10 TME bins takes place because of the fact that several differences in hardware have the same physical interpretation due to this symmetry. For example the differences: +1, -1, +17 and -17 all correspond to the TME bin #1. For the VHDL code this has the consequence that an additional mirror operation of the TME input is required to be able to take into account these additional differences, which are equivalent. The resulting LUT is:

LUT index	0	...	9	...	17	18	...	31
TME Bin	#0	...	#9	...	#1	x	...	x

η for muons η for muon conditions is written following the same principle as for calorimeter conditions. The hardware η scale at the moment is $\{-31, \dots, -0, +0, \dots, +31\}$ according to the η resolution of muon conditions. The η information for muons exactly fits into a 64-bit LUT.

LUT index	0	...	31	32	...	63
TME Bin	#32	...	#63	#31	...	#0

$\Delta\eta$ for muons The LUT that is used for $\Delta\eta$ of muons contains 128 bits. The η values are converted to a range from $\{0, \dots, 18\}$, using an internal conversion table and subtracted afterwards. The resulting LUT is:

LUT index	0	...	63	64	65	...	127
TME Bin	#0	...	#63	x	#63	...	#1

$\Delta\phi$ **for muons** $\Delta\phi$ for muons is implemented with a 144-bit LUT.

LUT index	0	...	71	72	73	...	143
TME Bin	#0	...	#71	#72	#71	...	#1

ϕ **for ETM** ϕ for ETM fits into a 128-bit LUT and has a resolution of 72 bins in the TME GUI. It is filled as follows, without mirroring.

LUT index	0	...	71	72	...	79
TME Bin	#0	...	#71	x	...	x

ϕ **for HTM** ϕ for HTM at the moment is implemented exactly the same way as ϕ for calorimeter objects.

Correlation conditions For correlation conditions involving calorimeter objects the η scales of “normal” calorimeter objects and forward jets are merged to a common scale, which implies an extension of the η range to +/- 0 .. 10. Muon η scales which have a better resolution in theory than calo η scales are downscaled to calorimeter resolution. The LUTs for correlation conditions with calorimeter conditions have 64 bits due to the common scales. Apart from that fact they are produced in the same way. The differences in $\Delta\eta$ are only relevant for the combinations calo-calo and calo-muon:

LUT index	0	...	13	14	...	18	19	...	63
TME Bin	#0	...	#13	x	...	x	#13	...	#1

For forward jets the table looks like:

LUT index	0	...	17	14	...	46	47	...	63
TME Bin	#0	...	#17	x	...	x	#17	...	#1

The $\Delta\phi$ LUT for the combinations calo-calo, calo-muon, calo-htm and htm-muon is defined as follows:

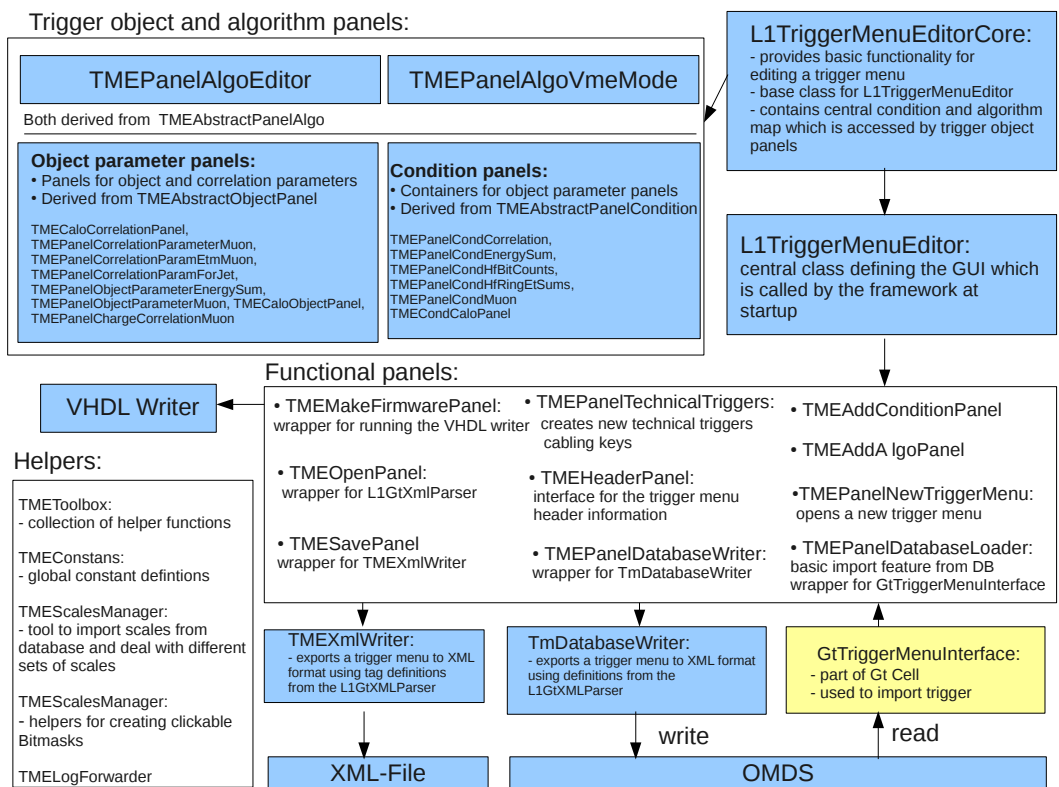
LUT index	0	...	9	...	17	18	...	31
TME Bin	#0	...	#9	...	#1	x	...	x

For ETM and muons a better resolution in $\Delta\phi$ is possible, therefore there is a 80-bits LUT:

LUT index	0	...	36	...	71	72	...	79
TME Bin	#0	...	#36	...	#1	x	...	x

Appendix B

Class Scheme of the L1 Trigger Menu Editor



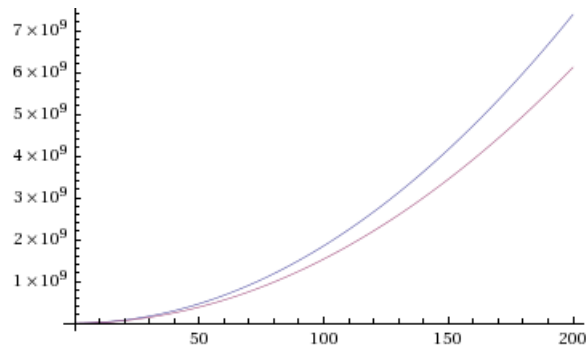
Appendix C

Trigger Rate Analysis Material

The statistical uncertainty of the luminosities

Since the statistical error of the luminosities was not yet officially given, it was estimated as follows: first it was assumed that the value of luminosity can be considered as constant for very few, consecutive luminosity sections. Then in total 42 intervals of consecutive luminosity sections for run 143953 were considered and a mean value for the luminosity for each of these intervals was calculated, together with its standard deviation. The mean value of these standard deviations was $\pm 0.0671 \times 10^{30} \text{cm}^{-2} \text{sec}^{-1}$. Taking into account that the luminosity for run 143953 is in the order of $10 \times 10^{30} \text{cm}^{-2} \text{sec}^{-1}$ this corresponds to a relative statistical error of about 1% for the luminosity.

Predicted rate from run 143953 vs measured rate from run 146511



The blue curve corresponds to the L1 trigger rate that was measured for run 143953 while the purple curve is the rate that was simulated using data from run 143953. It strikes out that the observed rate is always greater than the one that has been simulated. The fit results for both graphs are:

- Measured rate: $f_1(x) = 0.00588792 + 84685.2x + 184146x^2$, $\chi^2 = 351979$

- Predicted rate: $f_2(x) = -0.000130707 + 84261.7x + 152536x^2$, $\chi^2 = 51000.1$

Appendix D

Kurzzusammenfassung

Der Large Hadron Collider (LHC) am europäischen Kernforschungszentrum in Genf (CH) wurde gebaut, um die letzten noch offenen Fragen des Standard Modells der Teilchenphysik zu beantworten und soll gleichzeitig die Pforten für eine Physik jenseits des Standard Modells öffnen, da er es erlaubt, noch nie zuvor erreichte Energiebereiche zu untersuchen. Der LHC liefert eine relativ große Datenmenge bei jeder Kollision und produziert Kollisionen mit einer Frequenz von 40 MHz. Um mit dieser großen Rate an Ereignissen zurechtzukommen, sind die Experimente am LHC mit einem sogenanntem Trigger System ausgestattet, welches die vom physikalischen Standpunkt aus betrachtet interessanten Ereignisse von Hintergrundereignissen trennt, die keine neue Information liefern. Das Trigger System am CMS Experiment besteht aus insgesamt zwei Einheiten, einem L1-Trigger, welcher ein komplexes elektronisches System darstellt und einem High-Level Trigger, der im wesentlichen aus einer großen Computerfarm besteht. Hauptaufgabe des L1-Triggers ist es, die Frequenz von 40 MHz auf 100 kHz zu reduzieren, was der maximalen Inputrate für den High-Level Trigger entspricht. Er muss die Rate an Ereignissen also um einen Faktor von 10^7 reduzieren. Herzstück des L1-Triggers ist der Globale Trigger, der über eine in weiten Teilen frei programmierbare Logikeinheit verfügt, welche mit komplexen Algorithmen bestückt werden kann, die Daten mit zuvor definierten Auswahlkriterien vergleichen und deren Resultate darüber entscheiden, ob ein Ereignis zum High-Level Trigger weitergeleitet wird, oder ob es unwiederbringlich verworfen wird. Das Hauptziel dieser Diplomarbeit war es, eine Schnittstelle zu entwickeln, die es ermöglicht, diese Physikalgorithmen zu entwickeln und somit eine einfache Anpassung der Logik Einheit des Globalen Triggers an aus der Physik kommende Anforderungen erlaubt. Weiter müssen alle Informationen über das im Einsatz befindliche logische Setup des Triggers in der CMS Konfigurationsdatenbank gespeichert werden, damit sie für eine weitere Datenanalyse zugänglich sind. Ein weiteres Ziel dieser Arbeit war es, Triggerraten während der Anfangsphase des CMS Experiments zu analysieren, da sich während dieses Zeitraums die Luminosität des Beschleunigers, welche einen starken Einfluss auf die L1-Triggerraten hat, ständig erhöht. Die Steigerung der Luminosität erfolgt zum einen durch eine Erhöhung der Anzahl der Teilchen in den im Orbit zirkulierenden Teilchenpaketen und andererseits durch Erhöhung der Anzahl dieser Pakete selbst. Für einen reibungslosen Betrieb des Experiments ist es wichtig, den Zusammenhang zwischen Luminosität und Triggerrate

abschätzen zu können, damit die L1-Triggerrate immer unter der maximalen Inputrate für den High-Level Trigger gehalten wird, was durch ein zusätzliches Herunterskalieren („Prescaling“) von bestimmten Algorithmen erreicht werden kann. Weiter wurden auch die Raten einzelner Algorithmen analysiert und Korrelationen zwischen einzelnen Algorithmen untersucht, da diese Informationen hilfreich beim Abschätzen der Faktoren sind, um die einzelne Algorithmen herunterskaliert werden müssen.

Curriculum Vitae

29th of June 1986:

Born in Erlangen, Germany

2005:

General qualification for university entrance (“Abitur”) in Passau, Germany

Since 2005:

Studying physics at the University of Vienna

2006:

Passed first part of curriculum (“1. Studienabschnitt”) with award

Summer 2007:

Summer stay at the European Organization for Nuclear Research in Geneva, Switzerland for two month

Since November 2007:

Collaborator of the CMS Trigger group at the Institute of High Energy Physics of the Austrian Academy of Science

September 2008 – September 2009:

ERASMUS stay in Barcelona, Spain, at the UAB (Universitat Autònoma de Barcelona)

2010:

Diploma thesis with the title: “Interfacing the L1 Global Trigger of the CMS experiment at LHC with physics”